THERMAL AND HYDROTHERMAL STABILITY OF SELECTED POLYMERS IN A NUCLEAR REACTOR ENVIRONMENT

By

JINHO KIM

A DISSERTATION PRESENTED TO THE GRADUATE SCHOOL
OF THE UNIVERSITY OF FLORIDA IN PARTIAL FULFILLMENT
OF THE REQUIREMENTS FOR THE DEGREE OF
DOCTOR OF PHILOSOPHY

UNIVERSITY OF FLORIDA

2004

Copyright 2004

by

Jinho Kim

To my parent, my family and friends who love and support me.

ACKNOWLEDGMENTS

First, I appreciate God for giving me an opportunity to study and complete my degree with great happiness.

I would like to deeply thank Dr. Ronald Baney, my advisor, for guiding me through the doctoral study. I have learned from him how a researcher should pursuit his goal. I have also learned how an advisor should treat his students. His enthusiastic and devoted attitude toward research and teaching has strongly affected my attitude for my entire life. I will never forget my mentor, Dr. Ronald Baney. I also thank all my committee members. I am grateful to Prof. James Tulenko, who worked together with me during my entire doctoral study and helped me to understand the nuclear research field and supported me from the NERI project. I thank Dr. Darryl Butt who also worked on the same project, always gave me good advice and allowed me to share his excellent equipments. I also thank to Dr. Laurie Gower, Dr. Wolfgang Sigmund and Dr. Dow Whitney who gave me deep academic advice.

I deeply thank Dr. Glen Schoessow who ran over 50 samples in the Autoclave during my entire research period. Sincere gratitude is extended to Dr. Dean Schoenfeld who helped me to fabricate the irradiated polymer samples. I also thank staff members in MAIC and ERC to teach me how to use their equipments, i.e., FTIR, FESEM, ICP, SEM, XRD, AES, and XPS. I also appreciate my current group members, Kyle Kathan, Yunmi Kim, and Heather Trotter, and my former group members, Sangtae Park, Dongwon Lee, Paul Demkowicz, Noriko Shibuya and Lisa Argo. I would like to offer thanks to my

friends in Gainesville and Korea. I am truly thankful to Dr. Choi, my advisor in Korea, who guided me to study abroad. I also would like to thank my uncle and aunt in California.

Finally, I would like to say thanks to my family: my parent, my brother, my sister-in-law, my sister, my brother-in-law and my lovely three nieces and one nephew. Their love and support have encouraged me to overcome all difficulties while I have studied here. I dedicate this thesis to them.

TABLE OF CONTENTS

page

ACKNOWLEDGMENTS iv

LIST OF TABLES ix

LIST OF FIGURES xi

CHAPTER

1. INTRODUCTION 1

2. LITERATURE REVIEW 5

2.1 Application of Polymeric Materials to BPRAs in PWRs 5
2.1.1 Nuclear Power Plant 5
2.1.2 Primary Components and Materials of Nuclear Reactors 6
2.2 Moderation Effect 6
2.3 Burnable Poison Materials 8
2.4 Requirements for Polymeric Burnable Poison Materials 11
2.5 A Behavior of Polymeric Material in Near- and Supercritical Water 14
2.5.1 Definition of Near Supercritical Water (350 ^{0}C, 20.7Mpa) 14
2.5.2 Polymer Recycling by Using Near- and Supercritical Water 15
2.6 Polymer Degradation 17
2.6.1 Thermal Degradation 17
2.6.2 Chemical Degradation (Hydrolysis) 19
2.6.3 Degradation by High-energy Radiation 21
2.7 Water Absorption 22

3. POLY (DIACETYLENE-SILOXANE-CARBORANE): A POTENTIAL CANDIDATE POLYMERIC MATERIAL FOR BURNABLE POISON ROD ASSEMBLIES (BPRAS) IN PRESSURIZED WATER REACTORs (PWRs) 37

3.1 Introduction 37
3.2 Experimental 38
3.2.1 Synthesis of Poly (diacetylene-siloxane-carborane) 38
3.2.2 Characterizations 40
3.3 Results and Discussion 41
3.4 Summary 47

4. INTRODUCTION OF SILICON BASED POLYMERS TO POLY (DIACETYLENE-SILOXANE-CARBORANE): THEIR THERMAL & HYDROTHERMAL STABILITY....64

4.1 Introduction of Poly(diacetylene-siloxane) to Poly(diacetylene-siloxane-carborane)....64
4.1.1 Experimental....66
4.1.1.1 Sample preparation....66
4.1.1.2 Characterizations....67
4-1-2. Results and Discussion....67
4.2 Introduction of Dimethylsilane Linkages to Poly (diacetylene-siloxane-carborane)....69
4.2.1 Experimental....69
4.2.1.1 Sample preparation....69
4.2.1.2 Synthesis....69
4.2.1.3 Characterizations....70
4.2.2 Results and Discussion....71
4.3 Summary....74

5. SCREENING CANDIDATE MATRIX POLYMERS FOR POTENTIAL BURNABLE POISON ROD ASSEMBLIES (BPRAS) IN PRESSURIZED WATER REACTORS (PWRS)....89

5.1 Introduction....89
5.2 Experimental....90
5.2.1 Materials....90
5.2.1.1 Preparation of phenolic resins....90
5.2.1.2 Preparation of epoxy resins....91
5.2.1.3 Preparation of silicone resins....91
5.2.1.4 Preparation of Gamma irradiated high-density polyethylenes (HDPEs)....92
5.2.2 Characterizations....92
5.3 Results and Discussion....93
5.3.1 Phenolic resins....93
5.3.2 Epoxy resins....101
5.3.3 Silicone resins....102
5.3.4 Gamma irradiated high-density polyethylene....103
5.4 Summary....107

6. A CRITICAL FACTOR THAT DETERMINES THE HYDROTHERMAL STABILITY OF CROSS-LINKED POLYETHYLENES (XLPES) AT NEAR-CRITICAL WATER CONDITION....125

6.1 Introduction....125
6.2 Experimental....128
6.2.1 Sample Preparations....128
6.2.1.1 Silane, Peroxide and E-beam XLPEs....128
6.2.1.2 Gamma irradiated HDPE....128
6.2.2 Characterizations....128
6.3 Results and discussion....129
6.3.1 Characteristic Properties of Irradiated HDPE (Gamma XLPE)....129
6.3.2 Polymer Identification....132
6.3.3 A Critical Factor that Determines the Hydrothermal Stability of XLPEs133
6.4 Summary....135

7. PHYSICAL PROPERTIES OF HIGH GAMMA IRRADIATED HIGH-DENSITY POLYETHYLENE (HDPE) / GRAPHITE COMPOSITE....149

7.1 Introduction....149
7.2 Experimental....151
7.2.1 Sample Preparations....151
7.2.1.1 Materials....151
7.2.1.2 Composite and dogbone specimen fabrication....151
7.2.1.3 Gamma irradiation....152
7.2.2 Characterizations....152
7.3 Results and Discussion....153
7.4 Summary....157

8. CONCLUSIONS....168

9. FUTURE WORK....172

LIST OF REFERENCES....177

BIOGRAPHICAL SKETCH....186

LIST OF TABLES

Table page

2-1. Primary components and main materials of nuclear fission reactors. 27

2-2. Scattering properties of various nuclei. 28

2-3. Properties of moderators at 20°C. 28

2-4. Reactivity requirements for control mechanism in typical PWR. 28

2-5. Properties of burnable poison systems. 30

2-6. Essential properties to be used for BPRAs. 31

2-7. Weight percent of different elements in B_4C/Al_2O_3. 32

2-8. Estimating the number of H atoms/cc. 32

2-9. Evaluated data for centerline temperature in various BPRA materials. 33

2-10. Water absorption of various polymers 36

3-1. Cure and postcure condition for various samples. 57

3-2. Hydrogen content. 61

4-1. The glass transition temperature of copolymers. 76

4-2. The price for starting materials 77

4-3. Molecular structures, total weight per 1 mole and hydrogen and boron content for both DSCS and DS. 77

4-4. The general information of chemicals and derived polymers. 82

5-1. The essential properties that a polymer matrix should possess. 109

5-2. CHN analysis for phenolic resins with different curing temperature. 113

5-3. The gel content and the swelling ratio of irradiated HDPEs. 124

5-4. CHN element analysis for irradiated HDPEs 124

6-1. The oxidation index for various Gamma XLPEs. 139

6-2. Melting temperature, crystallization temperature, ΔH_f and crystallinity of the HDPE before and after gamma irradiation. 141

6-3. Mechanical properties of virgin HDPE and Gamma irradiated HDPE. 142

6-4. Autoclave test for various XLPEs 144

6-5. The swelling ratio of various XLPEs. 146

6-6. CHN element analysis for 4 different XLPEs 148

7-1. The radiation dose rate used in this experiment as a function of the distance from the ^{60}Co source 159

LIST OF FIGURES

Figure page

2-1. Nuclear fission and fission chain reactions. 24

2-2. Pressurized water reactors (PWRs). 25

2-3. PWR Fuel rod assemblies and BPRA locations. 26

2-4. Two different burnable poison system (a) BPRA plan view and cross section. (b) WABA plan view and cross section. 29

2-5. Phase diagram of supercritical water. 34

2-6. Ionic product, density, and dielectric constant of water versus temperature at a pressure of 24 MPa. 35

3-1. The chemical structure of poly (diacetylene-siloxane-carborane). 49

3-2. The synthesis and processing of poly (diacetylene-siloxane-carborane). 49

3-3. The synthesis apparatus. 50

3-4. The synthesis steps. 51

3-5. FTIR spectroscopy of (a) synthesized original viscous liquid poly (diacetylene-siloxane-carborane) (b) poly (diacetylene-siloxane-carborane) thermoset after curing at 350°C for 4 hours. 52

3-6. NMR spectroscopy of synthesized original viscous liquid poly (diacetylene-siloxane-carborane) (a) ^{1}H NMR Spectroscopy ($CDCl_3$): 0.1, 0.3(24H, Si-CH_3), 0.8-3.5(broad,10H, B-H), (b) ^{13}C NMR Spectroscopy ($CDCl_3$) : 0.549 (Si-C), 68.259(Si-C-B). 53

3-7. DSC scans showing cure exotherms of original polymer. 54

3-8. Chemical structures of ene-yne and butatriene. 55

3-9. TGA thermograms of poly (diacetylene-siloxane-carborane) under an Ar atmosphere. 56

3-10. FTIR spectroscopy of poly (diacetylene-siloxane-carborane) with different postcuring temperatures (a) 400°C (b) 600°C (c) 700°C. 58

3-11. An estimated hydrolysis reaction of poly (diacetylene-siloxane-carborane) under near-critical water conditions. 59

3-12. FTIR spectroscopy of poly (diacetylene-siloxane-carborane) with heat treatment (400°C, 2h & 600°C, 1h) (a) before autoclave test (b) after autoclave test. 60

3-13. SEM of poly (diacetylene-siloxane-carborane) with different annealing temperature (a), (b): fracture surface, (c), (d), (e): top surface. 62

3-14. EDX of spherical particles which appeared on the top layer pyrolyzed at 1000°C..63

4-1. The chemical structure of poly (diacetylene-siloxane)....76

4-2. Synthesis steps of poly (diacetylene-siloxane)....78

4-3. FTIR spectra for synthesized poly (diacetylene-siloxane): (a) before curing (b) after curing at 300°C for 4 hours. 79

4-4. DSC scan showing cure exotherms for synthesized poly (diacetylene-siloxane): (a) before curing, (b) after curing at 300°C for 4 hours. 80

4-5. TGA curves of poly (diacetylene-siloxane) after curing at 300°C for 4 hours 81

4-6. Synthesis step of poly (diacetylenedimethylsilane) and poly (diacetylenedimethylsilylethane) copolymer. 83

4-7. FTIR spectra of synthesized (A) poly (diacetylenedimethylsilane) and (B) poly (diacetylenedimethylsilylethane)....84

4-8. TGA curves of poly (diacetylenedimethylsilane) after curing at 300°C. 85

4-9. TGA curves of poly (diacetylenedimethylsilylethane) after curing at 350°C. 86

4-10. Infrared spectra of poly (diacetylenedimethylsilylethane) at 200°C, 360°C and 450°C and original polymer (2)....87

4-11. Scanning electron spectrum of poly (diacetylenedimethylsilylethane) after the autoclave test. 88

5-1. The diagram of HDPE sheet (A dose rate and the calculation of total doses). 110

5-2. A possible curing mechanism of resol type of phenolic resin. 111

5-3. TGA curves of P13470-180: — cured at 180°C for 20 mins and P13470-350: --- postcured at 350°C for 4 h. 112

5-4. SEM image of phenolic resin (P13470) with different pyrolyzing temperatures (a) P13470-350: postcured 350 °C for 4 hours (b) P350DRY: isothermal test (350°C/24h) in Ar (c) P170AUTO : autoclave test of P13470-170 (d) P350AUTO : autoclave test of P13470-350 114

5-5. FTIR spectra of phenolic resin (P13470) heat-treated at different temperature: (a) P13470-180: cured at 180 °C for 20mins (b) P13470-350: postcured 350 °C for 4 hours (c) P350AUTO: after the autoclave test (350°C/20.7MPa /24h) in water (d) P350DRY: isothermal test (350°C/24h) in Ar atmosphere. 115

5-6. Scanning electron spectra of phenolic resin (P13470) with different pyrolyzing temperatures (c) P13470-500 : 500°C for 1h (d) P13470-700 : 700°C for 1 hour 116

5-7. The variation of the density of P13470 with different pyrolyzing conditions.....117

5-8. TGA curve of cured epoxy resins (A) DER383® (B) DEN431® in Ar atmosphere. 118

5-9. FTIR spectra of Poly (methylsilsesquioxane)s (A) PMSSQ-A: after aging at room temperature for 2 weeks (B) PMSSQ-C: after curing consecutively at 130, 250, and 400°C for 4 hours. 119

5-10. TGA curves of Poly (methylsilsesquioxane)s (A) After aging at RT for 2weeks (B) After curing consecutively at 130, 250, and 400°C for 4 hours.....120

5-11. The estimated hydrolysis reaction of PMSSQ cage structure under near-critical water condition 121

5-12. TGA curve of (A) HDPE, (B) HDPE6940 (HDPE irradiated by 6940KGy).....122

5-13. SEM image for the fracture surface of HDPE6940 after the autoclave test.....123

6-1. The discoloration of cross-linked HDPE series with irradiation dose.....137

6-2. FTIR spectra of virgin and irradiated XLPEs.....138

6-3. T_m endotherm peaks and T_c exotherm peaks of virgin and irradiated HDPEs with different radiation intensity. 140

6-4. Elongation at break of virgin HDPE and irradiated HDPE. 142

6-5. FTIR spectra for 4 different XLPEs by (a) silane (b) peroxide (c) E-beam and (d) Gamma irradiated HDPE (2710KGy). 143

6-6. TGA diagram for HDPE and various XLPEs.....145

6-7. A cartoon of the cross-linked structures of (a) Gamma XLPE (6940 KGy) (2) Silane XLPE (3) Peroxide XLPE and (4) E-beam XLPE 147

7-1. Dog-bone samples mounted on the board before crosslinking in the irradiation chamber. 159

7-2. SEM of the fracture surface for HDPE/graphite power composite (x 1000) (a) 85/15 (b) 70/30 (c) 55/45 (c) 40/60 ratio of HDPE/graphite after quenching the samples160

7-3. SEM of the tensile fracture surface for HDPE/graphite power composite (x 1000) (a) 85/15 (b) 70/30 (c) 55/45 (c) 40/60 ratio of HDPE/graphite after 5254 KGy gamma irradiation (without quenching).....161

7-4. SEM of the tensile fracture surface for 70/30 HDPE/graphite (without quenching).162

7-5. Young modulus and Elongation at break of HDPE/graphite composite on the graphite content (a) before gamma irradiation (b) after gamma irradiation (5420KGy) 163

7-6. Relative electrical conductivity (σ_c/σ_m) of HDPE/graphite composite on the graphite content: (a) before gamma irradiation (b) after gamma irradiation. 164

7-7. Thermal conductivity (λ_c) of the graphite EG (■) and graphite KS (●) filled HDPE graphite on the volume filler content (ϕ_f). Solid lines – curve fitting. 165

7-8. TGA thermograms of graphite /HDPE composites.....166

7-9. TGA thermograms of graphite /HDPE composites after the radiation treatment. ...167

9-1. A special design of pellets that might show good thermal conductivity in the perpendicular direction.....176

Abstract of Dissertation Presented to the Graduate School
Of the University of Florida in Partial Fulfillment of the
Requirements for the Degree of Doctor of Philosophy

THERMAL AND HYDROTHERMAL STABILITY OF SELECTED POLYMERS IN A NULCEAR REACTOR ENVIRONMENT

By

Jinho Kim

December, 2004

Chair: Ronald H. Baney
Major Department: Materials Science and Engineering

The focus of this study is the development and understanding of polymer based burnable poison rod assemblies (BPRAs) in pressurized water reactors (PWRs). This material substitution reduces the water displacement penalty at the end of cycle (EOC) currently found with the B_4C/Al_2O_3 BPRAs that displace moderator water in PWRs. This gives rise to a longer fuel cycle due to the extra moderation from hydrogen in polymer structures. Finding synthetic polymers that endure a severe nuclear reactor circumstance is a challenge. Aside from the proper thermal stability at the range of 350-600°C in the core for a single cycle, the hydrothermal stability at near-critical water condition (350°C, 20.7MPa) is required to maintain the safe and controlled nuclear reaction because a danger comes if water might possibly penetrate inside the burnable poison rod by the failure of zircaloy cladding.

There are two approaches to obtain a boron source (burnable position material) in hydrogen containing polymers. One is to utilize the boron source directly by synthesizing boron-containing polymers. A second approach is to find commercial polymers that have an appropriate thermal, hydrothermal, radiational stability and high hydrogen content; and then add an inorganic boron source such as B_4C to form a composite material.

Poly (diacetylene-siloxane-carborane)s and other silicon based precursor polymers were introduced to observe their thermal and hydrothermal stability. However, we found that the degradation of Si-O-Si, which was presented in the polymer, was an unfavorable disadvantage under near-critical water (350°C, 20.7MPa) even though they formed dense network structures. In addition, the Si-O bond is quite sensitive to variety of reagents, including base and acid. Therefore, the degradation rate might be accelerated by high H^+ and OH^- ion concentrations at the near-critical water condition.

For the second approach, a number of candidate matrix polymers were screened for new polymeric BPRA system. Interestingly, phenolic resin showed strong condensation reactions at near-critical water condition, thus generating evolved gas followed by forming a highly ordered pore structure. Moreover, highly cross-linked polyethylene (XLPE), which was irradiated by 940 KGy and 1390 KGy, and silane XLPE also showed excellent hydrothermal stability under this condition. We found that the swelling ratio representing the network strength is a more critical factor to determine the hydrothermal stability of XLPEs.

XLPEs had a low ceiling temperature (~450°C), which does not fulfill the requirement of the high temperature stability above 500-600°C required by the temperature rise associated with neutron adsorption and low thermal conductivity. High

density polyethylene (HDPE)/graphite composite introduced to increase the thermal conductivity of pure HDPE. However, the development of an alternative for polymeric BPRA system, which has much higher thermal conductivity, still remains an important endeavor to make them commercial.

CHAPTER 1
INTRODUCTION

The use of burnable poisons has been studied extensively in the past decade resulting in dramatic improvements in fuel utilization and depletion and reduction of leakage of thermal neutrons from the core [1-4]. Extended lifetimes of fuel batches and higher burn-up have made nuclear power extremely cost-competitive.

The burnable poison material should burn out at approximately the same rate as the reactivity in fuel decreases. The problem related with an existing BPRA system, which consists of boron carbide (B_4C) in an alumina (Al_2O_3) matrix, is that at the end of cycle (EOC), when the burnable poison rod is no longer needed, it has a penalty on reactivity related to the loss of moderation due to occupying just the space with moderating water could occupy. An alterative technology, the wet annular burnable assemblies (WABAs) that allow the ingress of water by the use of a central annular hole are expensive to fabricate and still result in some moderator displacement [5]. However, the development of a polymeric burnable poison material could more effectively enhance burn-up and eliminate the water displacement penalty at EOC due to the extra moderation from hydrogen in polymer structures. The overall differences between two burnable poison systems (polymer based BPRA versus B_4C/Al_2O_3 BPRA) may only result in a change of about one percent of burn-up over the cycle of a core. However, because of the enormous costs to a utility during a shut-down, one percent of a two-year cycle could result in a savings of up to $6 million per reload to the utility [6].

Boron-10, which has a high neutron absorption cross section, has been used for a burnable poison material in order to have safe, controlled energy production. There are two approaches to develop the polymer based BPRA system depending on how to obtain a boron source in hydrogen containing polymers. One is to utilize the boron source directly by synthesizing boron-containing polymers. A second approach is to find commercial polymers that have an appropriate thermal, hydrothermal, radiational stability and high hydrogen content; and add an inorganic boron source such as B_4C to form a composite material.

Aside from the proper thermal stability at the range of 350-600°C in the core (inert atmosphere) for a single cycle which can range from 1 to 2 years, approximate hydrothermal stability under 350°C and 20.7MPa is required to maintain the safe and controlled nuclear reaction because a danger comes if water might possibly penetrate inside the burnable poison rod by the failure of the zircaloy cladding. Moreover, the requirement of the high temperature stability above 500-600°C might be reached due to the temperature rise associated with neutron adsorption and low thermal conductivity of a polymer. Therefore, the material having high thermal conductivity is needed.

Autoclave tests performed in this study were at 350°C and 20.7MPa. This region can be termed "near supercritical water" because the temperature is just below the critical point (T=374 °C, P=22.1MPa). The ion product, or dissociation constant (K_w), in this region representing H^+ and OH^- ion concentration of water goes through maximum. In fact, the dissociation of water itself in this condition generates a sufficiently high concentration that some acid-catalyzed organic reactions occur without any added acid [7-9]. As a result, water behaves like many organic solvents in that it has high solubility with

many organic compounds. Under these conditions, water has the ability to hydrolyze many compounds catalyzed by H^+ and OH^- ions [10].

Poly (diacetylene-siloxane-carborane)s were the initial starting material to develop a new polymer based BPRAs system [6]. Poly (diacetylene-siloxane-carborane)s are considered for this application due to their high thermal stability, high hydrogen content and their easy processing as well as ability to contain the boron [11-20]. In this study, thermal properties were measured by thermogravimetric analysis (TGA) and differential scanning calorimetry (DSC). An autoclave test was also performed to verify the hydrothermal stability at the near-critical water (350°C/20.7MPa). The chemical structure change and degradation mechanism during cure, postcure, autoclave test were analyzed by Fourier transform infrared spectroscopy (FTIR). The hydrogen content was monitored during the heat treatment to assure an adequate moderating benefit of the polymeric BPRAs. Moreover, the thermal and hydrothermal stability of other silicon based polymer precursors was examined to improve the hydrothermal stability of poly (diacetylene-siloxane-carborane). This could overcome the problems currently addressed in poly (diacetylene-siloxane-carborane), i.e., high cost, limited supply and high boron concentration.

In addition, a number of candidate polymer matrix materials were screened for the second approach. Thermosetting resins are one of the most difficult substances to decompose. Sugeta et al. showed that phenolic resin used as a matrix of fiber-reinforced plastics did not decompose under supercritical water at 380°C [21]. For these reasons, thermosetting resins such as phenolic resins, epoxy resins, silicone resins and cross-linked high-density polyethylenes were selected as candidate materials in this study. It

was also reported that the polyethylene main chain did not decompose at supercritical condition (380°C) [22]. Moriya et al. represented that the rate of supercritical water cracking in polyethylene is quite lower than that of thermal cracking [23]. These indications have challenged us to fabricate the cross-linked structure by using hydrothermally stable polyethylene linkages that would survive in severe autoclave condition. This study provides us to understand the behavior of selected polymers in the near-critical water condition and provided excellent evaluations of potential candidate materials.

CHAPTER 2
LITERATURE REVIEW

2.1 Application of Polymeric Materials to BPRAs in PWRs

2.1.1 Nuclear Power Plant

In a nuclear power plant, heat is generated in the reactor by nuclear fission as shown in Figure 2-1 [24]. When a free neutron is absorbed by a nearby uranium nucleus, that nucleus splits and releases more neutrons, which strike other nuclei. Thus, a chain reaction occurs, and the fission process becomes self-sustaining. A large amount of energy is released in the form of radiation and fragment kinetic energy during this reaction. The chain reaction that takes place in the core of a nuclear reactor is controlled by control rods, burnable poison rods, and chemical shim, which absorb neutrons to set the reactor at the required power level.

The principles for using nuclear power to produce electricity are the same for most types of reactor. The energy released from continuous fission of the atoms of the fuel generates heat and is used to produce steam. The steam is used to drive the turbines, which produce electricity.

Figure 2-2 shows typical pressurized water reactors (PWRs). This mainly consists of two separate circulations of water. The nuclear reactions take place inside the core in the fuel rod assemblies, the control rods, the moderator, and the coolant in the reactor vessel. The turbines, the heat exchanger, and part of the cooling system are located outside the core.

A typical fuel rod assembly in PWR is shown in Figure 2-3 [5]. These fuel rod assemblies are surrounded by a substance, called a moderator, to slow the speed of the emitted neutrons and thus enable the chance and probability of fission to occur. Water, heavy water, and graphite are used as moderators in different types of reactors. Usually pellets of uranium oxide (UO_2) are arranged in tubes to form fuel rods. Gray rods on the left corner in Figure 2-3 represent BPRA locations in fuel rod assemblies.

2.1.2 Primary Components and Materials of Nuclear Reactors

From an engineering viewpoint, it is a good idea to understand schematic characteristics of material composing of nuclear reactor. Table 2-1 shows the primary components and materials classified in seven main categories [25].

2.2 Moderation Effect

When a thermal neutron hits a U-235 nucleus, the nucleus generally splits into two big pieces and a few neutrons. These neutrons are used to sustain the chain reaction in the reactor. These fast neutrons have kinetic energies of 2MeV. However, this energy must be removed to change to a thermal neutron because only the thermal neutron can effectively break apart another uranium nucleus [26-28]. U-235 is most easily split by a thermal neutron with energy less then 1eV. Therefore, these fast neutrons should be slowed down or moderated to the thermal neutron by elastic and inelastic scattering with nuclei within the core in order to generate further fissions. The most efficient moderator for fast neutrons is hydrogen. The neutron can lose its energy significantly in one collision since the hydrogen atom has about the same mass as the neutron.

In scattering reactions, the net result is the exchange of energy between a neutron and a nucleus. In elastic scattering, the energy exchanged between the neutron and the nucleus is entirely kinetic in nature. Because neutrons generally have a higher kinetic

energy than atomic nuclei, the kinetic energy of the neutron is decreased in an elastic collision. In inelastic scattering, part of the kinetic energy of the neutron is transferred to the nucleus as internal energy. Elastic scattering is possible for all energies, but inelastic scattering can occur only when the neutron energy is large enough to produce an excited state of the nucleus. Most fast neutrons can be slowed down by elastic scattering.

In terms of kinetic energy, it is possible to express an average logarithmic energy decrement (ξ) as the describing term of the loss of neutron energy by collision of atoms as shown in Table 2-2 [27]. The table also shows that the mass of hydrogen is virtually identical to that of a neutron. Therefore, a 2MeV high energy neutron can be moderated to 1eV by an average of fifteen collisions with hydrogen atoms, which is the most effective way to reduce the kinetic energy of neutron [27,28]. To compare the total moderation effect of materials, the cross section of nuclei should be considered. A more actual moderation ability can be calculated by a combination of its average logarithmic energy decrement (ξ) and its cross section (σ) [27,28]. A microscopic elastic scattering cross section (σ_s) is a measure of an element probability of having a particular reaction with a particle. A macroscopic elastic scattering cross section (Σ_s) is the combination of σ_s and the number of density (atoms/cc) of materials. Therefore, the actual amount of moderation is considered to be the product of ξ and Σ_s. Both the high neutron scattering and the large cross section of the moderators imply frequent, large-angle collisions for a fast neutron to change to thermal neutron, thereby increasing the fission reactivity. In Table 2-3, ordinary water that has the value of $\xi \Sigma_s$ equal to 128 m^{-1} represents the most effective moderation.

2.3 Burnable Poison Materials

BPRAs are important to control the neutron flux and maintain a constant power level until the end of cycle (EOC). Boron-10, which has a high neutron absorption cross section, has been used for a burnable poison material in separate lattice pin or plate form of B_4C/Al_2O_3 in a zirconium alloy cladding tube. The primary purpose of a burnable poison is to offset excess reactivity required to sustain the reactor over time because of fuel depletion and fission product build-up. Boron-10 performs this function by absorbing thermal neutrons as the absorber material changes to lithium-7 and other isotopes or "burns" until just before EOC [5]. In order to have safe, controlled energy production, a nuclear reactor must always be under control within precise limits. The chain reaction in a nuclear reactor can be described quantitatively in terms of the multiplication factor, which is denoted by the symbol k [28].

$$k = \frac{\text{number of fissions in one generation}}{\text{number of fissions in preceding generation}}$$

If k is less than one, the chain would soon die out; this is known as subcritical (k<1). If exactly one neutron per reaction goes to take part in the chain reaction (k=1), the reactor is critical, meaning it is operating at constant power. The danger comes if more than one neutron per reaction goes on to sustain the chain; in this case the reactor would be supercritical (k>1). The rate of reaction would be out of control, and a meltdown could occur [26-28]. To control large amounts of excess reactivity at the beginning of cycle (BOC), control elements such as control rods, burnable poisons, and chemical shim are used in nuclear reactors to keep the reactor critical at a constant maximum power.

The most common method to control the excessive reactivity is the insertion or withdrawal of control rods made out of materials (poisons) having a large cross section

for the absorption of neutrons. This material is usually not totally burnable and can be usable only when loading a fresh fuel or shutting down the reactor. Hafnium, silver, indium, cadmium, and boron are currently used for this application [25].

Burnable poisons are materials that have a high neutron absorption cross section that are converted into materials of relatively low absorption cross section as the result of neutron absorption. After the burn-up of the poison material, the negative reactivity of the burnable poison decreases over core life. Ideally, these poisons should decrease their negative reactivity at the same rate the fuel's excess positive reactivity is depleted. Fixed burnable poisons are generally applied in the core with the fuel rod assemblies in the form of compounds of boron or gadolinium that are shaped into separate lattice pins or plates, or introduced as additives to the fuel. Since they can usually be distributed more uniformly than control rods, these poisons are more effective to control the core power distribution. Soluble poisons, called chemical shim, produce spatially uniform neutron absorption when dissolved in the water coolant. The most common soluble poison in commercial PWR is boric acid, which is often referred to as soluble boron. At BOC, enough boric acid is added to the coolant to allow the reactor to be just critical (k=1) with all control rods withdrawn. As fuel burnup takes place through power operation, the boric acid concentration in the coolant is reduced to sustain a nuclear reaction. If a cold shutdown is required, additional boric acid is added to compensate for the reactivity added as the moderator cools. With chemical shims, as temperature rises and the moderator expands, some moderator is pushed out of the active core area. Boron is also moved out, and this has a positive effect on reactivity. Excessive boric acid in water can be precipitated and the large amount of chemical shim in light water reactors can

lower the pH of the moderator, which leads to the corrosion of the cladding. Therefore, the role of burnable poison rod assemblies in nuclear fission reactor is important. Table 2-4 shows reactivity requirements or worth for control mechanism in typical PWR [29].

The use of burnable poisons have been extensively studied in the past decade; resulting in dramatic improvements in fuel utilization and depletion, or burn-up, improved overall conversion of uranium-238 into fissile plutonium, and reduction of leakage of thermal neutrons from the core [1-4]. Extended lifetimes of fuel batches and higher burn-up have made nuclear power extremely cost-competitive with other forms of energy production. Further improvements in burnable poisons could result in even greater fuel utilization and cost reduction. The wet annular burnable assemblies (WABAs) are one example of attempts to reduce the water displacement penalty.

The wet annular burnable assemblies (WABAs) in Figure 2-4 that allow the ingress of water by the use of a central annular hole are expensive to fabricate and still result in some moderator displacement [5]. From simulation study, our research group found that this new BPRA system with the carborane polymer consistently has a lower k-infinity value at beginning-of-cycle (BOC), indicating a harder spectrum; and a higher k-infinity at EOC, indicating a lower amount of burnable absorber present and a larger thermal flux at EOC. Based upon these considerations, the use of polymeric material in BPRAs would more effectively reduce the water displacement penalty than that of WABAs recently developed by Westinghouse.

The overall differences between two burnable poison systems (Polymer based BPRA versus B_4C/Al_2O_3 BPRA) may only result in a change of about one percent of burnup over the cycle of a core. However, because of the enormous costs to a utility

during a shut-down, one percent of a two-year cycle could result in a savings of up to $6 million per reload to the utility. It is therefore feasible to research new materials that could overcome some of the disadvantages listed in Table 2-5 even if the differences are subtle [5,6].

2.4 Requirements for Polymeric Burnable Poison Materials

In nuclear power generation it is possible to reduce the energy production cost by increase fuel burnup. Boron is often used in fuel (control rod and BPRA) or coolant (chemical shim) to control the excess reactivity at BOC, therefore optimizing reactivity and power distribution and eventually providing longer fuel cycles. In burnable poison rod, boron carbide (B_4C) in alumina (Al_2O_3) matrix is currently used in PWR.

The burnable poison material should burn out at approximately the same rate as the reactivity in fuel decreases. The problem related with an existing boron carbide (B_4C) in an alumina (Al_2O_3) matrix is that at EOC, when the burnable poison rod is no longer needed, it has a penalty on reactivity related to the loss of moderation due to occupying just the space with current burnable poison material. Tulenko et al. referred to the following critical conditions [6]. Listed below in Table 2-6 are essential properties that polymeric burnable poison material should possess.

First, the appropriate boron content in polymeric materials can be realized by substituting for boron carbide (B_4C) in the system. We have examined two approaches to obtain a boron source in hydrogen containing polymers. One is to utilize the boron source directly by synthesizing boron-containing polymers. A second approach is to find commercial polymers that have an appropriate thermal, hydrothermal, radiational stability and high hydrogen content; and add an inorganic boron source such as B_4C to

form a composite material. Table 2-7 shows the amount of boron in current B_4C/Al_2O_3 system.

Finding synthetic polymers that satisfy these criteria is a challenge. Most polymeric materials contain a sensitive organic part, which will decompose easily by oxidation and chain scission in the high temperature environment. Aside from the proper thermal stability at the range of 350-600°C in the core for a single cycle, which can range from 1 to 2 years, the hydrothermal stability at the near-critical water (350°C, 20.7MPa) is required because water may possibly penetrate inside the burnable poison rod by the failure of the zircaloy cladding. If this occurs, the polymeric materials should not decompose or melt and cannot lose boron from the polymer matrix to stay under safe nuclear reaction condition.

Moreover, it is also necessary to have high hydrogen content in polymeric materials as burnable poison materials to magnify the moderation effect. The hydrogen content can best be expressed in terms of the number of hydrogen atoms per unit volume for comparing the moderation effect. The density of water in PWR (320°C, 13.8MPa) will decrease because water expands; therefore the number of hydrogen atom also decreases as temperature and pressure increase. The density of water and the number of hydrogen at 335°C and 13.8MPa are 0.625g/cc and 418.0 x 10^{20} atoms/cc respectively. Therefore, the hydrogen content in PWR (320°C, 13.8MPa) will be higher than that in water (335°C, 13.8MPa). It is recommended to have at least 418.0 x 10^{20} atoms/cc of hydrogen atoms in polymer structures to give same moderation effect as water does in PWRs [28]. The hydrogen content of most polymeric material used in this study was higher than that of the moderator in PWR (320°C, 13.8MPa) as shown in Table 2-8. Cross-linked

polyethylene contains the highest amount of hydrogen atoms in the lists. The values are theoretical and depend on actual densities at the operating temperature. Some portion of hydrogen atoms may be released from polymer structure by radiolysis and thermolysis in the severe PWR operating condition. To monitor the exact amount of hydrogen atoms, it is necessary to use elemental analysis during the curing process.

In addition, thermal conductivity and radiation stability should also be considered to apply polymeric materials in BPRAs. Heat generated within the BPRA can be modeled using an MCNP energy deposition tally. The centerline temperature rise was calculated and the expected centerline temperature in various BPRA materials is shown in Table 2-9 [5]. A current B_4C/Al_2O_3 system has a maximum 440.41°C centerline temperature. However, high density PE showed > 600°C maximum centerline temperature. This temperature strongly depends on the thermal conductivity of materials. Many polymeric materials are used as insulators due to the low thermal conductivity. However, the introduction of graphite would increase the thermal conductivity and decrease the centerline temperature in BPRAs. The composite system may additionally provide the improvement of thermal stability of cross-linked HDPE.

Several types of radiation such as gamma ray, thermal neutron, and fast neutron occur in nuclear reactors. When this high-energy radiation passes through matter, a strong interaction occurs within the nucleus or within the orbital electrons resulting in the dissipation of a large portion of the incidental energy. The final result of such interaction in polymeric materials is the formation of ions and radicals followed by rupture of chemical bonds. Concurrently, new bonds are formed, followed by crosslinking and degradation at different rates. It is important to understand how many hydrogen atoms

would be knocked out under this condition because of the potential for hydriding of the zircaloy cladding and eventually the failure of the system.

2.5 A Behavior of Polymeric Material in Near- and Supercritical Water

2.5.1 Definition of Near Supercritical Water (350 °C, 20.7Mpa)

Water under high pressure and temperature conditions near and above its critical point (374 °C, 22.1MPa) is typically referred to as supercritical water. Conditions slightly lower than the critical point of water are generally referred to as subcritical water.

Autoclave test performed in our study were at 350°C and 20.7MPa, as shown in Figure 2-5. The region can be termed "near supercritical water" because the temperature is just below the critical point (T=374 °C, P=22.1MPa). The ion product, or dissociation constant (K_w) in this region (light gray), representing H^+ and OH^- ion concentration of water goes through maximum, which is about three orders magnitude higher than it is in ambient water. In fact, the dissociation of water itself in this condition generates a sufficiently high concentration that some acid-catalyzed organic reactions occur without any added acid. As a result, water behaves like many organic solvents in that it has high solubility with many organic compounds. Under these conditions, water has the ability to hydrolyze many compounds catalyzed by H^+ and OH^- ions or to dissolve organic substances that can provide a homogeneous phase. The dielectric constant is one of the most relevant physico-chemical properties for defining the solubility in fluids [30]. Therefore, the comparatively high ionic product under pressure and its quite low dielectric constant enhance organic compound dissolution by greater hydrolysis reactions.

In addition to ion concentration, water near the critical point shows different properties. Due to the large compressibility of supercritical water, small changes in pressure can produce very substantial change in density, which, in turn, affect viscosity,

diffusivity, dielectric, and solvation properties. The dielectric constant and density are much lower. The number and persistence of hydrogen bonds are both diminished. Diffusivity of water in supercritical water is much higher than for ambient water and they can readily penetrate porous and fibrous solids. Figure 2-6 depicted ionic product, density, and dielectric constant at near or supercritical water [31]. The gray color representing high ionic product and relatively low dielectric constant is our exact experimental region performed in this study. However, as exceeded the critical point, ionic constant rapidly decreases as shown in Figure 2-6. For example, ionic constant is about 12 orders of magnitude lower at 600°C and 24MPa than it is at the autoclave condition (350°C/20.7MPa) used in this study. Therefore, supercritical water at 600°C and 24MPa is a poor medium for ionic chemistry.

2.5.2 Polymer Recycling by Using Near- and Supercritical Water

In recent years, near- and supercritical water has been used as an inexpensive, nontoxic and nonpolar solvent for the chemical recycling of polymer waters. Separation and reaction process that utilize near- and supercritical water as a solvent is recently concerned due to its efficient and clean technology for recovery of fuels and chemicals from plastic wastes. Using near-critical or supercritical water instead of organic solvents in chemical processes offers environmental advantages and my lead to pollution prevention.

Near- or supercritical water is known as a good solvent and a reaction medium for the chemical recycling of polymer wastes. Connolly et al. published the first data on hydrocarbon solubilities in water at near-critical condition [32]. It was shown that water is completely miscible with a number of hydrocarbons, including pentane, heptane, benzene, and toluene. Under this condition, some hydrocarbon decomposition and condensation

reactions occurred without adding air or other potential oxidizers. Adschiri et al. also found that many polymers consisting of high molecular hydrocarbon could decompose to liquid product or to their monomers in the presence of high-temperature and high-pressure water [8]. The conversion appears to be most effective in the supercritical region (T>374 °C, P>22.1MPa). In the supercritical region, water achieves a highly compressible condition and further, the changes in physical properties of water allow it to dissolve many higher molecular weight hydrocarbons. For cellulose [33,34], poly (ethylene terephthalate) (PET) [35,36], nylon-66 [37-39], and other polymers [21,40-43], 100% liquid yield or 100% conversion with very low gas yield are obtained without catalysts under sub or supercritical water.

However, thermosetting resins are one of the most difficult substances to decompose. Their highly cross-linked structures improve chemical and thermal resistances [44]. They do not melt or cannot be depolymerized easily. Sugeta et al. showed that phenolic resin used as a matrix of fiber-reinforced plastics did not decompose under supercritical water at 380°C [21]. Suzuki et al. also confirmed that the decomposition of molding materials of phenolic resin started in supercritical water at 430°C into their monomers [41]. These are the main reasons in selecting thermosetting resins as candidate materials, such as phenolic resin, epoxy resin, silicone resin and cross-linked HDPE in this study.

Fang et al., Sasaki et al., Arai et al. and Smith et al. have studied phase behavior and reaction phenomena of polymer plus water systems [7-9,33,34,37,45]. In their work, a homogeneous phase was found for condensation polymer (polyethylene terephthalate, nylon) and cellulose in subcritical water. However, polyethylene could dissolve in

supercritical water only after it decomposed above 565°C [45]. Sako et al. also reported that the polyethylene main chain was stable at supercritical condition (380°C) [22]. Moriya et al. represented that the rate of supercritical water cracking in polyethylene is quite lower than that of thermal cracking [23]. They explained these phenomena because the water molecules intervene between the active molecules formed from the decomposition of HDPE. These indications have challenged us to fabricate the cross-linked structure by using hydrothermally stable polyethylene linkages that would survive in severe autoclave condition.

2.6 Polymer Degradation

It is important to understand the degradation mechanism of polymeric materials in this study. The degradation mechanism will be different as the circumstance where they are placed such as air, inert gas, water and vacuum etc. The interaction between the specimen and the medium will be treated and discussed in detail. Generally, the terms of polymer degradation is used to represent changes in physical properties caused both by chemical reactions, involving bond scission in the backbone of the macromolecules. It is useful to subdivide polymer degradation in terms of its various modes of initiation into thermal, mechanical, photochemical, radiation chemical, biological and chemical degradation [46,47]. In this study, we are more concerned about thermal, radiation chemical, and chemical degradation and will be treated in some detail.

2.6.1 Thermal Degradation

Polymers consisting of organic macromolecules are stable only below a certain limiting temperature range usually from 100°C to 200°C, in special cases a few hundred °C higher. If the temperature is increased to 1000°C or higher, organic molecules decompose into small fragments (free radical, free ions, H_2, CO etc). The rather high

thermal stability of organic substances derived from the fact that molecules are composed of atoms linked by covalent bonds. The strength of these bonds is limited. Dissociation energies of single bonds in the ground state are in the order of 150 ~ 400 kJ per mol at 25°C (e.g. O—O : 147, C—H : 320 ~ 420, C—C : 260 ~ 400, C—O : 330 kJ/mol). The bond breakage occur when the absorption of sufficient energy exceeds the dissociate energy of the single bonds at temperatures higher than 400 to 600°C.

In this study, we are concerned on finding polymeric materials with a high heat distortion temperature for the use of high temperature range in BPRAs. There are several routes to increase the heat stability: (a) Increase of the degree of crystallinity, (b) Incorporation of polar side groups, (c) Incorporation of aromatic and heteroaromatic ring, (d) Intermolecular chemical crosslinking, (f) Inorganic-organic hybrids.

The effect of (a) and (b) to increase the thermal stability is relatively smaller that that of (c), (d), and (f). However, we have selected polyethylene (HDPE) rather than other polyolefins because the influence of branching on thermal stability of polyolefins is negative as considering the thermal stability (PE > PP > branched PE > PIB). High-density polyethylene (HDPE) contains higher concentration of crystallinity than low-density polyethylene (LDPE). HDPE also showed the high thermal conductivity.

The attainment of chemical resistance at high temperatures was based essentially on the idea of avoiding chemical structures with weak linkages or sites possessing a strong tendency for rearrangement. Further criteria of importance of chemical stability concern resonance stabilization and structures with unstrained bond angles. Since occasional ruptures of chemical bonds cannot be totally prevented, the breakdown of the chemical structure was expected to be retarded to a significant extent by using double or

multiple strand structures, such as ladder, cage and network structures. Poly(methylsilsesquioxane)s (PMSSQs) with empirical formula of $(CH_3SiO_{3/2})_x$ and Poly(diacetylene-siloxane-carborane), which contains carborane cage structure, have been investigated in this study for this reason. The use of thermosetting polymer in this study would also provide the improvement of thermal stability for the same reason. In other attempts to improve the thermal stability, the chemical structure of polymers was modified by substituting C and H atoms by atoms of other elements such as Si, P, B, and F. It was reported that siloxane-containing polymer showed a good thermal stability because their strong bond energy of Si-O bonds. In this study, PMSSQ and other siloxane containing polymers were selected for further investigation.

Poly (diacetylene-siloxane-carborane) is the promising material that could satisfy all above criteria. As mentioned, the incorporation of inorganic elements into an organic polymeric system has the potential for extending temperature limitations. Polysiloxanes possess high thermal stabilities, exhibit hydrophobicity, are flexible, and have low melting and softening point. Adding an acetylene linkage through addition reaction without the evolution of volatiles in this system provides to form conjugated polymeric cross-linked networks structure. Moreover, by adding a carborane unit ($HCB_{10}H_{10}CH$) having cage structure in this system improve further thermal stability and remarkable chemical and exhibit good protection against oxidative degradation.

2.6.2 Chemical Degradation (Hydrolysis)

The chemical degradation is devoted by chemical reactions, which start spontaneously when certain low molecular weight compounds, are brought in contact with polymers. This type of degradation will also be related with the hydrothermal degradation in near-critical water that is interested in this study. Commonly, the rate of

chemical reactions is strongly dependent on temperature, which implies the thermal and chemical overlapping processes. Thermal degradation can be distinguished from chemical degradation. Generally, solvolysis reactions concern the breaking of C-X bonds, X designating hetero (non-carbon) atoms such as O, N, P, S, Si or halogen. The primary interest for solvolysis reactions of polymers containing hetero atoms is main chain rupture as indicated by reaction (1).

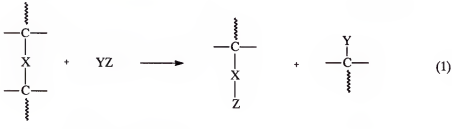

(1)

Common solvolysis agents (YZ) are water, alcohols, ammonia etc. For regarding polymer degradation hydrolysis (YZ=OH—H), water-soluble polymers (i.e., polysaccharides and cellulose) are good example that would be rather readily hydrolyzed. Generally, the mechanism prevailing in neutral or acidic media differs from that in alkaline media, as will be demonstrated here for an ester linkage.

At pH ≤ 7, hydrolysis is initiated by a protonation process (2) which is followed by the addition of H_2O and the cleavage of the ester linkage (3).

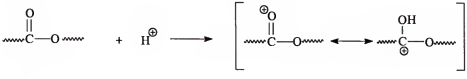

(2)

(3)

In alkaline condition, hydroxyl ions are attached to the carbonyl carbons. Subsequently ester linkages are ruptured, as illustrated for the case of polyester by the following reactions (4, 5).

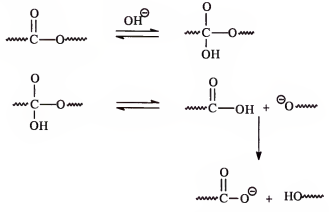

(4)

(5)

The autoclave tests performed in this study were 350°C and 20.7MPa. In this region, the ion product, or dissociation constant (K_w) representing H^+ and OH^- ion concentration of water goes through maximum. [30]. As a result, water in near-critical condition behaves like many organic solvents in that it has high solubility with many organic compounds.

2.6.3 Degradation by High-energy Radiation

When high-energy radiation [γ- and X-rays, neutron, electrons, protons, and deuterons] passes through matter, strong interaction occurs within the nucleus or within the orbital electrons resulting in the dissipation of a large portion of the incidental energy. The final result of such interaction in polymeric materials is the formation of ions and radicals followed by rupture of chemical bonds. Concurrently, new bonds are formed, followed by crosslinking and degradation at different rates. The rates of degradation are much lower for polymers containing aromatic rings because of resonance stabilization of the transient species. Generally, rigid molecular structures, i.e., thermoset materials are more resistant than flexible thermoplastic and elastomeric structures. Steric effects

contribute to the probability of ion- or radical recombination. Radiation resistance is usually improved by the addition of mineral fillers. The oxygen content of polymeric materials or the carbonyl content of cross-linked PEs has a considerable adverse effect on radiation resistance such as oxygen in phenolic resin. The main problem using polymeric material in nuclear radiation environment is primarily loss of mechanical strength and the evolution of gaseous by-products. This will also be critical problem to look at for new BPRA system.

2.7 Water Absorption

At the molecular level, a polymer surface consists of units such as $-CH_2-$, –CHO–, –CO– and aromatic rings, etc. Although crosslinking may make the polymer macroscopically quite rigid, at the molecular level, chain segments should have some mobility since they interact with geometrically adjacent segments by relatively weak forces of the van der Waals type [48]. At the molecular level, polyethylene surface should resemble that of a crystalline long chain alkane. In this point, it seems reasonable that the absorption of small molecules on molecular solids should give information relevant to the interaction potential between such molecules and a polymer surface. When a molecule such as hexane is placed in water, no appreciable hexane-water bonding occurs. Water only tries to interact with itself. Water forms a highly ordered structure (clatherate) around hexane molecules [48]. Even for cross-linked PE in water, the water incorporated in PE is mostly in the form of isolated molecules. [49]. In this case, it is difficult to expect any hydrolysis reaction at this condition. This is why polyolefins such as PE, PP, PIB and PS have low water absorption value as shown in Table 2-10 [50]. However, polymers synthesized by a condensation reaction with removing of water can be hydrolyzed in water. They contain water sensitive functional groups such as amide, imide, and ester

could be depolymerized reversibly with the route of hydrolysis reaction and more vigorous reaction will occur under near-critical water condition. Polytetrafluoroethylene (PTFE) has zero of water absorption and there was no weight loss after the autoclave test ($350^{\circ}C$/20.7MPa/24h) in our experiment. PTFE was not discussed in detail because of the depletion of hydrogen concentration. However, it showed excellent hydrothermal stability because the bulky structure of fluorine hardly make water molecules attack into the polymer specimen as well as hydrophobicity of fluorine also take greater role to improve hydrothermal stability.

Most water insoluble polymers are attacked very slowly by hydrolysis reaction. In this case, the occurrence of the reaction is restricted to the surface of the specimen and the ability of the polymer to absorb water. However, polymeric materials having the large amount of water absorption in the structure might be degraded easily under near-critical water condition. Therefore, water uptake property on polymeric material was a good parameter to be concerned about screening candidate materials in this study.

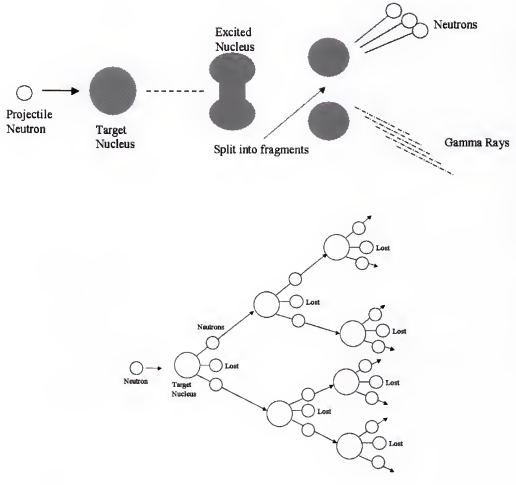

Figure 2-1. Nuclear fission and fission chain reactions [24].

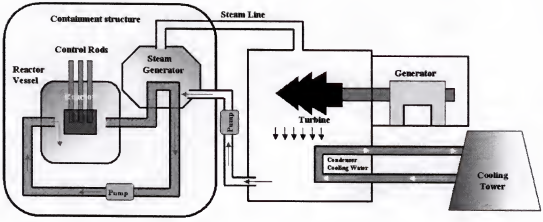

Figure 2-2. Pressurized water reactors (PWRs).

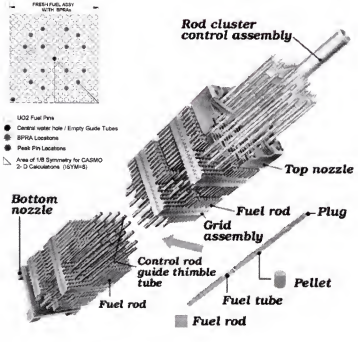

Figure 2-3. PWR Fuel rod assemblies and BPRA locations [5].

Table 2-1. Primary components and main materials of nuclear fission reactors [25].

Primary Component	Main Materials
(1) Nuclear fuel	Uranium oxide, plutonium oxide
(2) Structure	Zirconium alloys, mild steel, stainless steels, nickel alloys
(3) (a) Moderator and reflector (thermal reactors) (b) Blanket and reflector (fast reactors)	Graphite, heavy and light water, beryllium Depleted uranium, thorium, beryllium, graphite
(4) Control elements	Boron carbide, calcium, hafnium, boric acid, burnable absorbers
(5) Coolant	He, CO_2, light water, heavy water, liquid metals (NaK, Na)
(6) Shield	Light, medium, and heavy elements or components
(7) Safety systems	Pressure suppression system, emergency core cooling system, instrument monitoring system

Table 2-2. Scattering properties of various nuclei [27].

Element	Mass No.	α	ξ	Collisions to 1 eV
Hydrogen	1	0	1.000	15
Deuterium	2	0.111	0.726	20
Beryllium	9	0.640	0.207	70
Carbon	12	0.716	0.158	92
Oxygen	16	0.779	0.120	121
Uranium	238	0.983	0.0083	1700

* $\alpha = \left(\frac{A-1}{A+1}\right)^2$ $E_{max} = E_1(1-\alpha)$, ξ=Average logarithmic energy decrement

Table 2-3. Properties of moderators at 20°C [27].

Element	Mass No.	ξ	Density (g/cc)	Epithermal σ_s(barns)	Σ_s (m^{-1})	$\xi\Sigma_s$ (m^{-1})
Ordinary water	18	0.93	1.0	42	140	128
Heavy water	20	0.51	1.0	10.5	35	18
Beryllium	9	0.207	1.10	6.1	75	16
Carbon	12	0.158	1.70	4.8	41	6.5

Table 2-4. Reactivity requirements for control mechanism in typical PWR [29].

Control Rod	0.07
Burnable Poison Rod	0.08
Chemical Shim	0.17
Total	0.32

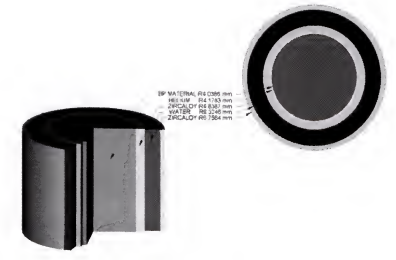

(a)

WATER R7 9579 mm
ZIRCALOY R6 3909 mm
HELIUM R5 3509 mm
BP MATERIAL R4 0386 mm
HELIUM R4 1183 mm
ZIRCALOY R4 8367 mm
WATER R5 3246 mm
ZIRCALOY R5 7964 mm

(b)

Figure 2-4. Two different burnable poison system (a) BPRA plan view and cross section. (b) WABA plan view and cross section [5].

Table 2-5. Properties of burnable poison systems [5].

Type	Advantages	Disadvantages
BPRA (B_4C-Al_2O_3)	-Inexpensive and easy to manufacture -Uniform boron distribution -Low swelling	-Some residual reactivity at EOC -Moderator displacement -Separate assembly creates an additional waste product
IFBA	-No moderator displacement penalty	-Helium gas produced by the burnup of boron adds to the fission gases inside the fuel rod and is a limiting criteria
Gd_2O_3-UO_2	-Gadolinium has a very high thermal neutron cross section -No moderator displacement penalty	-Reduces the melting point of uranium and thermal conductivity of the fuel -Daughter products have moderate cross sections for absorption
WABA	-Less excess reactivity because the annular design allows moderator to flow through the center of the rod enhancing boron burnup -A 21% smaller moderator displacement penalty than a BPRA	-Cost of manufacture for the annular design -Sill results in some moderator displacement

Table 2-6. Essential properties to be used for BPRAs [6].

- The material must contain adequate boron to control the excessive neutron and reactivity.
- The material must be thermally stable at 350-600°C in the core for a single cycle, which can range from 1 to 2 years *(or >600°C if the neutron adsorption energy release and low polymer thermal conductivity are considered).*
- The material must not dissolve or decompose if exposed to hydrothermal conditions of reactor *(350°C/20.7MPa in water in the event if clad failure).*
- The material should contain at least 5% of hydrogen to have an economic benefit.
- The material must be shapeable or moldable to conform to the shape of its containment.
- The material must be stable against breakdown into volatile species such as hydrogen in the radiation environment of a reactor core such as clad hydriding problems.
- The material must have adequate thermal conductivity to maintain equilibrium temperature during neutron adsorption.

Table 2-7. Weight percent of different elements in B_4C/Al_2O_3 [5].

Element	w%
Boron (natural)	2.77%
Carbon	0.76%
Aluminum	51.04%
Oxygen	45.43%

Table 2-8. Estimating the number of H atoms/cc.

Polymer	Mw (g/mol)	Density (g/cc)	H (10^{20} atoms/cc)
Poly (carborane-siloxane-acetylene)	454.8	1.0	448.8
Phenolic resin (resol type)	941.0	1.25	430.8
Polyborosilazane	333.8	1.0	595.1
Crosslinked Polyethylene	-	0.96	825.6
Ordinary water	-	1.0	670.0
Water at 335°C, 13.8 MPa	-	0.625	418.0
Water at 368°C, 20.7 MPa	-	0.467	312.2

*$N=\left(\sigma\frac{N_A}{M}\right)$, m=molecular atomic density(atoms/cc), ρ=mass density of the compound(g/cc), M=molecular weight of the compound, N_A=Avogadro's Number (atoms/mol)

Table 2-9. Evaluated data for centerline temperature in various BPRA materials [5].

	Thermal conductivity [W/cm °K]	Max difference between T_{MOD} and T_{CL} for BP rod [°C]	Linear q^1 value from MCNP [°C]	Linear q^1 value from Framatome [°C]
High density PE	0.0046	483.81	483.81	659.07
B_4C/Al_2O_3	0.02	63.46	393.46	449.41
Alumina	0.118	15.87	325.87	397.40

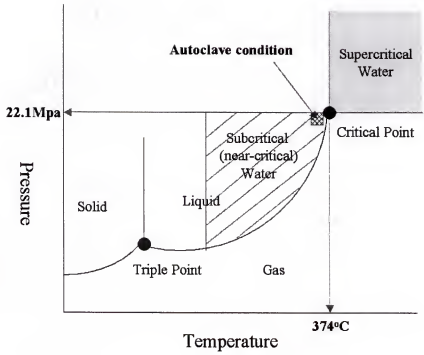

Figure 2-5. Phase diagram of supercritical water.

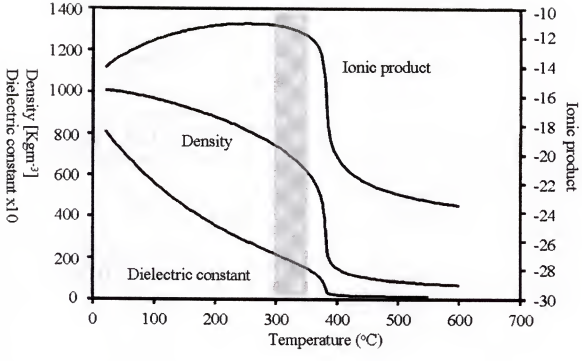

Figure 2-6. Ionic product, density, and dielectric constant of water versus temperature at a pressure of 24 MPa [31].

Table 2-10. Water absorption of various polymers [50].

Polymeric Material	Abbreviation	Water Absorption (mg in 24h) ASTM D570
Thermoplastic		
Low Density Polyethylene	LDPE	< 0.01
High Density Polyethylene	HDPE	< 0.01
Polypropylene	PP	0.01-0.03
Polyisobutylene	PIB	< 0.01
General Purpose Polystyrene	GPPS	0.03-0.1
Unplasticized Polyvinyl Chloride	RPVC	0.04-0.4
Polytetrafluoroethylene	PTFE	0
Polyimide	*PI*	*0.32*
Polyamide 66	*PA-66*	*1.5*
Polyethylene Terephthalate	*PET*	*0.3*
Thermoset		
Phenol-Formaldehyde (Phenolic Resin)	*PF*	*0.3-1.2*
Silicone Molding Compound	*Si*	*0.02*
Epoxy Resin	*EP*	*0.05-0.2*
Thermoset vs. Thermoplastic		
Polyurethane Thermoset	PUR	0.1-0.2
Polyurethane Thermoplastic Elastomer	PU	0.7-0.9

CHAPTER 3
POLY (DIACETYLENE-SILOXANE-CARBORANE): A POTENTIAL CANDIDATE POLYMERIC MATERIAL FOR BURNABLE POISON ROD ASSEMBLIES (BPRAS) IN PRESSURIZED WATER REACTORS (PWRS)

3.1 Introduction

Finding the synthetic polymers that satisfy these criteria is difficult. However, it is of interest to us to apply "carborane based polymers", which exhibits appreciable enhancement of thermal stability due to their cage structures [51-53]. Keller et al. introduced poly (diacetylene-siloxane-carborane)s (Figure 3-1), which are inorganic-organic hybrid polymers, shown to be thermally stable up to 1,000^{0}C and can be easily processed into shaped configurations. Besides "carborane cage structures", these polymers include "siloxanes" possessing good thermal and oxidative stability and high hydrophobicity. Incorporating inorganic elements, such as boron and silicon, into organic based polymers shows better thermo-oxidative stability relative to carbon [16]. Acetylenic units in the structure provide crosslinking and increases thermal stability. During reaction by heat treatment, a conjugated crosslinking structure is formed by 1,4-addition polymerization [54,55]. Figure 3-2 shows the schematic procedure for the synthesis of poly (diacetylene-siloxane-carborane)s and their processing.

Poly (diacetylene-siloxane-carborane)s are the starting material to develop new polymer based BPRAs system [6]. Poly (diacetylene-siloxane-carborane)s are considered in this application due to high thermal stability, high hydrogen content, their easy processing, and boron content [11-20]. This material substitution reduces the water displacement penalty at the end of cycle (EOC) and another added benefit is that near

EOC, carborane causes a shift in the neutron spectrum from the harder-B_4C-Al_2O_3 matrix spectrum to the soft spectrum of hydrogen in the carborane matrix assembly [5]. This gives rise to a longer fuel cycle due to the extra moderation from hydrogen in the BPRA at EOC.

Poly (diacetylene-siloxane-carborane) was synthesized by using the exactly same method as reported by Keller et al. [11,12]. This chapter discusses thermal properties of poly (diacetylene-siloxane-carborane)s by thermogravimetric analysis (TGA) and differential scanning calorimetry (DSC). Autoclave test was also performed to verify the hydrothermal stability at near-critical water condition (350°C/20.7MPa). The curing condition was optimized to monitor the hydrothermal stability and hydrogen content of the sample under the autoclave.

3.2 Experimental

3.2.1 Synthesis of Poly (diacetylene-siloxane-carborane)

All of the monomers were handled without air contact and stored in a moisture-free environment. 1,7-bis(chlorotetramethyldisiloxy)-m-carborane was purchased from Dexil Corporation. The anhydrous tetrahydrofuran (THF, 99.9%) and anhydrous diethyl ether (Et_2O, 99.5%) were used as received from Acros Organics. N-butyllithium (2.5M in hexane) and Hexachlorobutadiene were also obtained from Acros Organics and used without further purifications.

All syntheses were performed under an atmosphere of dry argon utilizing standard Schlenk techniques in order to prevent contact with oxygen or water. A syringe was used to make injections into the reactor during chemical transfers. A 100mL three necked

round bottom flask was equipped with a stir bar, gas inlet tube and thermometer. The bath was cooled down to -78°C by adding a dry ice/acetone as shown in Figure 3-3.

The synthesis of poly (diacetylene-siloxane-carborane) is a one-pot, two stage reaction. THF (8mL) was injected into a 100mL round bottom flask, connected to an argon source and cooled in a dry ice/acetone bath. N-butyllithium (10.6mL, 26.5mmol) was then added slowly and stirred for 5 minutes. Subsequently, hexachlorobutadiene (0.99mL, 6.3mmol) was introduced dropwise via syringe and stirred for 5-10 minutes at -78°C. After complete addition, the cold bath was removed and the mixture was stirred at room temperature for 2 hours. A dark brown 1,4-dilithio-1,3-butadiyne mixture was generated as shown in Figure 3-4. 1,4-dilithio-1,3-butadiyne was again cooled in a dry ice/acetone. Subsequently, equal amount of 1,7-bis(chlorotetramethyldisiloxy)-m-carborane (2.86mL, 6.3mmol) was injected via syringe and reacted to generate the linear poly (diacetylene-siloxane-carborane). After addition of 1,7-bis(chlorotetramethyldisiloxy)-m-carborane, the mixture was stirred at room temperature for 2 hours. The reaction mixture was then poured into dilute hydrochloric acid in 250mL separatory funnel and extracted with diethyl ether. The resulting two-phase mixture was separated. The dark organic phase (ethereal extract) was poured into an Erlenmeyer flask and dried over anhydrous sodium sulfate. Filtration into a round-bottom flask was followed by rotary evaporation. The rest of ether or THF was removed at room temperature for 5 hours to afford a dark brown and dried out in vacuum oven for overnight. The synthesis was performed three times and the yield of a viscous liquid polymer was with the average 85%.

3.2.2 Characterizations

The structure of poly (diacetylene-siloxane-carborane) synthesized in Figure 3-4 was confirmed by Fourier transform infrared spectroscopy (FTIR) and ^{1}H, ^{13}C - Nuclear magnetic resonance spectroscopy (NMR) (Gemini 300). The curing condition was monitored by both differential scanning calorimeter (DSC) and FTIR. Thermal stability and weight loss at elevated temperature was analyzed under an Ar atmosphere using a TGA2050 thermal gravimetric analyzer from TA instruments. The heating rate was 5°C/min. The flow rate was fixed at 130 mL/min and sample size was 5.00–10.00 mg. The degradation experiment in near-critical water (350°C/20.7MPa) was performed in a custom-built autoclave. The total charge of water was 50mL. The autoclave was maintained at 350°C for 24 hours. Each sample was run three times at the same condition and an average value was determined. The hydrogen content was measured by a conventional combustion technique, i.e., CHN Carlo Erba microanalyser. The chemical structure changes during cure, postcure, autoclave test were analyzed by transmission FTIR spectroscopy on a Nicolet MAGNA 760 Bench FTIR, equipped with a conventional DTS detector in the wave number range of 4000–600cm^{-1}. FTIR spectra were obtained from pellets containing 2 mg sample in approximately 100 mg potassium bromide (KBr). X-ray diffraction (XRD) measurements of the polymer and its pyrolyzed products were obtained with a Philips APD 3720 X-ray diffractometer using a Cu Kα source with a scan speed of 0.05 degree per second. The experimental density of the composites was obtained by the Archimedian method of weighing small pieces cut from first in air and then in water. The morphology of fracture surface and top layer was examined by field emission scanning electron microscope (FESEM). The composition in

the specimen was analyzed by scanning electron microscopy with an energy dispersive X-ray spectrometer (EDX).

3.3 Results and Discussion

The chemical structure of poly (diacetylene-siloxane-carborane) synthesized in this study was confirmed by both FTIR and NMR (^{1}H, ^{13}C) spectroscopy. From FTIR spectra of original viscous liquid poly (diacetylene-siloxane-carborane), the presence of prominent peak of C-H, B-H, C-Si, Si-O and diacetylene was observed as shown in Figure 3-5a. ^{1}H and ^{13}C NMR spectra also confirmed the chemical structures of original polymer as shown in Figure 3-6a,b.

Diacetylenes in viscous original polymer are known to undergo crosslinking reactions on exposure to heat or irradiation, which can be converted into a thermoset. DSC analyses under argon revealed a strong exotherm with an onset between 300 and 400 °C centered at 347°C as shown in Figure 3-7. This exothermic transformation is related to a thermally induced crosslinking through the diacetylene groups that modify irreversibly the backbone of the starting material. The integral under the DSC curve yielded the heat of reaction, which amounts to 285 $J \cdot g^{-1}$. A shiny void-free dark brown solid (thermoset) was produced by thermally curing at 350°C for 4 hours. The occurrence of curing reaction was monitored by FTIR. As shown in Figure 3-5b, the absorption band characteristic of $C \equiv C$ transition peak at 2070 cm^{-1} had completely disappeared.

Polymers that contain the crosslinkable acetylene moiety as a pendant functional group have been reported [11,13,55,56]. The incorporation of the acetylene group enhanced the thermal stability of respective polymers. The increase in thermal stability is believed to be due to generation of a cross-linked material. Corriu et al. have studied the evidence of

1,4- addition polymerization during crosslinking reaction of poly (dimethylsilylene-diacetylene). They suggested that cross polymerization of this poly (diacetylene) proceeds via a solid-state 1,4-addition reaction to generate mainly ene-yne and butatriene structures as shown in Figure 3-8 [54]. Poly (diacetylene-siloxane-carborane) synthesized in this study also showed that the IR spectrum of the cured sample exhibited three new absorptions at 2139 cm^{-1}, 1586 cm^{-1} and 1890 cm^{-1}, indicated of ene-yne and butariene structure respectively seen in Figure 3-5, thus of a 1,4-addition pathway. All other acetylene containing polymers, i.e., poly (diacetylene-siloxane), poly (diacetylenedimethylsilane) and poly (diacetylenedimethylsilylethane) synthesized in Chapter 4 also followed 1,4-addition crosslinking reaction.

The conversion of original viscous linear polymer to ceramic residues was shown in the TGA thermograms in Figure 3-9. This polymer gave high char yields when heated to 1,000°C under an argon atmosphere. The TGA trace showed that the weight loss was only 17.76% and occurred mainly between 450 and 700°C. This is the same result that Keller et al. reported [11,12].

In the first step, most of weight loss occurs between 200 and 400°C, which is mainly caused by the volatilization of residual solvents and unreacted monomers. The second step (400-700°C) is related to the extensive thermal degradation of the cross-linked material formed during the exothermic transformation of the diacetylene units. In this step, bond breakage and rearrangements and further networking occur with additional small molecule volatilization. Above 700°C, typically the chars are stabilized and no major loss is observed [12,15,18]. However, unexpectedly, this polymer showed additional 22w% weight loss around 1250°C as shown in Figure 3-9. This is a new finding that there

is a difficulty to apply this material at high temperature application. Elimination of CO corresponding to carbothermal reduction would be mainly coincident to the weight loss in this temperature region. The carbothermal reduction in an inert atmosphere follows the general equation shown below.

$$Oxide_{solid} + Carbon_{solid} \rightarrow Carbide_{solid} + CO_{gas}$$

This reduction is a negative reaction that the ceramic material produced from poly (diacetylene-siloxane-carborane) will give a limitation to apply in high temperature application (>1250°C). The samples pyrolyzed between 400°C and 1400°C under an argon atmosphere were analyzed with X-ray diffractometry. It appears that all samples had only a broad XRD peak consistent with disordered carbon and other disordered materials. No other peaks were detected in this temperature range.

Aside from the proper thermal stability at the range of 350-600°C in the core for a single cycle, which can range from 1 to 2 years, the hydrothermal stability at near-critical water condition (350°C/20.7MPa) is required because water might possibly penetrate inside the burnable poison rod by the failure of the zircaloy cladding. The material should not decompose or melt in order to stay under safe nuclear reaction.

Before running the autoclave test, all samples with different postcure temperature were prepared as shown in Table 3-1. We can expect to increase the thermal stability as performing the postcure treatment due to generating further network structures.

As shown in Table 3-1, all samples except S6, S9, S10 and S11, which were postcured above 600°C, were dissolved after the autoclave test. When preparing the postcured sample, the heating rate is important to minimize the thermal stress that induced the thermal shock as a result of changes in temperature. When the samples were

postcured at 600°C with 5°C/min of heating rate, they showed a surface crack and broke to pieces. However, the samples postcured with the heating rate 1°C/min did not break even though they had a slight surface crack.

After the autoclave test, S6, S9 and S10 postcured at 600°C showed about 30w% weight loss however, when postcuring at 700°C, S11 only showed less than 5% of weight loss. This result indicates that the structural change of thermoset polymer may occur between 450 and 700°C. Further network structure might form around 450°C, however as already discussed in previous section, a high weight loss occurred at this temperature region due to the extensive thermal degradation of the cross-linked material followed by bond breakage and rearrangements. Therefore, there are changes occurring at 700°C. Above 700°C, poly (diacetylene-siloxane-carborane) thermoset may change into ceramic material. Changes from 450 and 700°C are better followed by density measurement as shown in Table 3-1. Heating to 700°C resulted in 1.3011g/cm^3 density. A densification rapidly occurred around 700°C, which reflects the structural change from thermoset to ceramic material. This is the way that S11 is very stable at the autoclave condition. S6, S9 and S10 postcured at 600°C were not completely dissolved at the autoclave condition because they might possess the transitional structure between polymers and ceramics.

FTIR of samples heated at temperatures between 400°C and 700°C are in qualitative agreement with the above TGA results. Figure 3-10 shows the infrared spectra of poly (diacetylene-siloxane-carborane) pyrolyzed at (a) 400°C, (b) 600°C, and (c) 700°C, respectively. The presence of prominent peak of C-H, B-H, C=C, C-Si, and Si-O were exhibited below 600°C. However, all peaks were disappeared after pyrolyzing above 700°C.

Moreover, there are previous papers that have studied the degradation of Si-O-Si by the humidity. It was reported that polydimethylsiloxanes (PDMS) hydrolyzed predominantly through random scission of their Si-O-Si backbones in water environments [57]. Shim et al. also reported that the thermal depolymerization process of PDMS was enhanced under water vapor with high pressure [58,59]. This may be the reason that most samples postcured below 600°C in this study were dissolved after the autoclave test.

The bond energy of silicon-oxygen atoms in the PDMS is greater than that of the carbon-carbon bonds in various organic elastomers [60]. This property is contributed to higher thermal stability of silicon containing polymers. However, a water molecule is released from the condensation of the end groups of PDMS during the production of PDMS. An excess amount of water may accelerate a degradation reaction, that is, a reverse condensation reaction of PDMS [61]. In addition, the Si-O bond is quite sensitive to variety of reagents, including base and acid [62]. As explained in chapter 2, the dissociation of water itself at near-critical condition generates a sufficiently high concentration that some acid-catalyzed organic reactions occur without any added acid. Under these conditions, water enhances the ability to hydrolyze condensation polymers such as poly (ethylene terephthalate) [7,9] , nylon 66 [37-39], cellulous [33,34], polycarbonate [40], and polyurethane [63] catalyzed by H^+ and OH^- ions, and by hydrothermal cleavage with water molecules, and to dissolve organic substances that can provide a homogeneous phase for reactions. Figure 3-11 depicted the estimated degradation route of poly (diacetylene-siloxane-carborane) by hydrolysis reaction under near-critical water condition. FTIR test

has showed a good evidence to occur the reversible hydrolysis reaction at the autoclave condition.

The infrared spectrum of the product obtained under hydrothermal treatment at 350°C, 20.7MPa for 24 hours are presented Figure 3-12b. The new absorption band at around 3350 cm^{-1} ascribed to OH stretching vibrations was generated after the autoclave test. This result well explains the formation of –OH group under near-critical water condition due to the reversible hydrolysis reaction as depicted in Figure 3-11.

Scanning electron microscopy (SEM) showed all samples pyrolyzed at 400°C - 1400°C. As shown in Figure 3-13a,b, the samples postcured at 400°C and 600°C respectively showed a shiny void-free morphology on both top layer and fracture surface. The surface morphologies pyrolyzed with higher temperature at 700°C and 1000°C showed spherical particles (2-4μm) and occasional flat, triangle or hexagonal crystals as shown in Figure 3-13c,d. Keller et al. also reported the same morphology of top layer annealed at 900°C [15]. They explained that these spherical particles consisted of principally silicon dioxide and only a small amount of boron. This result is corresponding to that of our EDX experiment seen in Figure 3-14. Although it is unclear, the boron depletion of the outer layer is due to the oxygen originated in the polymer bulk or was an impurity in the argon atmosphere during the sample preparation. The spherical discontinuous top layers disappeared after pyrolyzing at 1400°C as shown in Figure 3-13e. This result is corresponding with that of TGA analysis that explained the severe weight loss due to the carbothermal reduction around 1250°C.

It is important to monitor hydrogen content during the postcure process to assure an adequate moderating benefit of the polymeric BPRAs. CHN analysis was performed

three times for each sample and the average value are shown in Table 3-2. The hydrogen content of poly (diacetylene-siloxane-carborane) is superior to that of water at near-critical water condition (350°C, 20.7Mpa) as explained in Chapter 2. It was one of advantages to use poly (diacetylene-siloxane-carborane) as a burnable poison material. When it consisted of polymeric structure with the high hydrogen content (thermoset), all samples were dissolved at the near-critical water. After passing through the organometallic-ceramic transition temperature, the sample pyrolyzed above 700°C survived at the autoclave test. However, as shown in Table 3-2, this material is already ceramic like that only contains 1.352w% hydrogen. There is no more an advantage to use this material for a new polymeric BPRA system because it is unlikely to expect the extra moderation effect due to the depletion of hydrogen concentration.

3.4 Summary

Poly (diacetylene-siloxane-carborane), which is a potential candidate polymeric material to be used for a new polymeric BPRA system, was introduced in this study. They are an inorganic-organic hybrid shown thermally stable up to 1,000°C, contain appropriate boron concentration and can be easily processed into shaped configuration to apply BPRAs. However, we found that the degradation of Si-O-Si was unfavorable disadvantage of poly (diacetylene-siloxane-carborane) under hydrothermal circumstance. Moreover, the hydrolysis reaction would be accelerated at the near-critical water condition (350°C, 20.7MPa) due to the characteristic properties of near-critical water such as high catalytic property of H^+ and OH^- ions, relatively low dielectric constant, and high diffusivity.

The very high cost (18,000 $/lb) and current limited supply of carboranes could wipe out any economic advantage for the utilization and development of polymers and

ceramics based on carborane units. Above 1250°C, the carbothermal reduction, which is a negative reaction, occurred. This is a new finding that the ceramic material produced from poly (diacetylene-siloxane-carborane)s would give a limitation to apply in high temperature application (>1250°C).

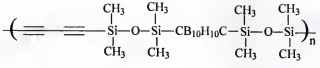

Figure 3-1. The chemical structure of poly (diacetylene-siloxane-carborane).

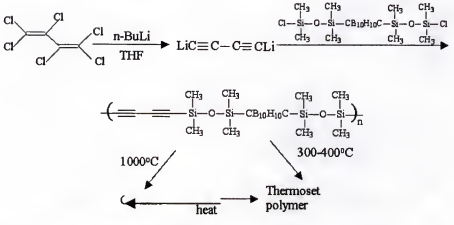

Figure 3-2. The synthesis and processing of poly (diacetylene-siloxane-carborane).

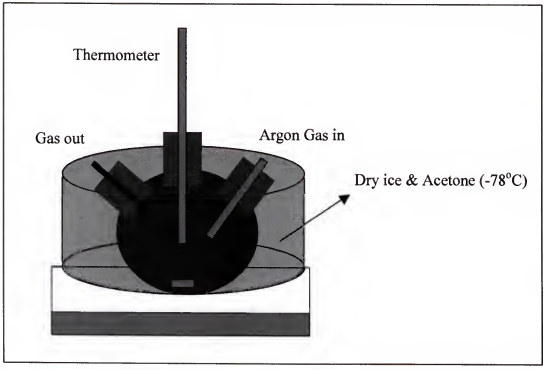

Figure 3-3. The synthesis apparatus.

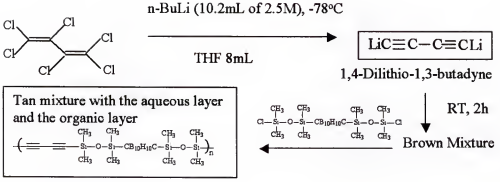

Figure 3-4. The synthesis steps.

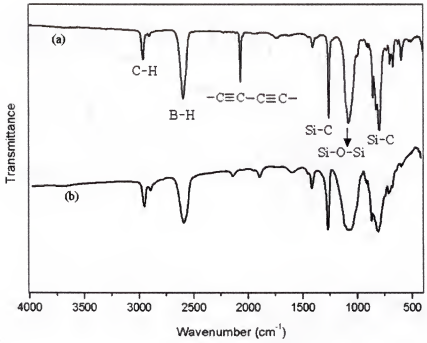

Figure 3-5. FTIR spectroscopy of (a) synthesized original viscous liquid poly (diacetylene-siloxane-carborane) (b) poly (diacetylene-siloxane-carborane) thermoset after curing at 350°C for 4 hours.

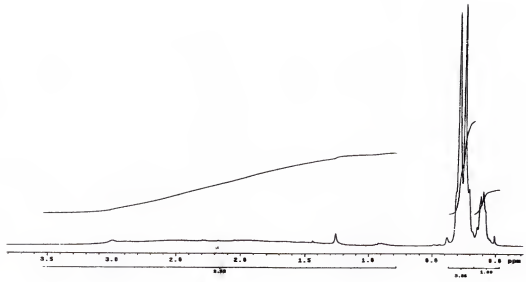

(a)

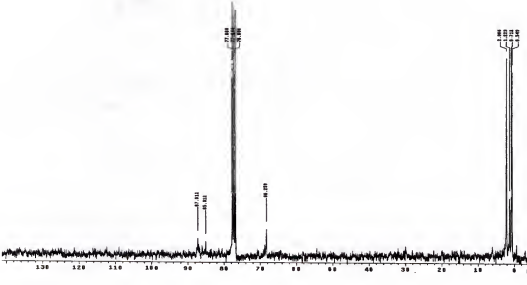

(b)

Figure 3-6. NMR spectroscopy of synthesized original viscous liquid poly (diacetylene-siloxane-carborane) (a)^{1}H NMR Spectroscopy ($CDCl_3$): 0.1, 0.3(24H, Si-CH_3), 0.8-3.5(broad,10H, B-H), (b)^{13}C NMR Spectroscopy ($CDCl_3$) : 0.549 (Si-C), 68.259(Si-C-B).

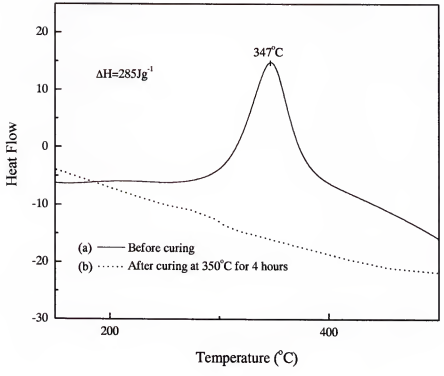

Figure 3-7. DSC scans showing cure exotherms of original polymer.

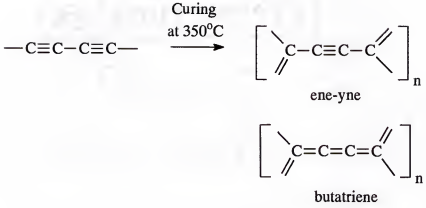

Figure 3-8. Chemical structures of ene-yne and butatriene [54].

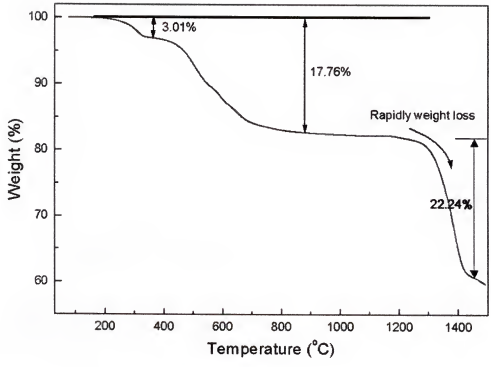

Figure 3-9. TGA thermograms of poly (diacetylene-siloxane-carborane) under an Ar atmosphere.

Table 3-1. Cure and postcure condition for various samples.

Sample	Cure condition*	Postcure condition*	Heating rate	Density	Sample status after postcure	Autoclave test
S1	300°C, 2h	None	5°C/min		Good	Dissolved
S2	350°C, 2h	None	5°C/min	1.0212	Good	Dissolved
S3	400°C, 2h	None	5°C/min		Good	Dissolved
S4	350°C, 4h	400°C, 1h	5°C/min		Good	Dissolved
S5	350°C, 8h	400°C, 2h	5°C/min		Good	Dissolved
S6	500°C, 3h	600°C, 1h	5°C/min		Break to pieces	26w% weight loss
S7	350°C, 4h	400°C, 2h	1°C/min		Good	Dissolved
S8	350°C, 4h	500°C, 2h	1°C/min	1.0387	Good	Dissolved
S9	350°C, 4h	600°C, 2h	1°C/min	1.0450	Slight surface crack	28w% weight loss
S10	400°C, 4h	600°C, 1h	1°C/min	1.0524	Slight surface crack	29w% weight loss
S11	400°C, 4h	700°C, 1h	1°C/min	1.3011	Break to pieces	No weight loss

* Temperature and isothermal period

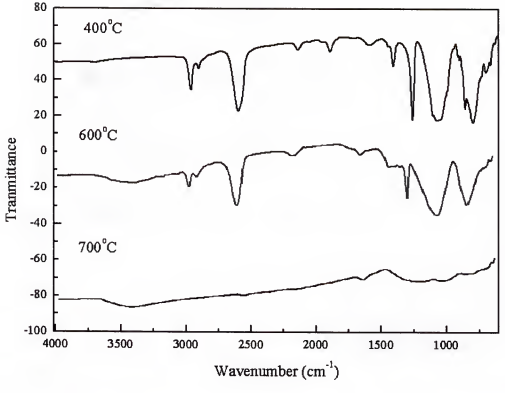

Figure 3-10. FTIR spectroscopy of poly (diacetylene-siloxane-carborane) with different postcuring temperatures (a) 400°C (b) 600°C (c) 700°C.

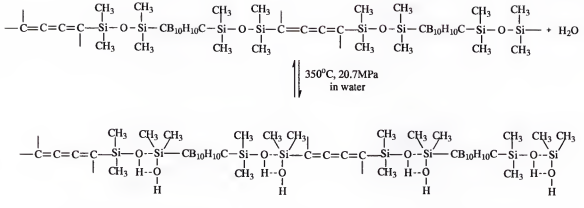

Figure 3-11. An estimated hydrolysis reaction of poly (diacetylene-siloxane-carborane) under near-critical water conditions.

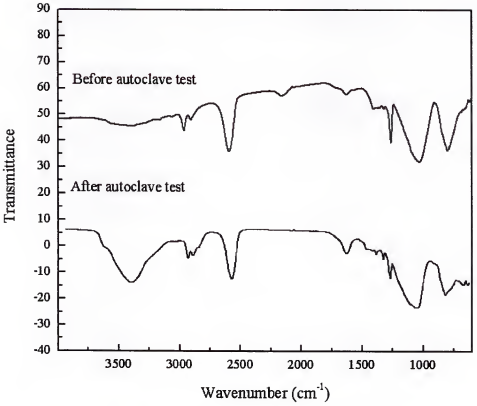

Figure 3-12. FTIR spectroscopy of poly (diacetylene-siloxane-carborane) with heat treatment (400°C, 2h & 600°C, 1h) (a) before autoclave test (b) after autoclave test.

Table 3-2. Hydrogen content.

CONDITION	H (W %)
Theoretical value	7.500
Original polymer	7.030
Curing at 400°C 2h & 600°C 1h Density = 1.0524	4.067
Curing at 400°C 2h & 700°C 1h Density = 1.3011	1.352

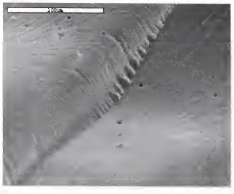

(a) 400°C

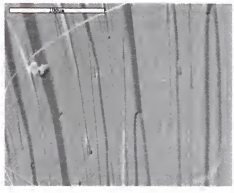

(b) 600°C

(c) 700°C

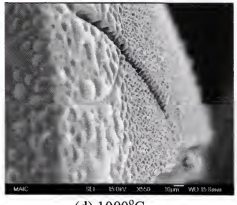

(d) 1000°C

(d) 1400°C

Figure 3-13. SEM of poly (diacetylene-siloxane-carborane) with different annealing temperature (a), (b): fracture surface, (c), (d), (e): top surface.

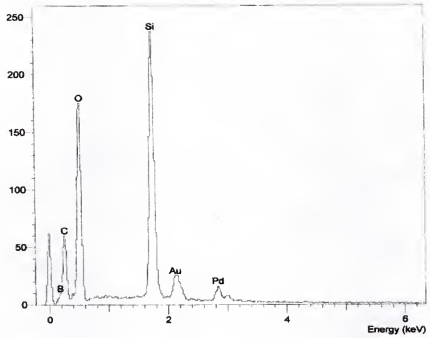

Figure 3-14. EDX of spherical particles which appeared on the top layer pyrolyzed at 1000°C.

CHAPTER 4
INTRODUCTION OF SILICON BASED POLYMERS TO POLY (DIACETYLENE-SILOXANE-CARBORANE): THEIR THERMAL & HYDROTHERMAL STABILITY

4.1 Introduction of Poly(diacetylene-siloxane) to Poly(diacetylene-siloxane-carborane)

In Chapter 3, the use of poly (diacetylene-siloxane-carborane) as a new burnable poison material was proposed due to its outstanding thermal stability, high hydrogen content, as well as the boron concentration in polymeric structures [11-13,15,17-19]. However, we found that the degradation of Si-O-Si under near-critical condition (350°C, 20.7MPa) was an unfavorable disadvantage to use in BPRAs [57]. A high cost (18,000$/lb) and current limited supply of carboranes could give rise to difficulties for the utilization and development of polymers and ceramics based on carborane units. Moreover, this material has some technological challenges that must be addressed. The boron content in poly (diacetylene-siloxane-carborane) is 23.8w% and it is too high as comparing with the current Al_2O_3/B_4C system (2.77w%). The boron content of poly (diacetylene-siloxane-carborane) should be diluted to keep same neutron capture capability as in the B_4C/Al_2O_3 system. This problem will be overcome by introducing more $(CH_3)_2SiO$ moieties or other silicon based polymers.

More importantly, the introduction of $(CH_3)_2SiO$ moieties or other silicon based polymers onto poly (diacetylene-siloxane-carborane) could be the most cost-effective method to solve the problem related to the extremely high cost and current limited supply of the carboranes based precursors.

It was reported that poly (diacetylene-siloxane-carborane) (DSCS) had excellent thermo-oxidative stability and a tough residue after curing. However, this cured resin showed a relatively low T_g (94°C) due to high flexibility of carborane-siloxane linkage [18]. Keller et al. [18] incorporated Poly (diacetylene-siloxane) (DS) polymer onto DSCS polymer to optimize thermo-oxidative stability and toughness of the DSCS thermoset and increase the glass transition of the DSCS thermoset. The schematic chemical structure of DS thermoset is presented in Figure 4-1. It was shown that both 90/10 and 50/50 of DS/DSCS random copolymer cured to a thermoset did not undergo T_g below 350°C as indicated in Table 4-1 and showed better thermal stability. Less than 0.5 % weight loss at the operating temperature (340°C) of PWRs was observed for both the 90/10 and the 50/50 of DS/DSCS [18].

There are several advantages to use high DS systems [12-14,18,64,65]:

(a) The rigid, highly cross-linked copolymer by short single siloxane repeats unit increase the glass transition temperature (T_g) (Table 4-1).

(b) The crosslinking density of DS is twice than that of DSCS.

(c) They are easy to fabricate and control the boron content. The current B_4C/Al_2O_3 system contains 2.77w% of boron. To make the same boron content in DS/DSCS system, 5.23w% of DSCS is necessary to keep the same neutron capture capability as in the B_4C/Al_2O_3 system.

(d) They are cost effective. The incorporation of DS can significantly reduce the cost less than 10% of original DSCS as explained in Table 4-2. It may be possible to reduce the cost still further by adding 3.53 w% of B_4C as a boron source instead of the expensive and scarce DSCS. From the above result, we can calculate hydrogen and boron

content in both DSCS and DS as shown in Table 4-3. The exact hydrogen content for 5.23w% of the DSCS and 94.77w% of the DC will be 6.71w%.

DS thermosets are highly cross-linked with diacetylene groups reacted to form stiff bulky crosslink with extended conjugation. The only source of flexibility is the short (Si-O-Si) backbone sequence between rigid crosslinking sites and crosslinking density of DS is twice than that of DSCS. A much higher T_g can be expected. DS/DSCS copolymer representing high T_g above the operating temperature (350°C) would have an opportunity to study its hydrothermal stability at the near-critical water.

In this study, thermal and hydrothermal stability of DS thermoset were observed. The potential hydrolysis degradation of the extra Si-O-Si moieties under subcritical water conditions of a PWR could prove to be a disadvantage for use in BPRAs as reported in previous Chapter 3. However, it would be expected that the highly cross-linked DS thermoset might improve the hydrothermal stability of the material.

4.1.1 Experimental

4.1.1.1 Sample preparation

All reactions are performed under an Ar gas using standard Schlenk line techniques. Tetrahydrofuran(8mL) was injected into a flame-dried 100mL round bottom flask, connected to an argon source. N-butyllithium (10.2mL of a 2.5 hexane solution, 26.4mmol) was added slowly and stirred for 5min. Hexachlorobutadiene (1.0mL, 6.2mmol) was introduced dropwise and stirred for 5-10 min. at -78°C and warmed to room temperature with stirring for 2 hours. From the above step, dilithiobutadiyn is generated. 1.25g of dichlorosiloxane, purchased from Gelest Corp. are added dropwise for 10 min to react with dilithiobutadiyn and form the linear polymer as illustrated in the reaction scheme shown in Figure 4-2. The mixture was warmed to room temperature and

stirred for 2 hours and then poured into dilute hydrochloric acid and extracted with ether. The ethereal extract was washed with water until neutral and dried over anhydrous sodium sulfate. The ether was removed at reduced pressure to afford a dark brown solid. It was then dried out in vacuum oven for overnight. Total polymer yield was about 80-90% in three different synthesis runs.

4.1.1.2 Characterizations

The structure of poly (diacetylene-siloxane) synthesized in Figure 4-1 was confirmed by FTIR. Thermal stability and weight loss at elevated temperature was analyzed under an Ar atmosphere using a TGA2050 thermal gravimetric analyzer from TA instruments. The heating rate was 5°C/min. The flow rate was fixed at 130 mL/min and sample size was 5.00–10.00 mg. The degradation experiment in near-critical water (350°C/20.7MPa) was performed in a custom-built autoclave. The total charge of water was 50mL. The autoclave was maintained at 350°C for 24 hours. Each sample was run three times at the same condition and an average value was determined. The hydrogen content was measured by a conventional combustion technique, i.e., The CHN Carlo Erba microanalyser. The chemical structure changes during cure, post cure, autoclave test were analyzed by transmission FTIR spectroscopy on a Nicolet MAGNA 760 Bench FTIR, equipped with a conventional DTS detector in the wave number range of 4000–600cm^{-1}. FTIR spectra were obtained from pellets containing 2 mg sample in approximately 100 mg potassium bromide (KBr).

4-1-2. Results and Discussion

The polymers described above were characterized by FTIR. As shown in Figure 4-3, the presence of prominent peak for C-H, C≡C, C-Si, and Si-O are observed and confirming the proposed structure for poly (diacetylene-siloxane). FTIR spectra clearly

showed the diacetylene C≡C stretching bands (2071cm^{-1}) in uncured poly (diacetylene-siloxane) as shown in Figure 4-3 (a). After curing at 300°C for 4 hours, the diacetylene peak clearly disappeared (Figure 4-3(b)). Heating to 300°C for 4 hours in an inert atmosphere converted the polymer into hard, visibly void-free thermoset.

Figure 4-4 shows the DSC analysis under argon reveals a strong exotherm. This exothermic transformation is related to a chemical process, which is a thermally induced crosslinking reaction through the diacetylene groups, which will modify irreversibly the backbone of the starting material. After complete curing at 300°C for 4 hours, this peak clearly disappeared as shown in Figure 4-4(b).

The TGA analysis showed poly (diacetylene-siloxane) thermosets to have good thermal stability. As shown in Figure 4-5, poly (diacetylene-siloxane) gave high char yield of 78% when heated to 1450°C under argon atmosphere. In the 400 °C to 700°C temperature range, bond breakage and rearrangements and further networking occur with additional small molecule volatilization. Above 700 °C, typically the chars are stabilized and no weight losses are observed. Poly (diacetylene-siloxane) showed excellent thermal stability even under extremely high temperatures (~1450°C).

CHN analysis was performed three times for each sample and took the average value. Poly (diacetylene-siloxane) thermosets cured at 300°C for 4 hours had 7.0w% of hydrogen content, which is more than adequate for our BPRA application.

Even though poly (diacetylene-siloxane) showed an excellent thermal stability, poly (diacetylene-siloxane) thermosets cured at 300°C for 4 hours decomposed after the autoclave test. The siloxane bond is relatively more stable to thermo-oxidative degradation than the aliphatic carbon-oxygen bond. However, in solution the Si-O bond

is very sensitive to variety of reagents, including base and acid. The dissociation of water itself at near-critical condition generates a sufficiently high concentration of H^- and OH^- ions. Even though poly (diacetylene-siloxane) thermosets consisted of highly dense cross-linked structures, the degradation started in the hydrolytically weak Si-O-Si linkages and it could be very serous at the autoclave condition.

At this point, we are focusing on using other silane groups instead of siloxane linkages that would be expected to be stable at the autoclave condition. This study is presented in the following section.

4.2 Introduction of Dimethylsilane Linkages to Poly (diacetylene-siloxane-carborane)

In this study, we are introducing other silane groups such as dimethyldichlorosilane and dimethyldichlorosilylethane instead of siloxane linkages (Si-O-Si) that would be expected to improve the hydrothermal stability at the near-critical water condition.

4.2.1 Experimental

4.2.1.1 Sample preparation

Two different types of dichlorosilanes were used, i.e., dimethyldichlorosilane and dimethyldichlorosilylethane in this study. The general information of chemicals and expecting polymers are represented in Table 4-4. Dimethyldichlorosilylethanes were used to increase the hydrogen content because they consist of ethylene between two dimethylsilane linkages.

4.2.1.2 Synthesis

All reactions are performed under an Ar gas using standard Schlenk line techniques. Tetrahydrofuran (8mL) is injected into a flame-dried 100mL round bottom flask, connected to an argon source. N-butyllithium (10.2mL of a 2.5 hexane solution,

26.4mmol) was added slowly and stirred for 5min. Hexachlorobutadiene (1.0mL, 6.2mmol) was introduced dropwise and stirred for 5-10min. at -78°C and warm to room temperature with stirring for 2 hours. From the above step, dilithiobutadiyn has generated. 0.80g of dimethyldichlorosilane or 1.35g of dimethyldichlorosilylethane, purchased from Gelest Corp. were added dropwise for 10 min to react with dilithiobutadiyn and form the linear polymer as illustrated in the reaction scheme shown in Figure 4-6. The mixture was warmed to room temperature and stirred for 2 hours and then poured into dilute hydrochloric acid and extracted with ether. The ethereal extract was washed with water until neutral and dried over anhydrous sodium sulfate. The ether was removed at reduced pressure to afford a dark brown and dried out in vacuum oven for overnight. Total polymer yield was about 80-90% in three different synthesis runs.

4.2.1.3 Characterizations

The structure of synthesized polymers in this study was confirmed by FTIR. Thermal stability and weight loss at elevated temperature was analyzed under an Ar atmosphere using a TGA2050 thermal gravimetric analyzer from TA instruments. The heating rate was 5°C/min. Flow rate was fixed at 130 mL/min and sample size was 5.00–10.00 mg. The degradation experiment in near-critical water (350°C/20.7MPa) was performed in a custom-built autoclave. The total charge of water was 50ml. The autoclave was maintained at 350°C for 24 hours. Each sample was run three times at the same condition and an average value was determined. The hydrogen content was measured by a conventional combustion technique, i.e., The CHN Carlo Erba microanalyser. The chemical structure changes during cure, postcure, autoclave test were analyzed by transmission FTIR spectroscopy on a Nicolet MAGNA 760 Bench FTIR, equipped with a conventional DTS detector in the wavenumber range of 4000–600cm^{-1}.

FTIR spectra were obtained from pellets containing 2 mg sample in approximately 100 mg potassium bromide (KBr). The morphology of fracture surface and top layer was examined by field emission scanning electron microscope (FESEM). The composition in the specimen was analyzed by scanning electron microscopy with an energy dispersive X-ray spectrometer (EDX).

4.2.2 Results and Discussion

The structures of poly (diacetylenedimethylsilane) and poly (diacetylenedimethylsilylethane) were confirmed by FTIR spectroscopy as shown in Figure 4-7. Heat treatment of both poly (diacetylenedimethylsilane) and poly (diacetylenedimethylsilylethane) results in a reaction between diacetylene units producing cross-linked polymers (thermosets).

As shown in Figure 4-7 (A), the absorption bands of poly (diacetylenedimethylsilane) represented strong acetylenic stretching (2070 cm^{-1}), and strong Si-C deformation (1260, 840, and 810 cm^{-1}). When a sample was heated to 350°C and the residue analyzed by FTIR spectroscopy, acetylenic absorption disappeared. Thus heating to 350°C is interpreted as an adequate enough temperature for conversion of the acetylenic units into a cross-linked system. An unexpected siloxane Si-O-Si asymmetric stretching vibration was also observed in the 1090-1020 cm^{-1} region. This peak would be generated by the contamination of water during the synthesis. The FTIR spectra of poly (diacetylenedimethylsilylethane) were shown in Figure 4-7 (B). They showed the same strong peaks (C≡C, Si-C) as poly (diacetylenedimethylsilane) had. They also showed the evidence of ethylene (-CH_2-CH_2-) with a strong and sharp peak in the 1180-1120cm^{-1} regions. This result indicated the confirmation of ethylene group between two

dimethylsilane linkages. When a sample was heated to 400°C, acetylenic absorption disappeared. Poly (diacetylenedimethylsilylethane) also showed an unexpected siloxane Si-O-Si asymmetric stretching vibration at 1055 cm^{-1}.

The residual mass as a function of temperature for each of the materials considered is presented in Figure 4-8 and Figure 4-9. The char yield of poly (diacetylenedimethylsilylethane) thermoset was slightly lower than that of poly (diacetylenedimethylsilane). For poly (diacetylenedimethylsilane) thermosets, the TGA trace showed that the weight loss was 22% when heated to 1450°C under argon atmosphere and occurred mainly between 450 and 750°C seen in Figure 4-8. As shown in Figure 4-9, poly (diacetylenedimethylsilylethane) thermosets gave 31% weight loss when heated to 1450°C under argon atmosphere. In the 400 °C to 600°C temperature range, poly (diacetylenedimethylsilylethane) may occur bond breakage, rearrangements and further networking with additional small molecule volatilization.

CHN analysis was performed three times for each sample and took the average value. Poly (diacetylenedimethylsilane) thermoset cured at 350°C for 4 hours showed 5.0w% of hydrogen content. Poly (diacetylenedimethylsilylethane) thermosets cured at 400°C for 4 hours showed 8.6w% of hydrogen content. The higher hydrogen value of poly (diacetylenedimethylsilylethane) thermosets is caused by the presence of ethylene linkage between two dimethylsilanes.

After the autoclave test (350°C/20.7MPa/24h), poly (diacetylenedimethylsilane) thermoset completely decomposed and poly (diacetylenedimethylsilylethane) thermoset partly decomposed with 45w% weight loss. The degradation may be induced from the unexpected siloxane linkages, which are unintentionally produced by the hydrolysis of

dimethyldichlorosilane and dimethyldichlorosilylethane monomer respectively. These unexpected siloxane linkage was already confirmed by FTIR study in previous section. Moreover, EDX experiment showed that poly (diacetylenedimethylsilane) and poly (diacetylenedimethylsilylethane) thermoset contained 3.68w% and 0.93w% oxygen respectively. The oxygen content represents quantitive Si-O-Si linkages. This result explained the reason that poly (diacetylenedimethylsilane) was completely degraded under near-critical water condition.

It is well known that dimethyldichlorosilane readily reacts with water by the hydrolysis reaction [66-68]. The hydrolysis of starting materials such as dimethyldichlorosilane and dimethyldichlorosilylethane was negative reactions that should not have happened. Corriu et al., who introduced poly (diacetylenedimethylsilylethane), did not mention the formation of siloxane linkages in their FTIR study, however, as shown in Figure 4-10, they also produced unexpected siloxane linkages near 1100 cm^{-1} [54]. Poly (diacetylenedimethylsilylethane) thermoset is newly introduced in our study and it also produced unexpected siloxane linkage. However, the reactivity of dimethyldichlorosilane generating siloxane linkages might be stronger than that of dimethyldichlorosilylethane.

All reactions during synthesis were performed under an atmosphere of dry argon gas utilizing standard Schlenk techniques. Even though we performed this synthesizing process several times, every time they generated Si-O-Si siloxane linkages.

Based on visual observation, poly (diacetylenedimethylsilylethane) thermoset was porous and broken easily during handling after the autoclave test. Figure 4-11 showed

very porous structure of poly (diacetylenedimethylsilylethane) thermoset after the autoclave test.

In water under the autoclave condition, the Si-O bond would be more sensitive to variety of reagents, including base and acid. Therefore, the potential hydrolysis of the unexpected siloxane Si-O-Si linkage in poly (diacetylenedimethylsilane) and poly (diacetylenedimethylsilylethane) thermoset could be accelerated under near-critical water condition. The result showed that poly (diacetylenedimethylsilylethane) containing less unexpected siloxane linkages improved the hydrothermal stability at the autoclave condition. This is the evidence that Si-C bond is quite stable under the near-critical water. Pure poly (diacetylenedimethylsilane) and poly (diacetylenedimethylsilylethane), which do not contain the unexpected Si-O-Si linkages, should show good hydrothermal stability at the autoclave condition. Therefore, it is necessary to develop a new synthesis method to produce pure poly (diacetylenedimethylsilane) and poly (diacetylenedimethylsilylethane) to avoid the hydrolyzing degradation under near-critical water condition.

4.3 Summary

Thermal and hydrothermal stability of poly (diacetylene-siloxane), poly (diacetylenedimethylsilane), and poly (diacetylenedimethylsilylethane) were examined in this study. The introduction of more $(CH_3)_2SiO$ moieties or other silicon based polymers onto poly (diacetylene-siloxane-carborane) expected to increase the hydrothermal stability and also overcome the problems currently addressed in poly (diacetylene-siloxane-carborane), i.e., high cost, limited supply and high boron concentration.

However, poly (diacetylene-siloxane) thermoset decomposed or depolymerized after the autoclave test (350°C/20.7MPa/24h). Poly (diacetylenedimethylsilane)

thermoset completely decomposed and poly (diacetylenedimethylsilylethane) thermoset partly decomposed with 45w% weight loss. The potential hydrolysis degradation of the Si-O-Si moieties in poly (diacetylene-siloxane) thermoset would be the starting point of degradation that it is difficult to overcome by their highly dense network structures. Moreover, an unexpected siloxane Si-O-Si linkage generated by the contamination of water during the synthesis might induce the weight loss of poly (diacetylenedimethylsilane) thermoset and poly (diacetylenedimethylsilylethane) thermoset under near-critical water condition. The result showed that poly (diacetylenedimethylsilylethane) containing less unexpected siloxane linkages improved the hydrothermal stability at the autoclave condition. Therefore, it is necessary to develop a new synthesis method to produce pure poly (diacetylenedimethylsilane) and poly (diacetylenedimethylsilylethane) to avoid the hydrolyzing degradation under near-critical water condition.

Poly (diacetylenedimethylsilylethane) is the novel polymer precursor introducing in this study. It is easy to process and convert into thermosets or ceramics since they are either liquids at room temperature or they are soluble in most organic solvents. Further tests are needed to observe this new polymer.

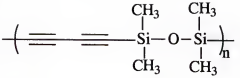

Figure 4-1. The chemical structure of poly (diacetylene-siloxane).

Table 4-1. The glass transition temperature of copolymers [18].

Polymer	Highest annealing temp. (°C)	Glass transition temp. (°C)
DS	300	>300
90:10	300	>300
50:50	300	>300
DSCS	300	94

Table 4-2. The price for starting materials.

Product	Price per 25g
1,3-dichlorotetramethylsiloxane	$36
1,7-bis(chlorotetramethyldisiloxy)-m-carborane	$1,000
Exact composition to use in BPRAs 5.23w% of 1,7-bis (chlorotetramethyldisiloxy)-m-carborane & 94.77w% of 1,3-dichlorotetramethylsiloxane	$86

Table 4-3. Molecular structures, total weight per 1 mole and hydrogen and boron content for both DSCS and DS.

Poly (diacetylene-siloxane-carborane) [DSCS]	Poly (diacetylene-siloxane) [DS]
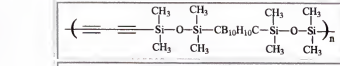	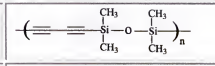
C: 12 x 14 = 168 Si: 28 x 4 = 112 B: 10.8 x 10 = 108 O: 16 x 2 = 32 H: 1 x 24 = 34	C: 12 x 8 = 96 Si: 28 x 2 = 56 O: 16 x 1 = 16 H: 1 x 12 = 12
Total weight per 1 mol = 454g/mol	Total weight per 1 mol = 180g/mol
Theoretical Hydrogen w% = 7.49 w% Theoretical Boron w% = 23.79 w%	Theoretical Hydrogen w% = 6.67 w% Theoretical Boron w% = 0 w%

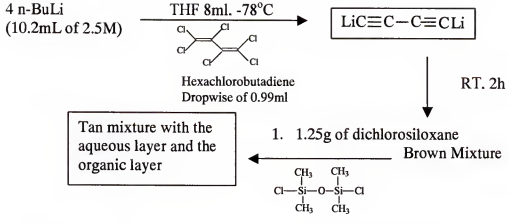

Figure 4-2. Synthesis steps of poly (diacetylene-siloxane).

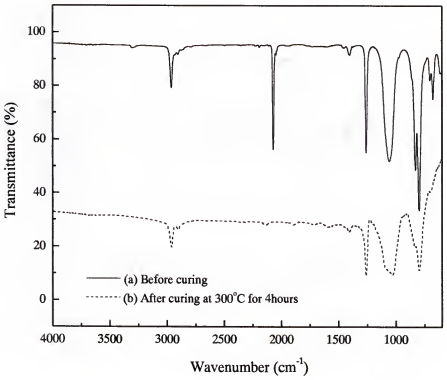

Figure 4-3. FTIR spectra for synthesized poly (diacetylene-siloxane): (a) before curing (b) after curing at 300°C for 4 hours.

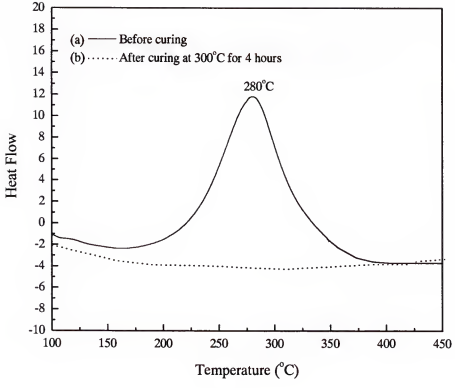

Figure 4-4. DSC scan showing cure exotherms for synthesized poly (diacetylene-siloxane): (a) before curing, (b) after curing at 300°C for 4 hours.

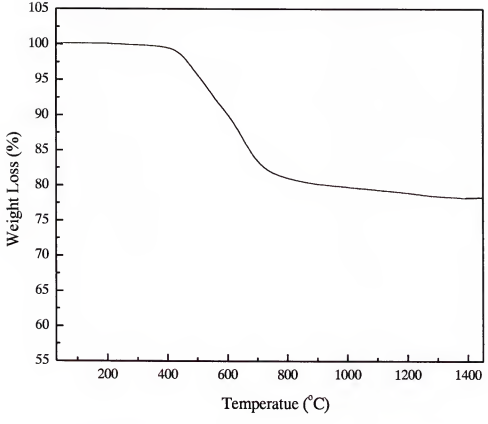

Figure 4-5. TGA curves of poly (diacetylene-siloxane) after curing at 300°C for 4 hours.

Table 4-4. The general information of chemicals and derived polymers.

Final product	Poly(diacetylenedimethylsilane)	Poly(diacetylenedimethylsilylethane)
Structure	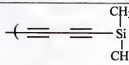	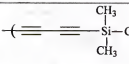
Monomer Mw	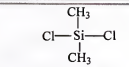 Mw = 129g/mol	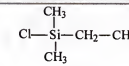 Mw =215g/mol
Price per 25g	$10 [90]	$25 [90]
Mw of Polymer	Total weight per 1 mol = 106.20g/mol	Total weight per 1 mol = 192.41g/mol
Composition	Theoretical Hydrogen w% = 5.69 w% Theoretical Boron w% = 0 w%	Theoretical Hydrogen w% = 8.38 w% Theoretical Boron w% = 0 w%

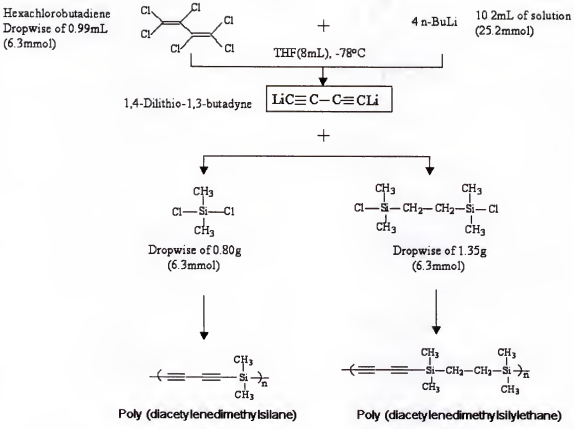

Figure 4-6. Synthesis step of poly (diacetylenedimethylsilane) and poly (diacetylenedimethylsilylethane) copolymer.

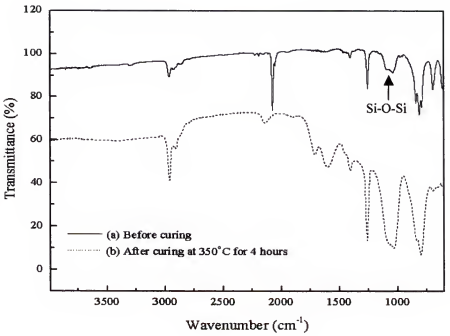

(A)

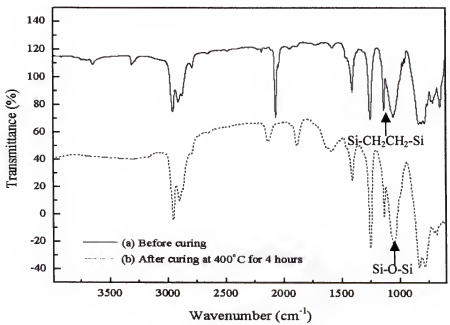

(B)

Figure 4-7. FTIR spectra of synthesized (A) poly (diacetylenedimethylsilane) and (B) poly (diacetylenedimethylsilylethane).

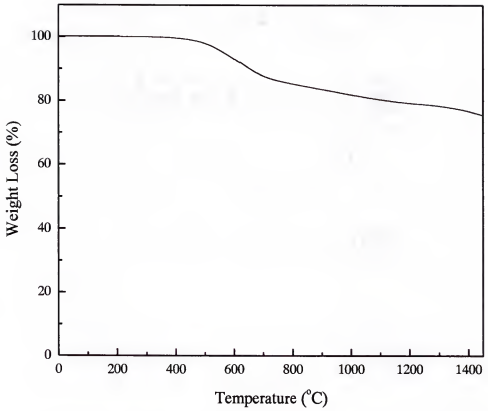

Figure 4-8. TGA curves of poly (diacetylenedimethylsilane) after curing at 300°C.

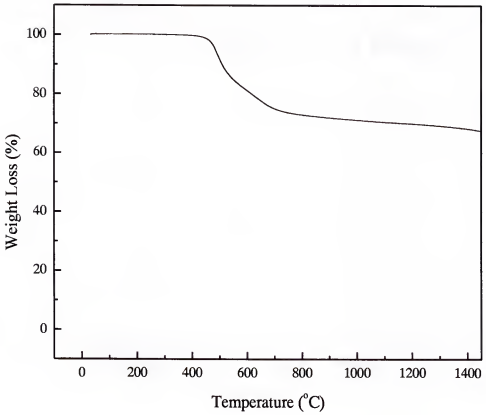

Figure 4-9. TGA curves of poly (diacetylenedimethylsilylethane) after curing at 350°C.

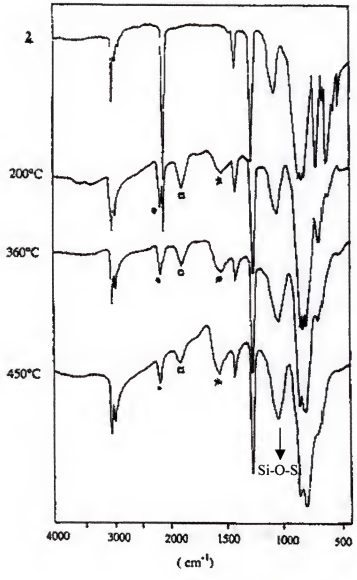

Figure 4-10. Infrared spectra of poly (diacetylenedimethylsilylethane) at 200°C, 360°C and 450°C and original polymer (2) [54].

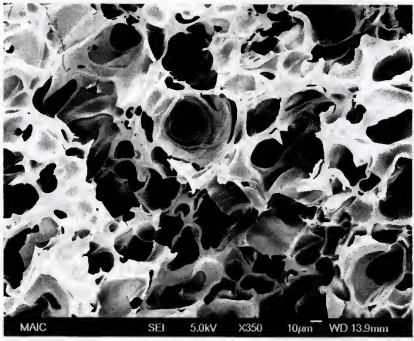

Figure 4-11. Scanning electron spectrum of poly (diacetylenedimethylsilylethane) after the autoclave test.

CHAPTER 5
SCREENING CANDIDATE MATRIX POLYMERS FOR POTENTIAL BURNABLE POISON ROD ASSEMBLIES (BPRAS) IN PRESSURIZED WATER REACTORS (PWRS)

5.1 Introduction

Keller et al. introduced poly (diacetylene-siloxane-carborane), which is an inorganic-organic hybrid shown thermally stable up to 1,000°C, and can be easily processed into shaped configuration to apply to BPRAs [11-13,15,17-19]. However, we found that the degradation of Si-O-Si under near-critical water condition (350°C, 20.7MPa) was an unfavorable disadvantage of poly (diacetylene-siloxane-carborane) [57]. A high cost (18,000$/lb) and current limited supply of carboranes could give rise to difficulties for the utilization and development of polymers and ceramics based on carborane units.

The second approach is believed to be a more promising method. In this chapter, the focus is on finding a candidate polymeric matrix that can replace a current alumina matrix.

Listed below in Table 5-1 are essential properties that matrix polymer should possess.

As was explained in background section, it was shown that water is completely miscible with a number of hydrocarbons, including pentane, heptane, benzene, and toluene. Under this condition, some hydrocarbon decomposition and condensation reactions occurred without adding air or other potential oxidizers. In addition, many polymers consisting of high molecular hydrocarbon could decompose to liquid product or to their monomers in the presence of high-temperature and high-pressure water [8].. In the

near- or supercritical region, water achieves a highly compressible condition and further, the changes in physical properties of water allow it to dissolve many higher molecular weight hydrocarbons. For cellulose [33,34], poly (ethylene terephthalate) (PET) [35,36], nylon-66 [37-39], and other polymers [21,40-43], 100% liquid yield or 100% conversion with very low gas yield are obtained without catalysts under sub or supercritical water.

Thermosetting resins, however, are one of the most difficult substances to decompose. Their highly cross-linked structures improve chemical and thermal resistances [44]. They do not melt or cannot be depolymerized easily. As explained earlier, It was reported that phenolic resin did not decompose in near-critical condition [41]. For these reasons, thermosetting resins such as phenolic resins, epoxy resins, silicone resins and cross-linked high-density polyethylenes were selected as candidate materials in this study.

5.2 Experimental

This study investigated phenolic resin, epoxy resin, silicone resin, and irradiated HDPE were investigated. Thermal stability of candidate materials was tested by thermal gravimetric analysis (TGA). Hydrothermal stability in near-critical condition (350°C/20.7MPa) was performed by custom-built autoclave constructed in our laboratory. Furthermore, FTIR technique was also used to characterize the structural change during curing process and autoclave test.

5.2.1 Materials

5.2.1.1 Preparation of phenolic resins

Resol-types of phenolic resin were supplied from Plenco Co, USA. P13470 resin is a powder product of Bisphenol-A, formaldehyde, and small amount of phenol. Bisphenol-A is usually used to increase flexibility for coating application [69]. The samples

were cured using a Teflon mold (3.0 cm × 3.0 cm × 0.2 cm) in a hot presser (180°C/ 20mins) with an air atmosphere. After curing, further a heat treatment or postcure was performed at 350°C for 4 hours in tube furnace in inert atmosphere (Ar).

5.2.1.2 Preparation of epoxy resins

Two epoxy resins supplied from Dow Chemical, USA were used in this study. DER 383® is a liquid product derived from bisphenol-A and epichlorohydrin. DEN431 Novolac resin® is a semi-solid reaction product of epichlorohydrin and phenol-formaldehyde novolac. Novolac epoxy resin provides additional reactive sites, as compared to a bisphenol-A type epoxy resin, produce tightly cross-linked systems. It shows better thermal stability and water resistance, which may be more suitable in our application. All samples were cured with Sulfanilamide (SSA) in a preheated Teflon mold (3.0 cm × 3.0 cm × 0.2 cm) using an air-circulating oven. The curing conditions were completed by heating the mixture at 150°C for 4 hours and 175°C for 1 hour, and 200°C for 4 hours, consecutively, allowing it to gradually cool down to room temperature.

5.2.1.3 Preparation of silicone resins

Poly(methylsilsesquioxane)s (PMSSQs) with empirical formula of $(CH_3SiO_{3/2})_x$ have been studied for many years since the first commercialization of silicon polymers as electrical insulation materials used at high temperatures [70,71]. A solution of PMSSQ was prepared as the mixture of 8mL of distilled methyltrimethoxysilane (MTMS) purchased from Gelest Co, USA, 1.5mL of water, and 1mL of methanol. This solution was cast on an untreated styrene dish at nitrogen atmosphere (21°C, 78% relative humidity) and allowed to cure for two weeks. The samples were subsequently further cured for 2 hours at 130, 250, and 400°C, respectively to make a complete cross-linked structure.

5.2.1.4 Preparation of Gamma irradiated high-density polyethylenes (HDPEs)

Sheets of 1/16" thickness HDPE were purchased from US Plastic Co, USA. After cutting to 12"x12" square, they were irradiated in a ^{60}Co facility, in air, at room temperature. Five dose rates, 0.5, 7.0, 10.4, 20.2, and 51.7KGy/hour determined with radiochromic film (FWT-60-00) dosimeter were selected in this study as shown in Figure 5-1. The total doses were from 72 to 6940 KGy depending on the radiation time of 6 days and 8 weeks.

5.2.2 Characterizations

Thermal stability and weight loss at elevated temperature was analyzed under an Ar atmosphere using a TGA2050 thermal gravimetric analyzer from TA instruments. The heating rate was 5°C/min. Flow rate was fixed at 130 mL/min and sample size was 5.00–10.00 mg. The degradation experiment in near-critical water (350°C/20.7MPa) was performed in a custom-built autoclave. The total charge of water was 50mL. The autoclave was maintained at 350°C for 24 hours. Each sample was run three times at the same condition and an average value was determined. The hydrogen content was measured by a conventional combustion technique, i.e., The CHN Carlo Erba microanalyser. The chemical structure changes during cure, postcure, autoclave test were analyzed by transmission FTIR spectroscopy on a Nicolet MAGNA 760 Bench FTIR, equipped with a conventional DTS detector in the wavenumber range of 4000–600cm^{-1}. FTIR spectra were obtained from pellets containing 2 mg sample in approximately 100 mg potassium bromide (KBr). The morphology of fracture surface was examined by field emission scanning electron microscope (FESEM). The polymer network analysis of the polyethylene samples was carried out by solvent swelling and gel content by the extraction of the sample under refluxing 50mL of *p*-xylene (bp=139°C) for 24 hours. The

experimental density of the sample pyrolyzed was obtained by the Archimedian method of weighing small pieces cut from first in air and then in isopropanol.

5.3 Results and Discussion

5.3.1 Phenolic resins

Phenolic resins are known to be quite temperature resistant polymeric materials and yield high amount of char during pyrolysis. Phenolic resins are divided into two broad classes: resols and novolacs. In this study, we choose the resol type of phenolic resin because the complete cure of resols leads to a high modulus, high cross-link density, and moderately high T_g exhibiting excellent moisture and heat resistance [72]. Further, Resol derived from Bisphenol-A instead of phenol increases economic benefits due to higher hydrogen content.

Resol type of phenolic resins can be cross-linked by heat curing. During this reaction water is evolved by the condensation reaction. Zinke et al. have reviewed the hardening routes of resol [73]. They summerized their thought on the structure of the phenolic resins produced under a variety of conditions: (a) resol is mixtures of substituted methylol phenols, (b) the primary reaction in the hardening process is the formation of ether and methylene bridges with the elimination of water explained in step (1) of Figure 5-2, (c) with further hardening or curing at higher temperatures (above 170°C), the ether bridges changes to methylene bridges as shown in step (2) of Figure 5-2.

After curing the final step, the resol type phenolic resins called "resites" are generated. Resites are amorphous and high crosslinking density polymers of heterogeneous structure. Conley et al. reported that resites preserved hardness up to 400°C and below that temperature in inert medium, only 3% gaseous products were evolved [72]. The polycondensation reaction continues up to 350°C and further cross-linked

structure of resites may be expected during this process [74]. Therefore, the postcure process was performed at the condition of 350°C, 4 hours in Ar atmosphere to make a fully cross-linked network structure.

Figure 5-3 showed TGA curve representing the weight loss of P13470 cured at 180 °C and 350°C respectively. P13470-180 showed the weight loss due to the condensation of aromatic ribbon molecules in the cured resin and the volatilization of low molecular weight species. However, after the postcure process at 350°C, P13470-350 was thermally stable up to 400°C in inert atmosphere. This is because it formed a fully cross-linked network structure and no more condensation reactions occurred between 300 - 400°C. In addition, a fully cross-linked structure may lead to a high glass transition temperature (T_g) with a firm and dense polymeric structure, and enhance thermal stability. Shalin et al. indicated that glass transition temperature of resite was over 350°C [74]. Moreover, the methylene bridge is well known to be thermodynamically the most stable cross-link site that is not easy to cleave [75,76]. It was confirmed that the weight loss (6.5w%) indicated in Figure 5-3 is mostly caused by water and paraformaldehyde [72,77] and the formation of these products is consistent to the further condensation to generate the methylene linkage. Ko et al. also represented that the amount of evolved gas between 400°C and 700°C was more than 90% of that evolved during pyrolysis [77].

The TGA result indicates a fully cross-linked phenolic resin may be a good candidate to use for the temperature range in BPRAs. However, it is important to monitor hydrogen content during the postcure process to assure an adequate moderating benefit. CHN analysis was performed three times for each sample and the average value are

shown in Table 5-2. It was confirmed that there was no significant decrease of hydrogen content during the postcure process at 350°C for 4 hours.

After the autoclave test (350°C/20.7MPa/24h), P13470-180 partly decomposed with 25.6w% of weight loss and P13470-350 also showed 17.5 w% of weight loss. Based on visual observation, both samples had a good shape with a smooth surface after the test. As was explained, the curing process of phenolic resin followed the condensation reaction with the evolution of water. Therefore, it would be expected that phenolic resin exhibited the same degradation mechanism as shown in condensation polymers such as poly (ethylene terephthalate), nylon 66, cellulous, polycarbonate, and polyurethane in the autoclave test. At this condition, water can easily hydrolyze condensation polymers by H^+ and OH^- ions, and by hydrothermal cleavage with water molecules, and to dissolve organic substances that can provide a homogeneous phase for reactions. For example, the hydrolysis of dibenzyl ether in phenolic resin thermoset would occur under this condition. However, further experiments, i.e., SEM, FTIR, XRD, and density measurement, have been performed and interestingly, they showed a totally different result.

A fracture surface was investigated by SEM (Figure 5-4). After curing at 180°C and 350°C, they showed void-free surface (Figure 5-4a). Ouchi et al. reported that the hydroxyl absorption peak at 3400cm^{-1} gradually started to decrease at 300°C. As increasing temperature, the rate of condensation reaction for resol type phenolic resin increases, and rapidly goes up between 400-600°C [78]. Therefore, as the increase of temperature, one would expect an increase in the pore structure by further condensation reactions. The moderate pore structure was found during isothermal experiment at 350°C for 24 hours as shown in Figure 5-4b. However, at the same temperature in the autoclave

condition (350°C/20.7MPa/24h), the porosity dramatically increased and a fine-porous microstructure with particle size in the range 1–10μm diameter was uniformly formed as shown in Figure 5-4c,d.

In order to better understand, each sample was studied by FTIR. Figure 5-5a, b shows the FTIR spectra of P13470-180 and P13470-350, respectively. It can be noted that with the increase of temperature the -OH stretching band at 3350 cm^{-1} shifts toward higher wave numbers. These observations are the same as reported by Morterra et al. They explained that the changes could take place in the H bonding as the number of -OH groups decreases [79]. This is probably due to the condensation reaction during the postcure process at 350°C. The 1360cm^{-1} -OH band decreases in intensity for the same reasons. The absorption bands at 1234cm^{-1} result from the stretching of the C-H bonds of a dibenzyl ether structure. The concentration of the dibenzyl ether link has almost disappeared after curing at 350°C as shown in Figure 5-5b and this result corresponds to that of curing mechanism explained in Figure 5-2. Figure 5-5c, d represented the FTIR spectra of P350AUTO (after autoclave test) and P350DRY (after isothermal test), respectively. As shown in Figure 5-5c, the intensity of -OH stretching band at 3400cm^{-1} has nearly disappeared after the autoclave test. This result is in agreement with the above analysis from the SEM micrograph. It is obvious that the strong condensation reaction preferably occurred at the near-critical water, thus forming numerous uniform pore structures.

The more evidence of condensation reactions at the near-critical water can be found on the FTIR spectra. The relatively new sharp band at 1256cm^{-1} indicates CO stretching vibration. This result shows that the following reaction occurs during the autoclave test.

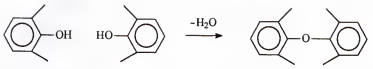

(5-1)

Morterra et al. and Jha et al. reported that a phenolic OH…OH condensation mechanism starts above 300°C and yields diphenyl ether linkages for novolac resin [79,80]. However, this peak was not observed during the postcure process in our study as shown in Figure 5-5b. These results may be related to structural difference between novolac and resol derived from bisphenol-A. The ether band was originally located at 1235cm^{-1} when it was cured at 180°C similar in the form of the dibenzyl ether as seen in Figure 5-5a. However, this peak disappeared during the postcure process (Figure 5-5b) and another new ether peak (diphenyl ether) was generated at 1256cm^{-1} after both autoclave and isothermal test. When comparing Figure 5-5c and Figure 5-5d, the reaction (1) may be more favored to form at autoclave condition than at inert atmosphere.

Ouchi et al. introduced the dehydration between phenolic hydroxyl group and methylene bridges. They suggested that the intensity of the methylene band at 1474cm^{-1} decreased and another strong band at 1465cm^{-1} at 400°C [78]. Figure 5-5c shows a relatively sharp band at 1465cm^{-1} indicating the following reaction preferentially occurs.

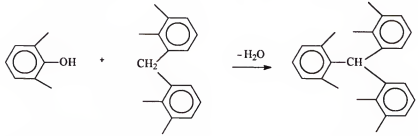

(5-2)

It was reported that the condensation reaction rate increased in acidic medium [81,82]. This reaction rate was proportional to the H-ion concentration. Knop et al. also explained the reaction between phenol and formaldehyde in the strong acidic pH range. The

methylol group is a transient intermediate under acidic conditions. Benzylic carbonium ions in Eq. 5-3 result under these conditions, which then react very fast with phenol, yielding dihydroxydiphenylamethane according to Eq. 5-4 [69]. The rate of formation of dihydroxydiphenlmethane was found to be more than 10-13 times [82].

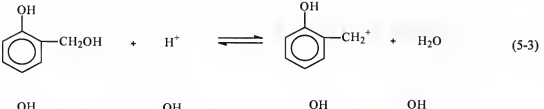

(5-3)

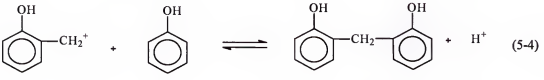

(5-4)

(5-5)

o-benzoquinone methide

Knop et al. explained " quinine methides" as intermediates in the heat curing of resols. However, it appeared at the initial time during prepolymer formation in their experiment. Hultzsch and Von Euler proposed quinine methides, which are intermediate in structure to quinines and quinodimethanes, but differ in their electron charge distribution [69]. As was explained in earlier, autoclave tests in this study use the condition of 350°C and 20.7MPa. In this region, the ion product, or dissociation constant (K_w), representing H^+ and OH^- ion concentration of water, goes through maximum which is about three orders magnitude higher than it is in ambient water [30]. The dissociation of water itself in this condition generates a sufficiently high concentration of H^+ and OH^-. At this point, we propose that o-benzoquinone methide would be possibly generated in this condition as seen in Eq. 5-5. Thus, they show a high reactivity to electrophiles as

well as nucleophiles. This would be the way that most –OH peaks easily disappeared under the autoclave condition. In the mean time, in water under near-critical condition, some acid-catalyzed organic reactions occur without any added acid. Therefore, we also propose that the additional condensation reaction preferably occur under acidic medium in the autoclave test and generate evolved gas followed by forming a highly ordered pore structure demonstrated in Figure 5-4c. It is possible to expect forming highly dense network structures followed by Eq. 5-3 and Eq. 5-4 under the autoclave condition. However, it is necessary to find the evidence or pathway to form "quinine methides" as intermediates as well as "benzylic carbonium ions" under near-critical water condition.

Ouchi et al. showed that all –OH peaks were disappeared after pyrolyzing above 600°C. In the 500-560°C, drastic changes occur in that the network collapses, aliphatic brides are destroyed. Hydrocarbonaceous residues are eliminated and those remaining are changed, polyaromatic domains form, and the resulting char is much like other intermediate temperature chars [79]. No specific peak was found after pyrolyzing above 600°C due to the transformation of phenolic thermoset resin into glass carbon ceramics. At this point, it would be expected that the property of P13470 after the autoclave test is different than that of pyrolyzing above 600°C even though they form the same porous structure. Moreover, P13470 thermoset in the near-critical water forms higher cross-linked network structure than that in the inert atmosphere at 350°C, therefore thermal and mechanical property will be enhanced.

The structural difference between two porous structures, generated by dry and wet conditions, was further compared by SEM and density measurement. There are two factors to determine the bulk density of the heat-treated samples [83]. One is pore formation,

and the other is chemical densification caused by the chemical structure change of the resin during the heat treatment. As discussed earlier, the pore structure was uniform and mainly consisted of narrow pores in the range 1–10μm diameter when P13470 resins were cured at the autoclave condition (Figure 5-4d). However, when they were pyrolyzed at 500°C and 700°C, a number of porous structures were formed. The evolved gases created irregular pores and diffused explosively from the bulk as shown in Figure 5-6a,b. Figure 5-7 represents the variation in the bulk density during pyrolysis. After the autoclave test (350°C/20.7MPa/24h), the density was much lower than that of sample cured with same temperature at 350°C. The more evolved gases generated the higher amount of pore structures at this condition because the condensation reaction was more accelerated in the high ion concentration of water at the autoclave condition.

As the material was pyrolyzed above 500°C, the polymeric structures of the resin started to transform into the glassy carbon structure. Thus the density should decrease as increasing temperature. Moreover, they also form a number of irregular pore structures. Figure 5-7 represents the overall net density of bulk material. The density of P350AUTO was even lower than that of P500DRY and P700DRY. This result indicates the sample cured at the autoclave condition still keep forming thermoset network structure, which has a much lower density than the carboneous ceramic.

It was reported that the carbonyl concentration at 1650cm^{-1} started to appear after heat-treatment in inert gas above 400°C due to the oxygen content in polymer structure. Conley et al. found that the primary degradation route for the phenolic resin is oxidation, regardless of whether the resin was exposed to elevated temperatures in air, argon, or nitrogen [72,84]. Any oxidative degradation was not observed at the near critical water in

this study as shown in Figure 5-5c. However, it will be expected to occur the oxidation reaction in supercritical water condition. For the future work, it will be interesting to compare the pyrolysis mechanism between wet and dry conditions at the same temperature (> 400°C).

In this study, emphasis was made by excellent hydrothermal stability of phenolic resin under near-critical water condition. However, further investigations of the structural properties such as type of pore shape, size and uniformity are planned to understand the difference between dry and wet pyrolysis. Their chemical, physical and mechanical properties will be discussed to understand the advantage of the new wet pyrolysis method of phenolic resin.

5.3.2 Epoxy resins

Two epoxy resins were used in this study. DER 383® is a liquid product derived from bisphenol-A and epichlorohydrin and DEN431 Novolac resin® is a semi-solid reaction product of epichlorohydrin and phenol-formaldehyde novolac. The curing process is a chemical reaction in which the epoxide groups in epoxy resin reacts with a curing agent to form cross-linked, three-dimensional network. All epoxy resins were cured for 9 hours with Sulfanilamide (SSA). The curing conditions were completed by heating the mixture at 150°C for 4 hours and 175°C for 1 hour, and 200°C for 4 hours, consecutively, allowing it to gradually cool down to room temperature. Novolac epoxy resin provides additional reactive sites, as compared to a bisphenol-A type epoxy resin, produce tightly cross-linked systems.

As expected, DEN431® displayed better thermal stability and higher char yield than DER383® as shown in Figure 5-8. However, all specimens after the autoclave test (350°C/20.7MPa/24h) decomposed or depolymerized. The hydrolysis of an epoxy resin

apparently is the main degradation reaction during the autoclave test. Fromonteil et al. showed the importance of hydrolysis phenomena on the epoxy resin. Hydrolysis of the epoxy resin was negligible up to 200°C. It became significant between 300 and 400 °C and the hydrolysis of the epoxy resin was accelerated when considering both high temperature and high pressure (24MPa). The complete destruction of the initial epoxy network occurred from 300°C [85]. Okajima et al. also presented the same result in their experiments [86,87].

As discussed earlier, the outline of the characteristics of water as a reactive solvent can be understood with both an ionic product and a dielectric constant. The overall breakdown rate of epoxy resin in near-critical water may be represented as the sum of hydrolysis and thermal breakdown contribution. Epoxy resins are therefore not good candidate materials to use in BPRAs. In addition to having a relatively weak thermal stability, epoxy resin is easily dissolved by a high hydrolysis reaction. Therefore, water at high temperature and pressure may accelerate the decomposition of the resin.

5.3.3 Silicone resins

Polysilsesquioxanes with empirical formula of $(RSiO_{3/2})_x$ Where R is hydrogen or an organic group, have been studied for many years since the first commercialization of silicon polymers as electrical insulation materials used at high temperatures [70]. The mixed cage/network structure of these materials can be expected to enhance the thermal and hydrothermal stability at the near-critical water [88].

Figure 5-9 shows the FTIR spectra of both PMSSQ-A and PMSSQ-C, respectively. After curing consecutively at 130, 250, and 400°C for 4 hours, a broad –OH peak at 3350cm^{-1} disappeared as shown in Figure 5-9a. This result confirms that PMSSQ forms a complete network structure of Si-O-Si linkages with all loss of SiOH structures during

heating up to 400°C. Figure 5-10 shows the TGA thermograms of the samples, measured at 5.0°C/min heating rate in an Ar atmosphere. PMSSQ-C does not show any weight loss up to 550°C. It has been reported that cured PMSSQ showed the significant weight loss above 550°C due to the thermal degradation of the network structure [71].

Even though they showed an excellent thermal stability, PMSSQ-C decomposed after the autoclave test. As discussed earlier, in solution the Si-O bond is very sensitive to variety of reagents, including base and acid. The method to preparing PMSSQ is polycondensation (step growth polymerization) of Methyltrimethoxysilane with water in solution. The dissociation of water itself at near-critical condition generates a sufficiently high concentration, therefore the sensitivity of Si-O to high H^+ and OH^- ion concentration would increase under the autoclave condition. In this condition, water has the ability to hydrolyze condensation polymers such as poly(methylsilsesquioxane), poly(ethylene terephthalate) [7,9], nylon 66 [37-39], cellulous [33,34], polycarbonate [40], and polyurethane [63] catalyzed by H^+ and OH^- ions, and by hydrothermal cleavage with water molecules, and to dissolve organic substances that can provide a homogeneous phase for reactions. Figure 5-11 represented a possible hydrolysis reaction of PMSSQ cage structure under near-critical water condition.

5.3.4 Gamma irradiated high-density polyethylene

Polyethylene in its simplest form consists of a long backbone covalently bonded carbon atom chain, $-(CH_2-CH_2)_x-$. This structure has over 14w% of hydrogen content. Polyethylene is generally cross-linked for following purpose: to improve its dimensional stability at elevated temperatures, to improve its impact resistance, or to reduce its propensity to stress crack [89]. Cross-linked polyethylene (XLPE) also does not melt when the crystalline melting temperature is exceeded. For these reasons, XLPE is widely used

for hot-water distribution system in the tubing industry required higher in-service temperature. Sako et al. reported that the polyethylene main backbone chain did not decompose under supercritical water condition (380°C) [22]. Moriya et al. also reported that the rate of supercritical water cracking in polyethylene is lower than that of its thermal cracking [23]. These indications have provided us an opportunity to fabricate the cross-linked structure by using hydrothermally stable polyethylene linkages that would survive in the severe autoclave condition. Generally, the cross-linked structure can be introduced to polyethylene either by conventional chemical means, usually involving functional silanes or free radical generating peroxides, or by exposure to ionizing radiation from either radioactive sources, or highly accelerated electrons.

The crosslinking and chain scission are the main reactions during irradiation and the balance of crosslinking and scission reactions in polyethylene chins exposed to high-energy radiation processes that produce free radicals is important to be used in our new applications.

The following major effects were observed when polyethylene was irradiated [90,91]:

i) The evolution of hydrogen and low molecular weight hydrocarbons.

ii) The formation of C-C bonds between molecules (crosslinking) converts the polymer into one, which is partly insoluble and infusible.

iii) An increase in unsaturation. At low dose, the degree of unsaturation is proportional to the dose but eventually tends to the maximum value.

iv) Destruction of crystallinity. The percentage of material present in the crystalline form at room temperature decreases with increasing dose.

v) Color changes. In common with many other polymers, polyethylene acquires a yellow tinge on irradiation.

vi) Oxidative reactions, particularly near the surface, when the irradiation is carried out in the presence of oxygen.

In our experiments, the cross-linked HDPE generated by high gamma radiation dose was used since a fully cross-linked network structure will enhance the hydrothermal stability in near-critical water. The discussion and characterizations are mainly based on the samples irradiated to a dose of 6940 KGy.

The thermal stability of irradiated HDPE was relatively higher than that of untreated HDPE as shown in Figure 5-12. Even though the melting temperature of HDPE is about 130°C, irradiated HDPE that contains higher cross-linked network structures is difficult to soften at high temperature applications.

After the autoclave tests, based on visual observation, HDPE cross-linked by gamma irradiation above 940 KGy (HDPE940) showed good shape retention and few defects before and after the test. However, at low gamma irradiation dose, all specimens partly melted or decomposed. SEM micrograph of the sample after the autoclave test illustrated in Figure 5-13. Highly cross-linked polyethylene showed a void-free smooth fracture surface after the autoclave test.

The study of the solubility and gel fraction of polymers is a good method to understand the structure of polymers cross-linked chemically or irradiated [90-93]. Most amorphous polymers or crystalline polymers at the melting point, if not cross-linked, dissolved readily in good solvents. However in the same solvent condition, cross-linked

polymers do not dissolve. They swell to an extent determined proportional to the crosslinking density at the gel fraction [90-93].

In our experiments, polymer network analysis of cross-linked HDPE was carried out by solvent swelling and gel content by the extraction of a sample under refluxing of *p*-xylene (bp=139°C) for 24 hours.

The gel content (%gel) and the swelling ratio (q) were calculated by following equation [92,94].

$$\%gel = \frac{w_{gel}(weight\ of\ gel)}{w_{ini}(initial\ weight)} \times 100\% \tag{5-6}$$

$$q = \frac{W_d + |W_g - W_d|K}{W_d} \tag{5-7}$$

K=the ratio of the density of the solvent to the polymer at immersion temperature, HDPE: 1.17 at 110°C
Wd=weight of dried gel
Wg=weight of swollen gel after the immersion period

As shown in Table 5-3, the gel content increased with the increase of irradiation dose and irradiated HDPEs with 1390 KGy and 6940 KGy (HDPE1390 and HDPE6940) also showed a small swelling ratio representing a lower solvent uptake into their network structures. These properties are directly affected to hydrothermal stability of irradiated XLPE. This result indicates the reason that HDPE cross-linked by a high irradiation dose survived after the autoclave test.

The major product of irradiation is hydrogen, and the evolution of each hydrogen molecule is accompanied by the formation of double bond C=C in the main chain, or by the linking together of two molecules ether side by side (crosslinking) or end (endlinking) [95,96]. As expected, the hydrogen content decreased with the increase of irradiation dose

(Table 5- 4). Approximately 2w% of hydrogen decreased with 940 KGy of irradiation and there was no significant change after this value.

5.4 Summary

A number of candidate polymeric materials were screened for potential polymeric BPRAs application. This study provides an understanding of polymeric material behavior in near- or supercritical water and provided excellent evaluations of potential candidate materials. The results present that phenolic resin and irradiated HDPE are promising materials for new BPRA system.

In this work, it was confirmed that reversible hydrolysis reaction occurred under the autoclave condition ($350^{o}C/20.7MPa$) for condensation polymers such as epoxy resin and PMSSQ. However, phenolic resins, which also follow condensation reaction during curing process, did not show reversible hydrolysis reaction at this condition. Interestingly, strong condensation reactions preferably occurred under high ion concentration condition at the near-critical water, thus generate evolved gas followed by forming a highly ordered pore structure.

The dissociation of water itself in this condition generates a sufficiently high concentration of H^{+} and OH^{-}. At this point, we proposed that o-benzoquinone methide would be possibly generated in this condition, thus they showed a high reactivity to electrophiles as well as nucleophiles. In addition, in water under near-critical condition, some acid-catalyzed organic reactions occur without any added acid. At this point, we also proposed that the additional condensation reactions preferably occurred under acidic medium in the autoclave test and generated evolved gas followed by forming a highly ordered pore structure. It was also confirmed by the density measurement that the sample cured at the autoclave condition still keep forming thermoset network structure, which

had much lower density than carboneous ceramic. Further investigations of the structural properties such as type of pore shape, size and uniformity are needed to understand the difference between dry and wet pyrolysis. Their chemical, physical and mechanical properties will be discussed to understand the advantage of the new wet pyrolysis method of phenolic resin.

Highly cross-linked polyethylene showed excellent hydrothermal stability under near-critical water condition. This was the evidence that our proposed idea that cross-linked polyethylene, which consisted of hydrothermally stable polyethylene linkages, would survive at the autoclave condition. Highly concentrated hydrogen in PE structure took an advantage to expect more moderadation effect when used as the matrix of burnable poison material.

Table 5-1. The essential properties that a polymer matrix should possess.

- The material must be thermally stable at 350°C in the core for a single cycle, which can range from 1 to 2 years.
- The material must not dissolve or decompose if exposed to hydrothermal conditions of reactor (350°C/20.7MPa in water).
- The material should contain at least 5% of hydrogen to have an economic benefit.
- The material must be shapeable or moldable to conform to the shape of its containment.
- The material must be stable against breakdown into volatile species such as hydrogen in the radiation environment of a reactor core – clad hydriding problems.
- The material must have adequate thermal conductivity to maintain equilibrium temperature during neutron adsorption.

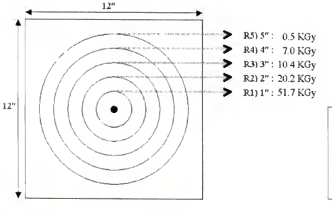

Figure 5-1. The diagram of HDPE sheet (A dose rate and the calculation of total doses).

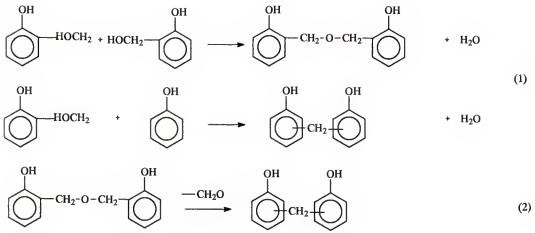

Figure 5-2. A possible curing mechanism of resol type of phenolic resin [73].

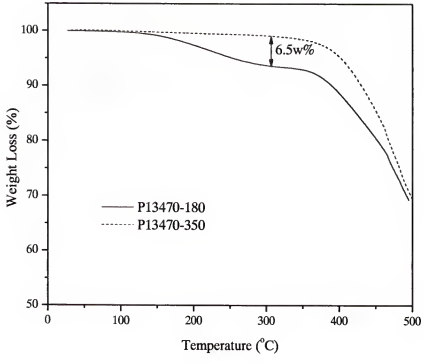

Figure 5-3. TGA curves of P13470-180: — cured at 180°C for 20 mins and P13470-350: --- postcured at 350°C for 4 h.

Table 5-2. CHN analysis for phenolic resins with different curing temperature.

Element / Material	C [w%]	H [w%]	N [w%]
P13470	72.43	6.40	0.00
P13470-180	76.35	6.27	0.02
P13470-350	79.63	6.19	0.20

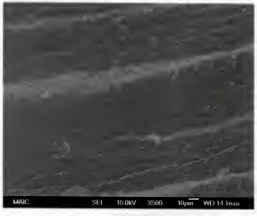

(a)

(b)

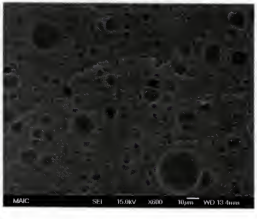

(c)

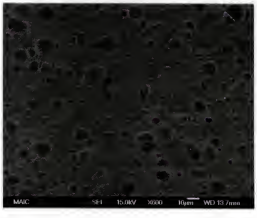

(d)

Figure 5-4. SEM image of phenolic resin (P13470) with different pyrolyzing temperatures (a) P13470-350: postcured 350 °C for 4 hours (b) P350DRY: isothermal test (350°C/24h) in Ar (c) P170AUTO : autoclave test of P13470-170 (d) P350AUTO : autoclave test of P13470-350

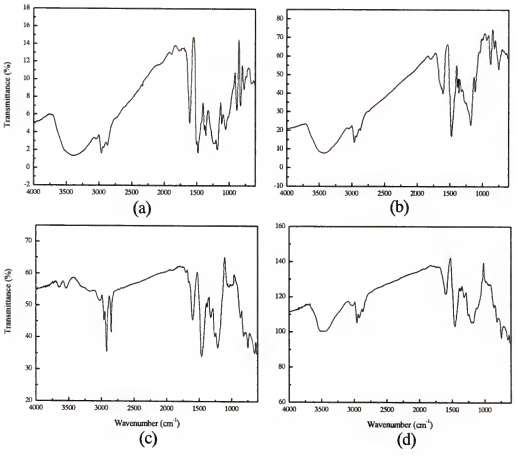

Figure 5-5. FTIR spectra of phenolic resin (P13470) heat-treated at different temperature: (a) P13470-180: cured at 180 °C for 20mins (b) P13470-350: postcured 350 °C for 4 hours (c) P350AUTO: after the autoclave test (350°C/20.7MPa /24h) in water (d) P350DRY: isothermal test (350°C/24h) in Ar atmosphere.

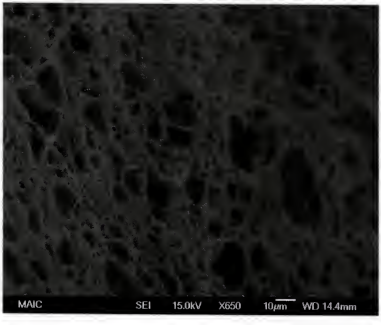

(a)

(b)

Figure 5-6. Scanning electron spectra of phenolic resin (P13470) with different pyrolyzing temperatures (c) P13470-500 : 500°C for 1h (d) P13470-700 : 700°C for 1 hour

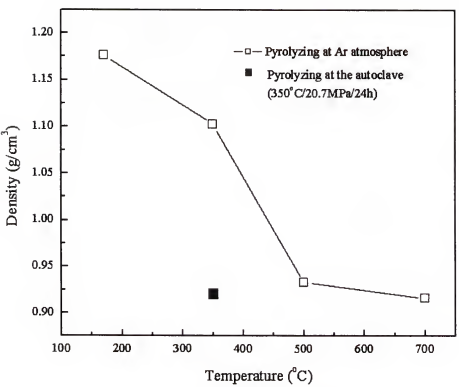

Figure 5-7. The variation of the density of P13470 with different pyrolyzing conditions.

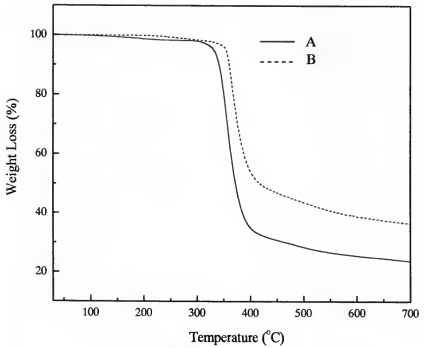

Figure 5-8. TGA curve of cured epoxy resins (A) DER383® (B) DEN431® in Ar atmosphere.

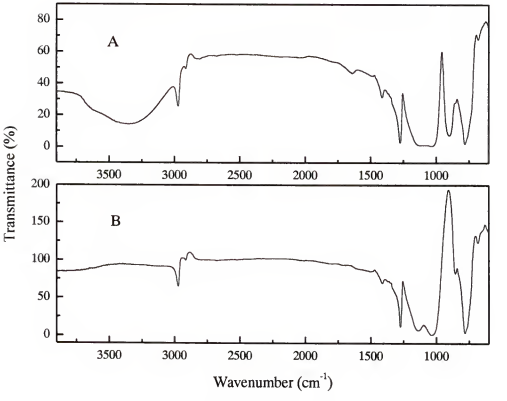

Figure 5-9. FTIR spectra of Poly (methylsilsesquioxane)s (A) PMSSQ-A: after aging at room temperature for 2 weeks (B) PMSSQ-C: after curing consecutively at 130, 250, and 400°C for 4 hours.

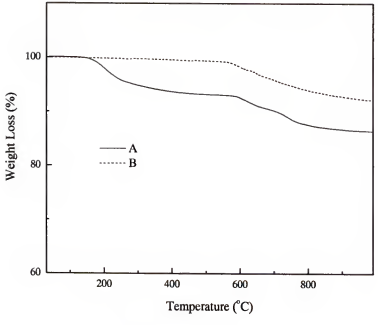

Figure 5-10. TGA curves of Poly (methylsilsesquioxane)s (A) After aging at RT for 2weeks (B) After curing consecutively at 130, 250, and 400°C for 4 hours.

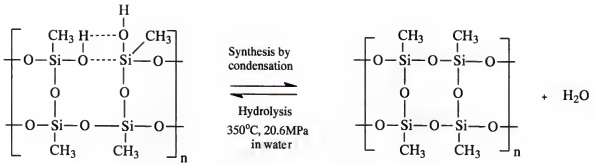

Figure 5-11. The estimated hydrolysis reaction of PMSSQ cage structure under near-critical water condition

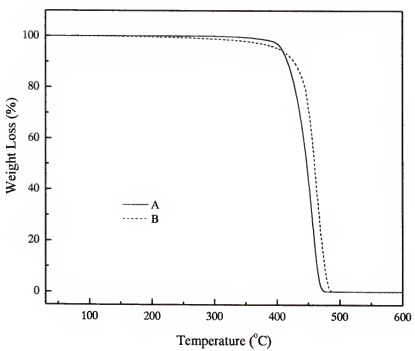

Figure 5-12. TGA curve of (A) HDPE, (B) HDPE6940 (HDPE irradiated by 6940KGy)

Figure 5-13. SEM image for the fracture surface of HDPE6940 after the autoclave test.

Table 5-3. The gel content and the swelling ratio of irradiated HDPEs.

Gamma irradiation	6940KGy	2710KGy	1390KGy	940KGy	670KGy
Gel content (%)	85.9	80.7	73.3	65.5	61.1
Swelling ratio	1.8	-	2.0	-	-

Table 5-4. CHN element analysis for irradiated HDPEs

Element / Material	C [w%]	H [w%]	N [w%]
HDPE	87.34	16.12	0.02
Irradiated HDPE (940 KGy)	83.03	14.32	0.03
Irradiated HDPE (1390 KGy)	83.31	13.81	0.07
Irradiated HDPE (2690 KGy)	83.34	14.08	0.03
Irradiated HDPE (6940 KGy)	83.41	14.21	0.83

CHAPTER 6
A CRITICAL FACTOR THAT DETERMINES THE HYDROTHERMAL STABILITY OF CROSS-LINKED POLYETHYLENES (XLPES) AT NEAR-CRITICAL WATER CONDITION

6.1 Introduction

The previous Chapter 5 comprised a literature survey and review, as well as screening candidate polymeric materials that would be potentially suitable for the second approach in new BPRA system. The result indicated that high irradiation HDPE and phenolic resin provided acceptable thermal and hydrothermal stability (350°C, 20.7MPa), which is possible to apply to new polymer based BPRA system. However, it is expected that cross-linked polyethylenes would be better candidate material due to their high hydrogen content (>14w%).

Near- or supercritical water is known as a good solvent and a reaction medium for the chemical recycling of polymer waters. Fang et al.[9,45], Sasaki et al. [34], Arai et al. [7,8] and Smith et al. [37] have studied phase behavior and reaction phenomena of polymer plus water systems. In their work, a homogeneous phase was found for condensation polymer such as polyethylene terephthalate (PET), nylon and cellulose in near- or supercritical water. However, polyethylene could dissolve in supercritical water only after it decomposed above 565°C [45]. Sako et al. also reported that the polyethylene main chain did not decompose at supercritical condition (380°C) [22]. Moriya et al. represented that the rate of supercritical water cracking in polyethylene is quite lower than that of thermal cracking [23]. They explained these phenomena because the water molecules intervene between the active molecules formed from the decomposition of HDPE. These

indications have challenged us to fabricate the cross-linked structure by using hydrothermally stable polyethylene linkages that would survive in severe autoclave condition.

At the molecular level, polyethylene surface should resemble that of a crystalline long chain alkane. In this point, it seems reasonable that the absorption of small molecules on molecular solids should give information relevant to the interaction potential between such molecules and a polymer surface. When a molecule such as hexane is placed in water, no appreciable hexane-water bonding occurs. Water only tries to interact with itself. Water forms a highly ordered structure (clatherate) around hexane molecules [48]. Moreover, polyethylene has its simplest form consisting of a long backbone covalently bonded carbon atoms with a pair of hydrogen atoms. Highly concentrated hydrogen (>14 w%) in PE structure took an advantage to expect more moderadation effect when used as matrix of burnable poison material.

These indications have challenged us to fabricate the cross-linked structure by using hydrothermally stable polyethylene linkages that would survive in severe autoclave condition. For cross-linked PE in water, the water incorporated in PE is mostly in the form of isolated molecules. [49]. It is difficult to expect any hydrolysis reaction at this condition.

Generally, the cross-linked structure can be introduced to polyethylene either by conventional chemical means, usually involving silanes or peroxides, or by exposure to ionizing radiation from either radioactive sources, or highly accelerated electrons.

Peroxide XLPE: The peroxides provide a source of free radicals when heated above their decomposition temperature. These free radicals are capable of extracting hydrogens

from the polyethylene backbone, thus transferring the free radical site to the polyethylene. Finally, two polyethylene chains get together and form crosslinking structures [97].

Silane XLPE: The way of making crosslinkable polyethylene through the silane method is the grafting of a silane on to the polyethylene and subsequently followed by the condensation reaction by moisture. A silane molecule has four potential sites to be cross-linked, so that up to 4 polyethylene molecules may be joined at any crosslinking points. This is the benefit to make consistent and uniform crosslinking structure [97].

E-beam XLPE and Gamma XLPE: In this case, free radicals formed on the polyethylene backbone are result of electron beam or gamma irradiation. The most common commercial sources of ionizing radiation are ^{60}Co and ^{137}Cs for gamma irradiation, and electron accelerators for e-beam (beta) irradiation. The irradiation of polyethylene results in the formation of new bonds, free radicals, double bonds, etc., which can react with other atoms or molecules to modify the original polymeric structure such as crosslinking and main-chain scission [90,95].

In this study, Gamma irradiated polyethylenes (Gamma XLPE), which are irradiated high-density polyethylenes, were prepared by exposing to gamma irradiation in a ^{60}Co source to obtain in dose range of between 72 and 6970 KGy. Peroxide XLPE, silane XLPE, and E-beam XLPE were obtained commercially. The purpose of the present work is to investigate a critical factor that determines the hydrothermal stability of XLPE at near-critical water condition. Four different XLPEs having different gel content and swelling ratio were selected to compare and clarify the result. In addition, the optimal gamma irradiation doses of Gamma XLPEs were also determined among the various ranges of irradiation doses. The autoclave test at 350°C and 20.7MPa was performed to

verify the hydrothermal stability of various XLPEs. The polymer network analysis of various XLPEs was carried out by solvent swelling and gel content by the extraction of the sample.

6.2 Experimental

6.2.1 Sample Preparations

6.2.1.1 Silane, Peroxide and E-beam XLPEs

All three commercial PE pipe cross-linked by silane, peroxide and e-beam were purchased by following companies. Silane XLPE commercially named "QuesPEX" was provided by Zurn Corporation. Peroxide XLPE was from Golan Plastics and E-beam XLPE pipe called " DURA-PEX " was supplied by CPI Corporation.

6.2.1.2 Gamma irradiated HDPE

Sheets of 1/16" thickness HDPE were purchased from US Plastic Co, USA. After cutting to 12"x12" square, they were irradiated in a ^{60}Co facility, in air, at room temperature. Five dose rates, 0.5, 7.0, 10.4, 20.2, and 51.7KGy/h determined with radiochromic film (FWT-60-00) dosimeter were selected in this study as shown in Figure 5-1. The total doses were from 72 to 6940 KGy depending on the radiation time of 6 days and 8 weeks.

6.2.2 Characterizations

A FTIR technique (Nicolet MAGNA 760 FTIR Bench) equipped with a conventional DTS detector in the wavenumber range of 4000–600cm^{-1} was performed to verify various XLPEs, and to correlate the structural changes between the irradiated and unirradiated samples. The degradation experiment at the near-critical water (350^{o}C/20.7MPa) was performed in a custom-built autoclave. The total charge of water was 50mL. The autoclave was maintained at 350^{o}C for 24 hours. Each sample was run

three times at the same condition and an average value was determined. Thermal stability of candidate materials was tested by thermal gravimetric analysis (TGA). Hydrothermal stability in near-critical condition (350°C/20.7MPa) was performed by custom-built autoclave constructed in our laboratory. FTIR technique was also used to characterize the structural change for Gamma XLPEs that have various ranges of irradiation doses.

The crystalline behaviors of semi-crystalline HDPE and XLPEs were studied with differential scanning calorimeter (DSC).

A polymer network analysis was carried out by solvent swelling and extraction of the sample under refluxing p-xylene (bp 139°C). The hydrogen content was measured by a conventional combustion technique, i.e., The CHN Carlo Erba microanalyser. Tensile properties were evaluated by using an Instron machine.

6.3 Results and discussion

6.3.1 Characteristic Properties of Irradiated HDPE (Gamma XLPE)

The use of radiation in the processing of polymers is receiving increasing interest because it can be suggested as an alternative to the traditional chemical methods to modify the molecular structure of polymers. Several studies on gamma-radiation-induced modifications of polymers have been reported [95]. It is well known that the main effect of the interactions between gamma rays and polymers is the formation of free radicals, whose further evolution can cause scission, with decrease in the molecular weight, and chain branching, with increase in the molecular weight up to crosslinking [90]. Usually both processes (crosslinking vs. scission) take place simultaneously, the prevalence of each depending on many factors which can affect the concentration of the reactive species and, consequently, the kinetics of the reactions involved [90,98,99].

Generally, polymers can be divided into two types: those which predominantly cross-link when exposed to radiation, and those which undergo primarily chain scission. Radiation can affect the molecular weight in two ways. Crosslinking leads to an increase in molecular weight while scission decreases molecular weight. Polyethylene, polypropylene, poly (methyl acrylate), polystyrene, etc., belong to the former, and polyisobutylene, poly (methyl methacrylate) (PMMA), poly (vinyldine chloride), polycarbonate, etc., belong to the latter [98,99].

Polyethylene used in this study is predominated by crosslinking. The degree of crosslinking and degree of degradation (i.e., chain scission and oxidation) are directly proportional to the radiation dose [90]. Therefore, highly cross-linked polyethylene with high gamma irradiation can maintain their shape and useful properties at high temperature application – i.e., they do not flow. The radiation dose carried out in this study is up to 6940KGy that is not practical to use in other application. However, it is focused on high-energy irradiated polyethylene because it is expected that the higher cross-linked structures will enhance the hydrothermal stability.

After crosslinking by gamma irradiation, the color of the HDPE cross-linked in air turned from white to yellowish brown and the discoloration increased with dose as shown in Figure 6-1. The experiment, which is carried out in air atmosphere, increases the effect of oxidation reaction especially at the surface.

The oxidation reaction was clearly observed by FTIR spectra in Figure 6-2. The carbonyl peak increased with the increase of irradiation dose. The carbonyl group indicating the oxidative degradation rapidly increased at the irradiation dose above 940 KGy.

The oxidation index was calculated by the following equation.

$$\text{Oxidation index} = \frac{A_{1712cm^{-1}}}{A_{1463cm^{-1}}}$$

Where, $A_{1712cm^{-1}}$ is the absorption peak of carbonyl group (-C=O) and $A_{1463cm^{-1}}$ is the absorption peak corresponding to scission motion of methyl or methylene groups (H-C-H) which may be one of most stable bands in their structure. The intensity of carbonyl group at 1712cm^{-1} was normalized to the absorption peak at 1463cm^{-1} as an internal standard as shown in Table 6-1, since as thicken the sample thickness, the absorption intensity is increased according to Beer-Lambert law [100,101].

The oxidation index rapidly increased at 740KGy irradiation dose. The gamma irradiation in the air easily induces carbonyl formation, accompanied by the molecular chain scission, leading to the decrease in crystallinity and melting temperature. The crosslinking reaction, which forms a three-dimensional network structure, simultaneously occurs at the high radiation dose.

The destruction of crystallinity was one of major effects during the irradiation. DSC curves of T_c and T_m in HDPE, which are before and after irradiation in air, are presented in Figure 6-3. The influence of the radiation dose on the thermal parameters (melting temperature, crystallization temperature and crystallinity degree) of HDPE is shown in Table 6-2. The melting and crystalline temperature of HDPE decreased with the increase of the dose. However ΔH_f and ΔH_c, which indicate the area of melting and crystalline peak became wider and decreased as increasing the dose.

It is difficult to generate the cross-linked network structure in crystalline regions because the crystalline structure is closely packed with lamellar structures and the

radicals formed in this region hardly escape to outside [90]. However, at the high radiation dose, one is able to reduce the cage effect and induce the decrease of crystallinity in semi-crystalline PE structure. At the low dose, crosslinking reaction dominantly occurred at the amorphous region and tie molecules, which is located outside of crystalline region due to capturing the radical species in crystalline region. However, with high dose above 1500 KGy, the crystallinity indicating "the thickness and long-range ordering of crystallites" apparently decreased in agreement with the result in DSC measurements.

Gamma irradiations strongly influence on the mechanical properties of HDPE as summarized in Table 6-4. Young's modulus rapidly increased when it was irradiated by 150KGy dose. It has almost reached to maximum value, which is closed to HDPE irradiated with 6940KGy dose. This result is corresponding to that of Elongation at break as shown in Figure 6-4.

6.3.2 Polymer Identification

In this study, four different cross-linked polyethylenes (XLPEs) containing quantatively different gel content and swelling ratio were selected to observe a critical factor to determine the hydrothermal stability at the near-critical water. They formed the network structure by Silane, Peroxide, E-beam and Gamma methods. Their chemical structures were verified by FTIR as shown in Figure 6-5. The crosslinking of silane XLPE was achieved between polyethylene backbones to form Si-O-Si structure with the loss of water and the evidence of Si-O and Si-C bands was represented at $1590cm^{-1}$ and $1367cm^{-1}$ respectively in Figure 6-5a. All other XLPEs showed the similar spectra because they were constituent with only hydrocarbon in their structure. For peroxide XLPE (Figure 6-5b), the OH band at $3450cm^{-1}$ was obtained by poly (ethylene vinyl

alcohol) (EVOH) because manufacturers usually added them to provide the excellent gas barrier features to give blocking features against oxygen and carbon dioxide. The XLPE by gamma irradiation in Figure 6-5d showed the characteristic peak at 1700cm^{-1} representing a carbonyl bond (C=O) due to the degradation by oxidative reaction.

6.3.3 A Critical Factor that Determines the Hydrothermal Stability of XLPEs

After the autoclave test, HDPE cross-linked by gamma irradiation (Gamma XLPE) above 940 KGy and silane XLPE showed the reasonable hydrothermal stability as shown in Table 6-4. Based on visual observation, Gamma XLPE irradiated by above 940 KGy showed a smooth surface and silane XLPE also showed a good shape that hardly finds any difference before and after the autoclave test. However, all other samples softened or decomposed after the test.

Interestingly, Gamma XLPE with 940 KGy and 1390 KGy showed most stable hydrothermal stability with the weigh loss less than 1.3 w%. With further irradiation dose, their weight loss after the autoclave test increased. Gamma XLPE 6940 KGy showed much higher weight loss with 5.6w%. This result indicated that the small chain segments, which are formed by chain scission, are dissolved in the water during the autoclave test. This result well corresponds to that of TGA experiment in Figure 6-6 and oxidation index in Table 6-1. The thermal stability of virgin HDPE and various XLPEs was measured by TGA in Ar atmosphere. All specimens showed approximately the same TGA diagram, which has the ceiling temperature around 450°C. However, the weight loss of Gamma XLPE has started to occur at low temperature region due to the evaporation of small molecules formed by the chain scission reaction. The oxidative degradation induced by chain scission reaction would be main degradation reaction especially in high dose range. The oxidation index rapidly increased at 2740KGy representing the dominant oxidative

degradation by chain scission reactions. It must be concluded from these result that the gamma irradiation dose between 940 KGy and 1390 KGy would provide the optimum hydrothermal stability under the autoclave condition. Silane XLPE also showed the excellent hydrothermal stability under the autoclave condition.

The study of the solubility and gel fraction of polymers is a good method to understand polymeric structure, which is cross-linked chemically or irradiated [90-93]. In this study, four different cross-linked polyethylenes containing quantatively different gel content and swelling ratio were selected to find a critical factor that determines their hydrothermal stability at near-critical water condition [92-94].

The gel content is a relative measurement to observe the homogeneity of the polymer network and the solvent ratio is relative measurement of the network strength of the gel fraction [92-94]. As shown in Table 6-5, the gel content increased with the increase of irradiation dose, Gamma XLPE with 1390 KGy and 6940 KGy showed very small swelling ratio representing a lower solvent uptake into their network structures. These properties are directly affected to hydrothermal stability of Gamma XLPEs.

Silane XLPE also showed the small swelling ratio representing the strong network strength. The swelling ratio might more directly affect the hydrothermal stability of XLPEs and this is the reason that Silane XLPE and Gamma XLPE with a high gamma irradiation survived in the autoclave test.

Silane XLPE contained "silane molecules" and one silane molecule supplies four potential sites to be cross-linked to form strong network structures as shown in Figure 6-7b. For Gamma XLPEs, hydrothermal stability increased with the increase of dose due to their high gel content and small swelling ratio. Their estimated structures are shown in

Figure 6-7a. Meanwhile, Peroxide XLPE is usually manufactured in a hot extruder and crosslinking on the melt leads to homogenous distribution of links. Figure 6-7c represented homogenous network structures of Peroxide XLPE. In Table 6-5, the gel content of peroxide XLPE was about 88w%, which has the highest value among various XLPEs. However, peroxide XLPE dissolved at the autoclave condition due to its weak network strength. In the mean while, even though silane XLPE had only 75w% gel content, it showed very stable hydrothermal property at the autoclave condition because they had small swelling ratio, which means the strong network strength.

The major product of irradiation is hydrogen, and the evolution of each hydrogen molecule is accompanied by the formation of double bond C=C in the main chain, or by the linking together of two molecules ether side by side (crosslinking) or end (endlinking) [95,96]. With the highly concentration of hydrogen in PE structure, it would be expected the more moderadation effect. To obtain precise data, CHN analysis was performed three times for each sample and the average value were described in Table 6-6. As expected, the hydrogen content decreased with the increase of irradiation dose. Approximately 2w% hydrogen decreased with 940 KGy of irradiation and there was no significant change after this value. This result also supported that chain scission would be more dominant above 940 KGy irradiation dose.

6.4 Summary

In a literature review, Fang et al. reported that the spherule of polyethylene began to expand at above 450°C and underwent a color change to red at about 570°C in supercritical water condition. It was also found that the rate of supercritical water cracking in polyethylene is quite lower than that of thermal cracking. This implies that polyethylene linkage is more stable at near- or supercritical water condition than that in

inert atmosphere. These phenomena are possibly explained because the water molecules, which are intervening between the active molecules, formed from the decomposition of HDPE. These indications have challenged us to fabricate the cross-linked structure by using hydrothermally stable polyethylene linkages that would survive in severe autoclave condition. Our proposed idea was proven in this study. The result showed that polyethylene, which has highly cross-linked network structure, i.e., Gamma XLPE above 940 KGy dose and Silane XLPE, survived at the autoclave condition. From TGA and autoclave test, it was also proven that the gamma irradiation dose between 940 KGy and 1390 KGy could provide the optimum hydrothermal stability at the near-critical water condition.

Moreover, four different cross-linked polyethylenes containing quantatively different gel content and swelling ratio were selected to find a critical factor that determines their hydrothermal stability at the near-critical water. The result indicates that the solvent ratio representing the network strength is more critical factor to determine the hydrothermal stability under near-critical water condition.

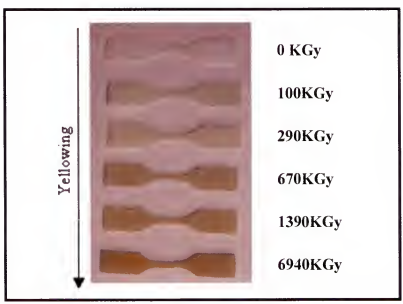

Figure 6-1. The discoloration of cross-linked HDPE series with irradiation dose.

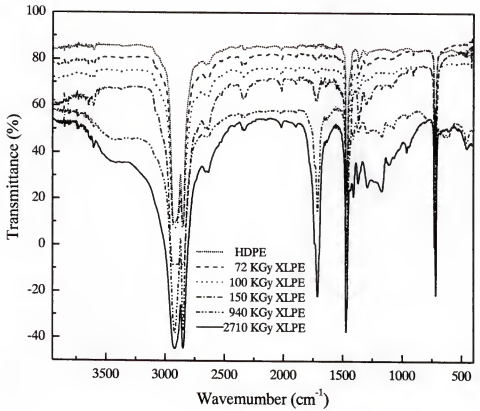

Figure 6-2. FTIR spectra of virgin and irradiated XLPEs.

Table 6-1. The oxidation index for various Gamma XLPEs.

Sample	$A_{1650\ to\ 1800cm^{-1}}$	$A_{1420\ to\ 1550cm^{-1}}$	Oxidation index
Virgin HDPE	0.053	10.713	0.005
72 KGy XLPE [1]	0.334	11.387	0.029
150 KGy XLPE	0.398	11.873	0.033
740 KGy XLPE	12.315	24.622	0.500
940 KGy XLPE	23.800	35.762	0.665
2710 KGy XLPE	28.276	26.949	1.049

[1] It is indicated that "cross-linked by gamma irradiation with 72 KGy dose".

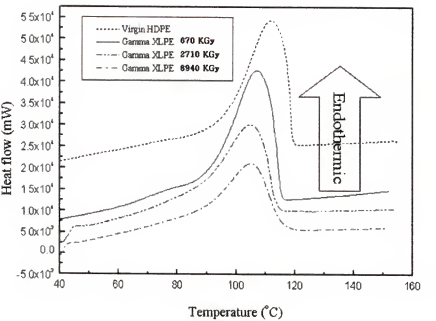

(a)

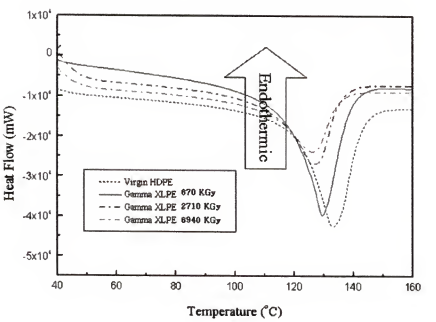

(b)

Figure 6-3. T_m endotherm peaks and T_c exotherm peaks of virgin and irradiated HDPEs with different radiation intensity.

Table 6-2. Melting temperature, crystallization temperature, ΔH_f and crystallinity of the HDPE before and after gamma irradiation.

Samples	T_m	T_c	ΔH_f	% Cryst
HDPE	133.2	112.1	253.2	87.3
Gamma XLPE (670KGy)	129.5	107.1	241.0	83.1
Gamma XLPE (2710 KGy)	127.0	105.0	199.0	68.6
Gamma XLPE (6940 KGy)	126.0	104.0	172.6	59.5

Table 6-3. Mechanical properties of virgin HDPE and Gamma irradiated HDPE.

Samples	Young's Modulus	Break Stress	Stress At Yield	Strain At Break	Strain At Yield	El At Break	El. At Yield
HDPE	695.667	34.542	25.419	7.275	0.071	178.087	1.724
150 KGy	993.609	22.916	22.916	0.050	0.050	1.215	1.215
670 KGy	1049.127	25.758	25.751	0.056	0.053	1.361	1.293
1390 KGy	1027.758	26.581	26.565	0.058	0.057	1.420	1.388
2710 KGy	1063.889	28.551	28.550	0.060	0.059	1.466	1.440
6940 KGy	1114.687	30.153	30.153	0.056	0.056	1.373	1.373

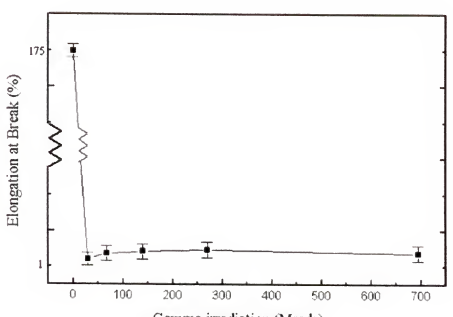

Figure 6-4. Elongation at break of virgin HDPE and irradiated HDPE.

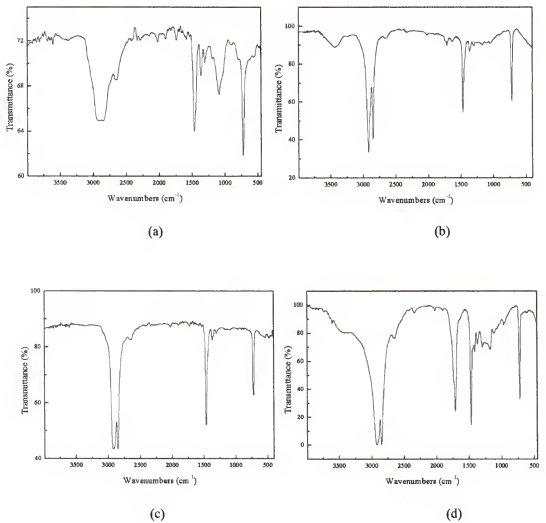

Figure 6-5. FTIR spectra for 4 different XLPEs by (a) silane (b) peroxide (c) E-beam and (d) Gamma irradiated HDPE (2710KGy).

Table 6-4. Autoclave test for various XLPEs

Sample	Weight loss during autoclave test (w%)
Gamma XLPE (6940KGy)	5.6
Gamma XLPE (2710KGy)	3.5
Gamma XLPE (1390KGy)	0.3
Gamma XLPE (940KGy)	1.3
Gamma XLPE (670KGy)	6.5
Silane XLPE	0.2
E-Beam XLPE	Decompose or soften
Peroxide XLPE	Decompose or soften

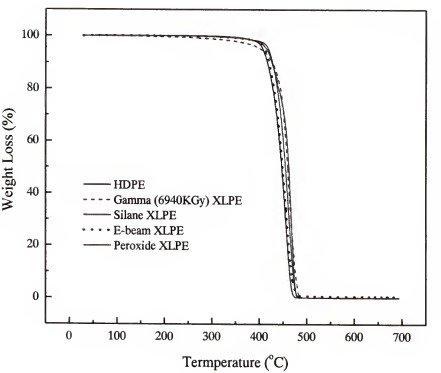

Figure 6-6. TGA diagram for HDPE and various XLPEs.

Table 6-5. The swelling ratio of various XLPEs.

Polymers	Gel content (%)	Swelling ratio
E-beam XLPE	71.4	9.0
Silane XLPE	75.4	3.3
Peroxide XLPE	88.8	6.4
Gamma irradiated HDPE (1390KGy)	73.2	2.0
Gamma irradiated HDPE (6940KGy)	85.4	1.8

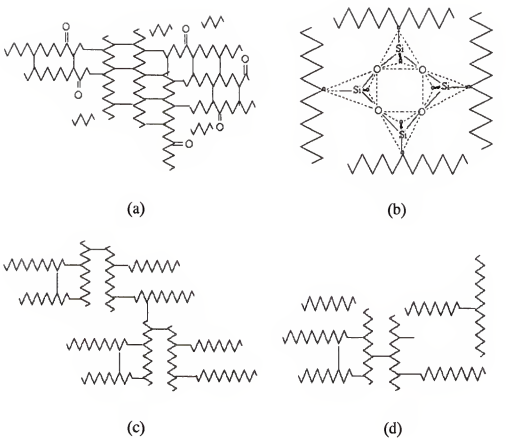

Figure 6-7. A cartoon of the cross-linked structures of (a) Gamma XLPE (6940 KGy) (2) Silane XLPE (3) Peroxide XLPE and (4) E-beam XLPE

Table 6-6. CHN element analysis for 4 different XLPEs

Element / Material	C [w%]	H [w%]	N [w%]	Total [w%]
HDPE	86.51	16.12	0.03	102.66
Gamma XLPE (940KGy)	83.43	14.32	0.03	97.78
Gamma XLPE (1390KGy)	82.88	14.30	0.07	97.25
Gamma XLPE (2690KGy)	83.34	14.08	0.03	97.37
Gamma XLPE (6940KGy)	83.41	14.21	0.83	98.45
Silane XLPE	83.49	14.55	0.04	98.04
Peroxide XLPE	85.80	15.70	0.10	101.50
E-beam XLPE	86.45	15.82	0.16	102.43

CHAPTER 7
PHYSICAL PROPERTIES OF HIGH GAMMA IRRADIATED HIGH-DENSITY POLYETHYLENE (HDPE) / GRAPHITE COMPOSITE

7.1 Introduction

Screening candidate polymeric material was based on thermal and hydrothermal stability in previous chapters. Cross-linked polyethylene had a low ceiling temperature (~450°C), which does not fulfill the requirement of the high temperature stability above 500-600°C required by the temperature rise associated with neutron adsorption and low thermal conductivity. Therefore, the development of thermally conductive polymer system still remains an important endeavor to commercialize new polymeric BPRA system.

The maximum centerline temperature within the BPRA is especially important for selection of a polymeric BPRA because most polymers have low ceiling temperature above, which they completely and rapidly revert back to their monomers or constituent species. Therefore, polymeric materials should possess an appropriate thermal conductivity to avoid the thermal degradation because centerline temperature could exceed their ceiling temperature.

Typical thermal conductivity values for some materials concerned in this study are 0.2 to 0.3 for polymers, 39 for alumina and 600 for graphite (all values in W/mK). High-density polyethylene (HDPE) shows a higher value (0.5 W/mK) in polymers due to its high crystallinity. The thermal conduction of polymers depends on the degree of crystallinity. A polymer with a highly crystalline and ordered structure will have a greater

conductivity than the equivalent amorphous materials. This is due to the more effective coordinated vibration of the molecular chains for the crystalline state [102]. However, the thermal conductivity possessed by HDPE is only slight higher than that of other polymeric materials.

A composite is combined material created by synthetic assembly of two or more compounds such as selected filler or reinforcing agent and compatible matrix binder to obtain specific characteristics and properties. The addition of high conductive filler material such as graphite would be a promising method to figure out the problem related to the high centerline temperature in polymeric BPRA system. There are many references in the literature concerning adding various conductive carbon fillers such as graphite, carbon black and carbon fiber to a polymer matrix to produce a more thermally and electrically conductive material [103-109]. King et al. reported that synthetic graphite particles showed the largest increase in composite thermal conductivity among various carbonaceous fillers [108,109].

In this study, up to 60w% graphite powder was formulated into a HDPE matrix to increase the thermal conductivity before gamma irradiations. It is not a critical issue that polymeric burnable poison material has weak mechanical properties for new BPRA system. Due to the high hydrogen content, the composite system with 60w% graphite still has about 6w% hydrogen content, satisfying our criteria discussed earlier. The calculation of the maximum temperature (Tcl) also was modeled using Monte Carlo Neutron Photon Transport Code (MCNP) energy deposition tally [5].

It is difficult to prepare well-dispersed HDPE/graphite composite containing over 35w% of graphite using a conventional mixer or extruder. To overcome this limitation,

Calleja et al. have prepared the composite by dry mixing as powder form and compress molding consecutively [110]. The small particle size of fillers should be more effective to increase the thermal conductivity due to their high surface area with the connection to increase possibility to contact for each particle [111].

Aside from mainly increase in thermal conductivity, the incorporation of an inorganic material into a polymer will exhibit a wide range of multifunctional properties. For instance, the interaction between graphite and polyethylene matrix after the exposure in high gamma irradiation circumstances might generate additional advantages for their properties. Electrical conductivity, thermal resistance, and heat distortion temperature are also observed in this study.

7.2 Experimental

7.2.1 Sample Preparations

7.2.1.1 Materials

The powder form of HDPE was obtained from Clariant Corp. The density, molecular weight (M_w), melting point and softening point are 0.958g/cm^3, 80,000g/mol and 134°C, respectively. The particle size range was 60-95μm. The natural crystalline flake type of graphite powders (Micro 850) were supplied from Asbury Graphite Mills Corp. They showed 98.5% of carbon content and 2.24g/cm^3 of density. The particle size of the graphite filler was 5μm.

7.2.1.2 Composite and dogbone specimen fabrication

The different content of graphite (85/15, 70/30, 55/45 and 40/60 of HDPE/graphite) was applied and maximum graphite content was 60w% because of requiring minimum hydrogen content (5w%). The HDPE powder and fillers were first dry-mixed in a mechanical mixer for 5 mins to achieve a reasonable uniform dispersion, and then spread

in a 5inch x 5inch aluminum mold. The mold was placed in Carver hydraulic presser and heated to 170°C. A pressure of 1,000 psi was applied and held for 3 mins to completely melt the HDPE. To increase the specimen uniformity, all composite sheets have been cut in half, stacked and subsequently remolded (3 times). After fabricating sheets of composite with the dimension of 5inch x 5 inch x 0.3inch, they were cutting to donebone shape by using a metal puncher designed by ASTM 638-M-3.

7.2.1.3 Gamma irradiation

The dogbone specimens were mounted on the board as described in Figure7-1. After preparing, they were placed into ^{60}Co chamber at room temperature in air atmosphere to get a gamma irradiation. The radiation dose rate in this experiment was explained in Table 7-1.

7.2.2 Characterizations

Four-point probe method was used to measure the electrical conductivity. Four electrodes are placed on the same sample surface, two are used to pass current and two to sense voltage. The laser flash method was used to measure thermal diffusivity. The front face of a right cylindrical sample was instantaneously heated using an intense laser pulse and then measured the temperature rise on the back face with respect to time. The experiment was performed by averaging the signals obtained in 20-100 laser shots. The averaged signal as a function of time was transferred to a microcomputer and then fitted to a theoretical expression to give the thermal diffusivity (D). The thermal conductivity (K) of the sample was calculated from the relation, $K = dC_pD$, where d is the density and C_p is the specific heat.

A FTIR technique (Nicolet MAGNA 760 FTIR Bench) equipped with a conventional DTS detector in the wavenumber range of 4000–600cm^{-1} was performed to

verify various XLPEs, and to correlate the structural changes between the irradiated and unirradiated samples. FTIR spectra were obtained from pellets containing 2 mg sample in approximately 100 mg potassium bromide (KBr). Thermal stability and weight loss at elevated temperature was analyzed under an Ar atmosphere using a TGA2050 thermal gravimetric analyzer from TA instruments. The heating rate was 5°C/min. Flow rate was fixed at 130 mL/min and sample size was 5.00–10.00 mg. The degradation experiment in near-critical water (350°C/20.7MPs) was performed in a custom-built autoclave. The total charge of water was 50mL and the autoclave was steadily maintained at 350°C for 24 hours. Each sample was run three times at the same condition and the result took an average value. Hydrogen content was measured by a conventional combustion technique, named CHN Carlo Erba microanalyser. Scanning electron microscopy (SEM) was employed to observe the fracture surface of the composites. Tensile properties were evaluated by using an Instron machine.

7.3 Results and Discussion

It is well known that the electrical conductivity of composites depends on the dispersion state of conducting particles in a matrix polymer. Many researchers have studied the electrical conductivity of the composites containing randomly dispersed conducting particles in an insulating polymer matrix [106,110-113]. The drastic increase of electrical conductivity was observed around a particular concentration of the filler. This concentration is generally called percolation concentration. Generally, at least one infinite cluster of particles is formed in polymeric matrix. This cluster penetrates throughout the sample while the particles in the cluster are in close contact and represents a conductive path for a movement of electrons throughout the sample. In the case of HDPE, the percolation concentration is dependent on particle size and shape of conducting particles

[106,111]. In this study, fine natural crystalline flake type of graphite particles with the size of 5μm was used to magnify the increase of thermal conductivity.

Figure 7-2 showed the fracture surface of composite materials prepared in this study. The specimen was prepared in the liquid nitrogen to get a flat fractured surface. The graphite particles homogeneously dispersed at the entire region for all compositions. The graphite particles were placed by the form of flake with about 5μm of particle size and each particles were closely contacted together when the graphite content was reached to over 45w% as shown in Figure 7-2 (c) and (d). After obtaining the desired gamma irradiation (5254 KGy dose), there was no significant difference between the samples before (Figure 7-3) and after (Figure 7-4) the gamma irradiation.

As shown in Figure 7-4, the fracture surface of 70/30 HDPE/graphite followed highly ductile fracture with the formation of necking, thus it is difficult to find micrographs of graphite powers on the fracture surface without quenching. Therefore, all specimens in Figure 7-3 obtained the fracture surface after quenching the specimen into liquid nitrogen. However, after the gamma irradiation, the tensile fractured specimens were used without further treatment because each specimen follows more brittle fracture without any plastic deformation due to the chain scission and crosslinking reaction by a high gamma irradiation.

This result is well corresponding to that of elongation at break as shown in Figure 7-5. The dependence of elongation at break on the graphite content is very critical as shown in Figure 7-5a. The elongation at break stiffly diminished when the graphite content was only 15w% and kept decreasing up to 60w% graphite content. Young's modulus increased as the increase of graphite content due to the high modulus of graphite

(Figure 7-5a). After the gamma irradiation (5420KGy), the elongation at break of pure HDPE rapidly dropped from 178 mm to 1.4 mm. Each specimen displayed more brittle fracture without any plastic deformation than that of the sample untreated due to the chain scission and crosslinking reaction by a high gamma irradiation.

The dependencies of relative electrical conductivity of HDPE/graphite composites representing before and after irradiation versus volume portion of the filler are shown in Figure 7-6. All samples seen in Figure 7-6b were cross-linked by 5254 KGy gamma irradiation. In all cases (Figure 7-6a,b), the electrical conductivity dramatically decreased around 21.8v% (45w%) filler content. This result is corresponding to that of SEM morphology presented in Figure 7-3. The influence of high gamma irradiation on the electrical conductivity of HDPE/graphite composites was not significant when they were compared to that in Figure 7-6b.

The thermal conductivity in HDPE/graphite composite was measured by ASTM E1461. The mechanism of thermal conductivity is somewhat different from that of electrical conductivity. The thermal conduction of solids is fairly well understood on the basis of the transport of phonons and electrons considering various scattering processes for heat carriers, especially in the case of single-phase nearly perfect crystals. Concerning thermal transport in heterogeneous solids, however here are numerous problems for further study. There are two kinds of approaches for understanding the thermal conduction of heterogeneous solids. One is the connection between thermal resistances of composite solids. In other approach the disturbance of heat flow through a medium by the presence of the regions of different thermal conductivity is considered [114,115]. It is concentrated on the particle-dispersed medium in this study that is the simplest example

of heterogeneous systems. It can be seen in many experimental studies for the thermal conductivity that have been carried out for various combinations of medium and particles [108,109,116-120]. Nakamura et al. reported that the thermal conductivity changes with the increase of particle content at first linearly and then more rapidly [118]. Krupa et al. showed the thermal conductivities of HDPE/graphite composite [106]. Two grade graphite was used. KS graphite was smaller and narrower than KS graphite. The blends were prepared by mixing both components in a 50mL-mixing chamber of Brabender Plasticorder PLE 331 at 200°C for 10 min at the mixing speed 35rpm. As shown in Figure 7-7, a nonlinear increase of thermal conductivities was observed with an increase in graphite content up to 29.1v% (60w%). The thermal conductivities of composites filled with graphite KS were higher than the thermal conductivity of material filled with the same concentration of graphite EG. The highest value of thermal conductivity was 1.8 W/mK with 60w% graphite KS.

HDPE showed relatively higher thermal conductivity, 0.5 W/mK when compared to other polymeric materials due to highly crystalline and ordered structure. However, the portion of ordered crystalline structures in HDPE would decrease as the gamma irradiation dose increases. Moreover, the effect of graphite to increase the thermal conductivity would be more critical to control the entire value of thermal conductivity on composite system. In our study, the thermal conductivity of 40/60 HDPE/graphite had 3.18 W/mK, which is much higher value than Krupa's because we used finer graphite particles (5μm) and prepared well-dispersed HDPE/graphite mixing technique explained in experimental section. After getting the high gamma irradiation (5254 KGy), the

thermal conductivity decreased with the average value, 2.52 W/mK. However, the value further decreased with the value of 0.98 W/mK when it was tested at 350°C.

At the temperature of 350°C, crosslinked polyethylene would be rubbery state, which does not contain any ordered crystalline structures. Moreover, the graphite powder, which forms conductive chains in the matrix at 25°C, would be disconnected or disoriented at this condition. It must be concluded from this result that the HDPE/graphite system is not a good method to figure out the problem related to the centerline temperature in BPRA system.

TGA investigation of HDPE/graphite composite under argon atmosphere is shown in Figure 7-8. The char yields of each sample for both Figure 7-8 and Figure 7-9 represented the graphite content in each composite system, i.e., 15 (b), 30 (c), 45 (d) and 60 (e) w% of graphite. The thermal stability of pure HDPE rapidly increased when it was irradiated by 5254 KGy dose (Figure 7-8a versus Figure 7-9a). The onset temperature of irradiated HDPE (Figure 7-9a) was 20°C higher than that of non-treated HDPE. Before irradiation, the onset temperature of thermal decomposition rapidly increased when added over 30w% of graphite seen in Figure 7-8. After irradiation, the onset temperature of thermal decomposition increased when 45w% of graphite was added (Figure 7-9). The ceiling temperature of irradiated 40/60 HDPE/graphite increased to around 480°C, which was 40°C higher than that of pure HDPE.

7.4 Summary

In this work, the results about the thermal conductivity and electrical conductivity, and heat distortion temperature before and after the gamma irradiation treatment are reported. An influence of both the graphite content and the dose rate was critical to determine to increase the thermal distortion temperature. The ceiling temperature of

irradiated 40/60 HDPE/graphite increased to around 480°C, which was 40°C higher than that of pure HDPE. The maximum value of thermal conductivity was 3.18 W/mK for our system, which is much higher value than Krupa's because we used finer graphite particles (5μm) and prepared well-dispersed HDPE/graphite mixing technique explained in experimental section. However, the thermal conductivity of irradiated 40/60 HDPE/graphite at 350°C was 0.98 W/mK. This result indicated that the HDPE/graphite system was not a good method to figure out the problem related to the centerline temperature in BPRA system. The development of an alternative for polymeric BPRA system, which has much higher thermal conductivity, still remains an important endeavor to make them commercial.

Table 7-1. The radiation dose rate used in this experiment as a function of the distance from the ^{60}Co source

Location	Dose Rate [KGy/hr]	Dose/Day [KGy]	Dose/Week [KGy]	Dose/10 wks [KGy]
1"	3.12	75	525	5254
2"	1.22	29	205	2053
3"	7.00	17	118	1176
4"	3.06	7	51	514
5"	2.27	5	38	381

Figure 7-1. Dog-bone samples mounted on the board before crosslinking in the irradiation chamber.

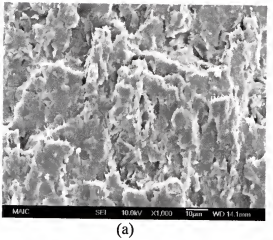

(a)

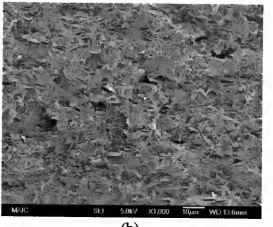

(b)

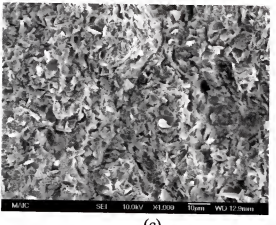

(c)

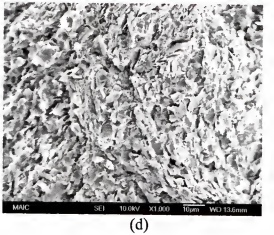

(d)

Figure 7-2. SEM of the fracture surface for HDPE/graphite power composite (x 1000) (a) 85/15 (b) 70/30 (c) 55/45 (c) 40/60 ratio of HDPE/graphite after quenching the samples

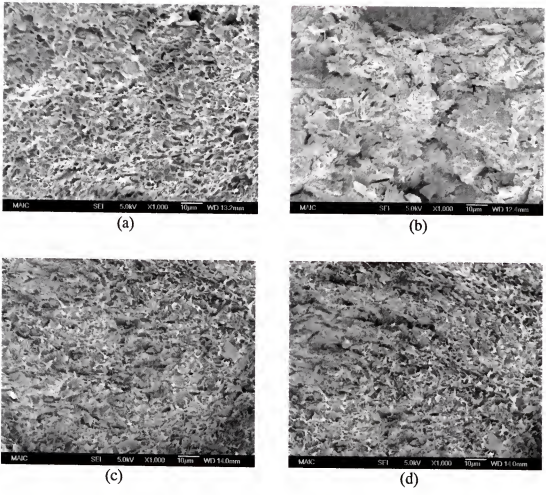

Figure 7-3. SEM of the tensile fracture surface for HDPE/graphite power composite (x 1000) (a) 85/15 (b) 70/30 (c) 55/45 (c) 40/60 ratio of HDPE/graphite after 5254 KGy gamma irradiation (without quenching).

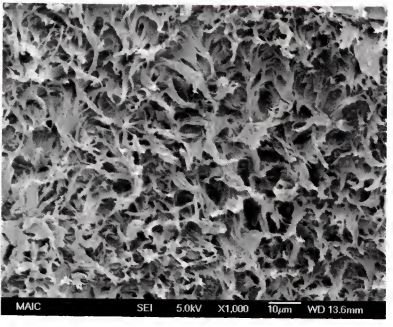

Figure 7-4. SEM of the tensile fracture surface for 70/30 HDPE/graphite (without quenching).

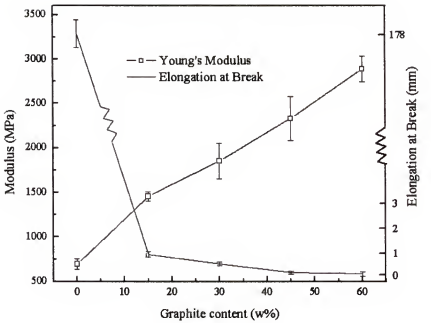

(a)

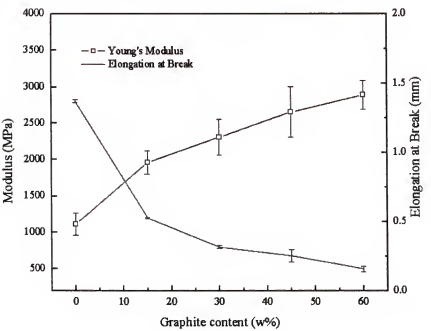

(b)

Figure 7-5. Young modulus and Elongation at break of HDPE/graphite composite on the graphite content (a) before gamma irradiation (b) after gamma irradiation (5420KGy)

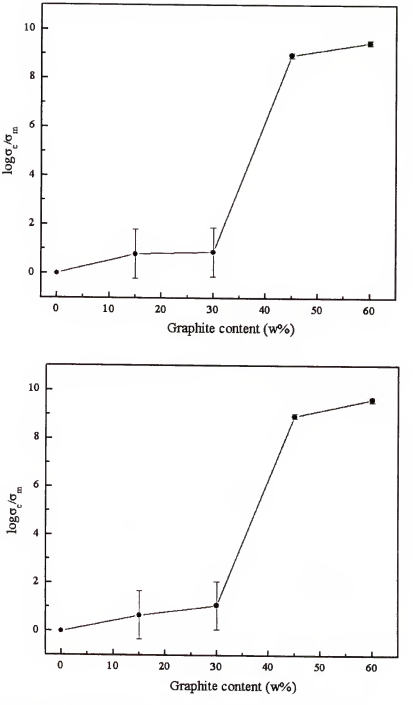

Figure 7-6. Relative electrical conductivity (σ_c/σ_m) of HDPE/graphite composite on the graphite content: (a) before gamma irradiation (b) after gamma irradiation.

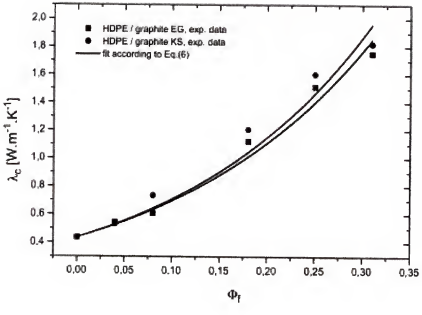

Figure 7-7. Thermal conductivity (λ_c) of the graphite EG (■) and graphite KS (●) filled HDPE graphite on the volume filler content (ϕ_f). Solid lines – curve fitting [106].

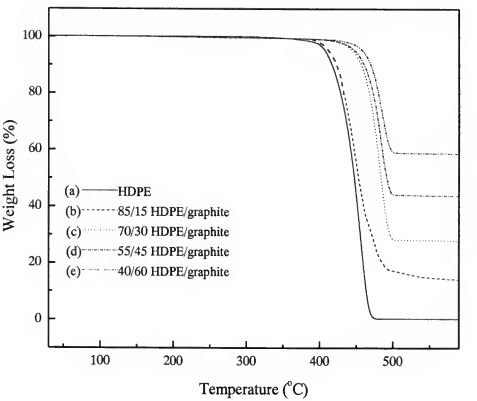

Figure 7-8. TGA thermograms of graphite /HDPE composites.

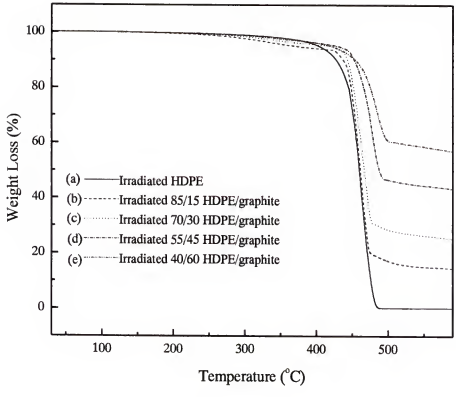

Figure 7-9. TGA thermograms of graphite /HDPE composites after the radiation treatment.

CONCLUSIONS

Understanding the degradation mechanism of polymeric materials, i.e., thermal degradation and hydrothermal degradation, under nuclear reactor environment was essential for advancement to find the candidate polymeric burnable poison material in this study. Poly (diacetylene-siloxane-carborane)s were the starting material to develop new polymer based burnable poison material. However, the degradation of Si-O-Si under near-critical water (350°C, 20.7MPa) was an unfavorable disadvantage. Other silicon based polymer precursors such as poly (diacetylene-siloxane), poly (diacetylenedimethylsilane) and poly (diacetylenedimethylsilylethane) were investigated to overcome the problems currently addressed in poly (diacetylene-siloxane-carborane), i.e., hydrothermally weak siloxane linkages, high cost, limited supply and high boron concentration. However, the result showed even though they formed highly cross-linked network structure, the hydrolysis of Si-O-Si linkage was the starting point to degrade and this reaction could be accelerated by H^+ and OH^- ions under near-critical water condition. Moreover, an unexpected siloxane Si-O-Si linkage generated by the contamination of water was the problem for poly (diacetylenedimethylsilane) thermoset and poly (diacetylenedimethylsilylethane). The result showed that poly (diacetylenedimethylsilylethane) containing less unexpected siloxane linkages improved the hydrothermal stability at the autoclave condition. Therefore, it is necessary to develop a new synthesis method to produce pure poly (diacetylenedimethylsilane) and poly

(diacetylenedimethylsilylethane) for avoiding the hydrolyzing degradation under near-critical water condition.

For the second approach, a number of candidate matrix polymers were screened. Based on a literature survey and review, thermosetting resins such as phenolic resins, epoxy resins, silicone resins and cross-linked high-density polyethylenes were selected as candidate materials in this study. However, it was confirmed that reversible hydrolysis reaction occurred under the autoclave condition for condensation polymers such as epoxy resin and PMSSQ. However, phenolic resins, which also follow condensation reaction during curing process, did not show reversible hydrolysis reaction at this condition. Interestingly, strong condensation reactions preferably occur under high ion concentration condition at the near-critical water, thus generate evolved gas followed by forming a highly ordered pore structure. The dissociation of water itself in this condition generates a sufficiently high concentration of H^+ and OH^-. At this point, we proposed that o-benzoquinone methide would be possibly generated in this condition, thus they showed a high reactivity to electrophiles as well as nucleophiles. In addition, in water under near-critical condition, some acid-catalyzed organic reactions occurred without any added acid. At this point, we also proposed that the additional condensation reaction preferably occurred under acidic medium in the autoclave test and generate evolved gas followed by forming a highly ordered pore structure. It was also confirmed by the density measurement that the sample cured at the autoclave condition still kept forming thermoset network structure, which had much lower density than carboneous ceramic. Further investigations of the structural properties such as type of pore shape, size and uniformity are needed to understand the difference between dry and wet pyrolysis. Their

chemical, physical and mechanical properties will be discussed to understand the advantage of the new wet pyrolysis method of phenolic resin.

From the literature review, Fang et al. reported that the spherule of polyethylene began to expand at above 450°C and underwent a color change to red at about 570°C in supercritical water condition. This implies that polyethylene linkage is more stable at near- or supercritical water condition than that in inert atmosphere. These phenomena are possibly explained because the water molecules, which are intervening between the active molecules, formed from the decomposition of HDPE. These indications have challenged us to fabricate the cross-linked structure by using hydrothermally stable polyethylene linkages that would survive in severe autoclave condition. Our proposed idea was proven in this study. The result showed that polyethylene, which has highly cross-linked network structure, i.e., Gamma XLPE above 940 KGy dose and Silane XLPE, survived at the autoclave condition. From TGA and autoclave test, it was also proven that the gamma irradiation dose between 940 KGy and 1390 KGy could provide the optimum hydrothermal stability at the near-critical water condition. Moreover, four different cross-linked polyethylenes containing quantatively different gel content and swelling ratio were selected to find a critical factor that determines their hydrothermal stability at the near-critical water. The result indicated that the solvent ratio representing the network strength is more critical factor to determine the hydrothermal stability under near-critical water condition.

Screening candidate polymeric material was based on thermal and hydrothermal stability. However, cross-linked polyethylene does not fulfill the requirement of the high temperature stability above 500-600°C required by the temperature rise associated with

neutron adsorption and low thermal conductivity. HDPE/graphite composite increased the thermal conductivity of pure HDPE. The maximum value of thermal conductivity was 3.18 W/mK for our system, which was much higher value than Krupa's because we used finer graphite particles (5μm) and prepared well-dispersed HDPE/graphite mixing technique. However, the value at 350°C was 0.98 W/mK. This result indicated that the HDPE/graphite system was not a good method to figure out the problem related to the centerline temperature in BPRA system. The development of an alternative for polymeric BPRA system, which has much higher thermal conductivity, still remains an important endeavor to make them commercial.

FUTURE WORK

The possible application of polymeric materials in a nuclear reactor environment as a new potential burnable poison material has been studied. The analysis for finding a candidate was based on thermal and hydrothermal properties in PWR nuclear reactor condition. XLPEs and phenolic resins were found to be possible candidate material for new polymeric BPRA systems. However, there are several critical problems to be addressed.

First, it is important to develop an alternative method to increase the thermal conductivity to a much higher value. The polymeric BPRA system should fulfill the requirement of the high temperature stability above 500-600°C required by the temperature rise associated with neutron adsorption and low thermal conductivity. However, XLPEs has a low ceiling temperature (~450°C) and phenolic resins would lose hydrogen content in their structures when they transferred from polymeric material to ceramic material above 500°C. Moreover, the XLPE/graphite composite system showed less thermal conductivity than our expectation due to its amorphous structures at 350°C. Therefore, it would be necessary to cool the centerline temperature down to below 400°C by developing other alternative methods. The following diagram in Figure 9-1 outlines alternative approaches that would be ideal to solve the problem. A thin cylindrical shape of graphite or metal sheet might be placed between every separate lattice pin or plate form of burnable poison material in a zirconium alloy cladding tube. This system will fit well into XLPE especially because polyethylene contains more than adequate of >14w%

hydrogen in their structures. The special shape as shown in Figure 9-1 will supply the identical temperature for both parallel and perpendicular direction as cooling down by the coolant (~350°C).

Second, "thermal expansion coefficient" should be considered to design the burnable poison rod. BPRA plan view in Figure 2-4 represented a space occupied by helium gas between burnable poison pellet and zirconium alloy cladding. The gap for current B_4C/Al_2O_3 system was 4.1783 mm. However, this gap would be variable depending on the thermal expansion coefficient of each polymeric material. Most polymers expand and contract more than metals or ceramics do when subjected to the same thermal loading. This may complicate the design of the burnable poison rods.

Thirdly, it is necessary to develop the system, which protects the dehydration of zirconium alloy with hydrogen atoms knocking off in the polymeric material by a high radiation. Several types of radiation such as gamma ray, thermal neutron, and fast neutron are found in a nuclear reactor. When polyethylene or other polymeric materials are exposed to such a high energy radiation, the main effects are the formation of new bonds, free radicals, double bonds, etc., which can react with other atoms or molecules to modify the original polymeric structure. From these interactions, hydrogen gas (H_2) would be evolved. Therefore, it is important to monitor how many hydrogen atoms will be knocked out at this condition. The University of Florida Training Reactor was used to perform this experiment. However, the thermal neutron fluxes in the reactor core were $1.5x10^{12}$ n cm^{-2} s^{-1}, which was too weak to analyze their effect. It would be expecting that phenolic resin is one of the most stable polymers with respect to radiation and very large doses are required to produce any noticeable changes. However, the development of the system,

which can protect the dehydration of zirconium alloy, is necessary because most polymeric system would produce hydrogen gas in the range of 1-2 years of fuel cycle under sever radiation condition of a nuclear reactor. A ceramic coating method would be promising approach to solve this problem. It has been already extensively studied to develop a protecting coating system for the corrosion of the zirconium alloy cladding in a previous NERI project (#DE-FG03-99SF21882) titled " An innovative ceramic corrosion protection system for zirconium alloy cladding". However, at this time, it is not necessary to consider the waterside corrosion of zirconium alloy, which was a primary limiting factor in the previous study. Therefore, it should be much easier to develop the inner protecting layer by using the knowledge and skill accumulated from previous studies. Alumina coating prepared by sol-gel method and deposited by dip coating could be a promising method to solve this problem.

Finally, it was confirmed that Si-C bond was quite stable under the near-critical water in this study. The development of copolymers containing 5~6w% poly (diacetylene-siloxane-carborane) with poly (diacetylenedimethylsilane) and poly (diacetylenedimethylsilylethane) could solve the problem related to the extremely high cost and current limited supply of the carboranes based precursors. More importantly, these copolymers showed very excellent thermal stability, high hydrogen content (> 6 w%) and easy processing. In addition, it is more difficult to lose their boron content under hydrothermal condition due to a strong chemical bond between boron and polymers in their structures. A well-defined synthesis method should be developed to fabricate pure poly (diacetylenedimethylsilane) and poly (diacetylenedimethylsilylethane) without any unexpected siloxane linkages. Moreover, monomers used in this study, i.e.

dimethyldichlorosilane and dimethyldichlorosilylethane, were purchased from Gelest and used without further purification even though they contained 99% and 90% purity respectively. Therefore, it is necessary to refine these monomers without any contamination of water.

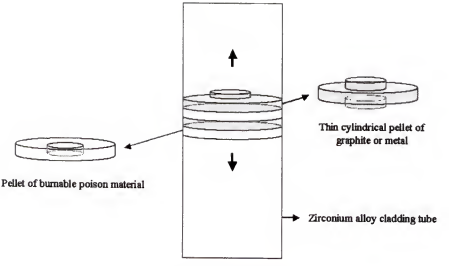

Figure 9-1. A special design of pellets that might show good thermal conductivity in the perpendicular direction.

LIST OF REFERENCES

1 Durmazucar HH, Colak U, Sarikaya B, Gunduz G: Burnup characteristics and performance of boron nitride and boron coated urania and urania-gadolinia fuels. *Nuclear Engineering and Design* 2001; **203**: 57-64.

2 Galperin A: Gd burnable poison system for reactivity control of the first cycle of a PWR. *Annals of Nuclear Energy* 1987; **14**: 53-57.

3 Kloosterman JL: Application of boron and gadolinium burnable poison particles in UO2 and PUO2 fuels in HTRs. *Annals of Nuclear Energy* 2003; **30**: 1807-1819.

4 Asou M, Porta J: Prospects for poisoning reactor cores of the future. *Nuclear Engineering and Design* 1997; **168**: 261-270.

5 Allen K. Advanced polymeric burnable poison rod assemblies for pressurized reactors: Nuclear and Radiological Engineering, Master dissertation, University of Florida, 2003.

6 Tulenko JS, Baney RH. An advanced poison materials for burnable poison rod assemblies and spent fuel shipping containers, Proposed to department of energy NERI program, 2000.

7 Arai K: Conversion of polymers and biomass to chemical intermediates with supercritical water. *Macromolecular Symposia* 1998; **135**: 205-214.

8 Arai K, Adschiri T: Importance of phase equilibria for understanding supercritical fluid environments. *Fluid Phase Equilibria* 1999; **158-160**: 673-684.

9 Fang Z, Smith RL, Inomata H, Arai K: Phase behavior and reaction of polyethylene terephthalate water systems at pressures up to 173 MPa and temperatures up to 490 degrees C. *Journal of Supercritical Fluids* 1999; **15**: 229-243.

10 Shaw RW, Brill TB, Clifford AA, Eckert CA, Franck EU: Supercritical Water - a Medium for Chemistry. *Chemical & Engineering News* 1991; **69**: 26-39.

11 Henderson LJ, Keller TM: Poly(Carborane-Siloxane-Acetylene) as Precursor to High-Temperature Thermoset and Ceramic. *Inorganic and Organometallic Polymers II* 1994; **572**: 416-426.

12 Henderson LJ, Keller TM: Synthesis and Characterization of Poly(Carborane Siloxane Acetylene). *Macromolecules* 1994; **27**: 1660-1661.

13 Son DY, Keller TM: Oxidatively Stable Carborane-Siloxane-Diacetylene Copolymers. *Journal of Polymer Science Part a-Polymer Chemistry* 1995; **33**: 2969-2972.

14 Son DY, Keller TM: Synthesis and Characterization of Linear Siloxane Diacetylene Polymers. *Macromolecules* 1995; **28**: 399-400.

15 Pehrsson PE, Henderson LJ, Keller TM: High-temperature oxidation of carborane-siloxane-acetylene-based polymer. *Surface and Interface Analysis* 1996; **24**: 145-151.

16 Bucca D, Keller TM: Thermally and oxidatively stable thermosets derived from preceramic monomers. *Journal of Polymer Science Part a-Polymer Chemistry* 1997; **35**: 1033-1038.

17 Keller TM, Son DY: Blending studies of poly(siloxane acetylene) and poly(carborane siloxane acetylene). *Synthesis and Characterization of Advanced Materials* 1998; **681**: 248-258.

18 Armistead JP, Houser EJ, Keller TM: Diacetylene-siloxane-carborane thermosets and ceramic precursors. *Applied Organometallic Chemistry* 2000; **14**: 253-260.

19 Keller TM: Oxidative protection of carbon fibers with poly(carborane-siloxane-acetylene). *Carbon* 2002; **40**: 225-229.

20 Kolel-Veetil MK, Keller TM: The effects of concentration dilution of cross-linkable diacetylenes on the plasticity of poly(m-carborane-disiloxane-diacetylene)s. *Journal of Materials Chemistry* 2003; **13**: 1652-1656.

21 Sugeta T, Nagaoka S, Otake K, Sako T: Decomposition of fiber reinforced plastics using fluid at high temperature and pressure. *Kobunshi Ronbunshu* 2001; **58**: 557-563.

22 Goto T, Yamazaki T, Okajima I *et al*: Decomposition of silane-crosslinked polyethylene for material recycling by using supercritical methanol. *Kobunshi Ronbunshu* 2001; **58**: 703-709.

23 Moriya T, Enomoto H: Characteristics of polyethylene cracking in supercritical water compared to thermal cracking. *Polymer Degradation and Stability* 1999; **65**: 373-386.

24 Gupta CK: Materials in Nuclear Energy Applications. Boca Raton, Fla. : CRC Press, 1989.

25 Ma BM: Nuclear Reactor Materials and Applications. New York : Van Nostrand Reinhold Co., 1983.

26 Cameron IR: Nuclear Fission Reactor. New York : Plenum Press, 1982.

27 Glasstone S, Sesonske A: Nuclear Reactor Engineering. New York, NY : Chapman & Hall, 1994.

28 Lamarsh JR: Introduction to Nuclear Engineering. New York, Addison-Wesley Publishing Company, 1982.

29 Duderstadt JJ, Hamilton LJ: Nuclear Reactor Analysis. John Wiley & Sons Inc., 1976.

30 Savage PE: Organic chemical reactions in supercritical water. *Chemical Reviews* 1999; **99**: 603-621.

31 Kritzer P: Corrosion in high-temperature and supercritical water and aqueous solutions: a review. *The Journal of Supercritical Fluids* 2004; **29**: 1-29.

32 Connolly JF: Solubility of Hydrocarbons in Water near Critical Solution Temperatures. *Journal of Chemical and Engineering Data* 1966; **11**: 13-&.

33 Fang Z, Minowa T, Smith RL, Ogi T, Kozinski JA: Liquefaction and gasification of cellulose with Na2CO3 and Ni in subcritical water at 350 degrees C. *Industrial & Engineering Chemistry Research* 2004; **43**: 2454-2463.

34 Sasaki M, Fang Z, Fukushima Y, Adschiri T, Arai K: Dissolution and hydrolysis of cellulose in subcritical and supercritical water. *Industrial & Engineering Chemistry Research* 2000; **39**: 2883-2890.

35 Smole MS, Zipper P: The influence of different treatment media on the structure of PET fibres. *Materials Research Innovations* 2002; **6**: 55-64.

36 Yang Y, Lu YJ, Xiang HW, Xu YY, Li YW: Study on methanolytic depolymerization of PET with supercritical methanol for chemical recycling. *Polymer Degradation and Stability* 2002; **75**: 185-191.

37 Smith RL, Fang Z, Inomata H, Arai K: Phase behavior and reaction of nylon 6/6 in water at high temperatures and pressures. *Journal of Applied Polymer Science* 2000; **76**: 1062-1073.

38 Alm TM: Solution O-17 NMR study of thermal hydrolysis in nylon 6,6. *Polymer* 2003; **44**: 6531-6536.

39 Meng LH, Zhang Y, Huang YD, Shibata M, Yosomiya R: Studies on the decomposition behavior of nylon-66 in supercritical water. *Polymer Degradation and Stability* 2004; **83**: 389-393.

40 Tagaya H, Katoh K, Kadokawa J, Chiba K: Decomposition of polycarbonate in subcritical and supercritical water. *Polymer Degradation and Stability* 1999; **64**: 289-292.

41 Suzuki Y, Tagaya H, Asou T, Kadokawa J, Chiba K: Decomposition of prepolymers and molding materials of phenol resin in subcritical and supercritical water under an Ar atmosphere. *Industrial & Engineering Chemistry Research* 1999; **38**: 1391-1395.

42 Shibasaki Y, Kamimori T, Kadokawa J-i, Hatano B, Tagaya H: Decomposition reactions of plastic model compounds in sub- and supercritical water. *Polymer Degradation and Stability*; **83**: 481-485.

43 Dai ZY, Hatano B, Tagaya H: Decomposition of a polyol in supercritical water. *Polymer Degradation and Stability* 2003; **80**: 353-356.

44 Ozaki J, Djaja SKI, Oya A: Chemical recycling of phenol resin by supercritical methanol. *Industrial & Engineering Chemistry Research* 2000; **39**: 245-249.

45 Fang Z, Smith RL, Inomata H, Arai K: Phase behavior and reaction of polyethylene in supercritical water at pressures up to 2.6 GPa and temperatures up to 670 degrees C. *Journal of Supercritical Fluids* 2000; **16**: 207-216.

46 Hamid SH, Amin MB, Maadhah AG: Handbook of polymer degradation. New York, M. Dekker, 1992.

47 Dvornic PR, Lenz RW: High temperature siloxane elastomers. Huthig&Wepf, Basel, 1990.

48 Rowland SP: Water in Polymers. Washington, D.C. : American Chemical Society, 1980.

49 Svorcik V, Proskova K, Rybka V, Hnatowicz V: Water diffusion in polyethylene modified by ion irradiation. *Polymer Degradation and Stability* 1998; **60**: 431-435.

50 Progelhof RC, Throne JL: Polymer Engineering Principles: Properties, Processes, Tests for design. Hanser, 1993.

51 Schwamm D, Kulig J, Litt MH: X-Ray Photoelectron Spectroscopic Depth Profiling of an Atomic Oxygen Resistant Poly(Carborane Siloxane) Coating. *Chemistry of Materials* 1991; **3**: 616-620.

52 Sundar RA, Keller TM: Synthesis and characterization of linear boron-silicon-diacetylene copolymers. *Macromolecules* 1996; **29**: 3647-3650.

53 Packirisamy S: Decaborane(14)-based polymers. *Progress in Polymer Science* 1996; **21**: 707-773.

54 Corriu RJP, Gerbier P, Guerin C, Henner BJL, Jean A, Mutin PH: Organosilicon Polymers - Pyrolysis Chemistry of Poly (Dimethylsilylene)Diacetylene. *Organometallics* 1992; **11**: 2507-2513.

55 Homrighausen CL, Keller TM: High-temperature elastomers from silarylene-siloxane-diacetylene linear polymers. *Journal of Polymer Science Part a-Polymer Chemistry* 2002; **40**: 88-94.

56 Sundar RA, Keller TM: Linear diacetylene polymers containing bis(dimethylsilyl) phenyl and/or bis(tetramethyldisiloxane)carborane residues: Their synthesis, characterization and thermal and oxidative properties. *Journal of Polymer Science Part a-Polymer Chemistry* 1997; **35**: 2387-2394.

57 Xu SH: Hydrolysis of poly(dimethylsiloxanes) on clay minerals as influenced by exchangeable cations and moisture. *Environmental Science & Technology* 1998; **32**: 3162-3168.

58 Shim SE, Isayev AI: Effects of the presecne of water on ultrasonic devulcanization of polydimethylsiloxane. *Journal of Applied Polymer Science* 2003; **88**: 2630-2638.

59 Shim SE, Yashin VV, Isayev AI: Environmentally-friendly physico-chemical rapid ultrasonic recycling of fumed silica-filled poly(dimethyl siloxane) vulcanizate. *Green Chemistry* 2004; **6**: 291-294.

60 Brook MA: Silicon in organic, organometallic, and polymer chemistry. John Wiley & Sons, Inc., 2000.

61 Clarson SJ, Semlyen JA: Siloxane Polymers. Englewood Cliffs, NJ, Prentice-Hall, 1993.

62 Allcock HR, Lampe FW: Contemporary polymer chemistry. New York, Prentice Hall, 1992.

63 Dai Z, Hatano B, Kadokawa J, Tagaya H: Effect of diaminotoluene on the decomposition of polyurethane foam waste in superheated water. *Polymer Degradation and Stability* 2002; **76**: 179-184.

64 Ijadimaghsoodi S, Barton TJ: Synthesis and Study of Silylene Diacetylene Polymers. *Macromolecules* 1990; **23**: 4485-4486.

65 Son DY, Keller TM: Linear Siloxane-Acetylene Polymers as Precursors to High-Temperature Materials: Fire and Polymers Ii. Washington, AMER CHEMICAL SOC, 1995, vol 599, pp 280-290.

66 Seyferth D, Prudhomme C, Wiseman GH: Cyclic Polysiloxanes from the Hydrolysis of Dichlorosilane. *Inorganic Chemistry* 1983; **22**: 2163-2167.

67 Seyferth D: Dimethyldichlorosilane and the direct synthesis of methylchlorosilanes. The key to the silicones industry. *Organometallics* 2001; **20**: 4978-4992.

68 Field RJ, Olson EW: Surface-treatment chemistry in the manufacture of aerogels: computational modelling of cyclic and linear siloxanes. *Journal of Non-Crystalline Solids* 2001; **285**: 194-201.

69 Knop A, Pilato LA: Phenolic Resins;Chemistry, Applications and Performance. Berlin ; New York : Springer-Verlag, 1985.

70 Baney RH, Itoh M, Sakakibara A, Suzuki T: Silsesquioxanes. *Chemical Reviews* 1995; **95**: 1409-1430.

71 Oh W, Hwang Y, Park YH *et al*: Optical, dielectric and thermal properties of nanoscaled films of polyalkylsilsesquioxane composites with star-shaped poly([epsiv]-caprolactone) and their derived nanoporous analogues. *Polymer* 2003; **44**: 2519-2527.

72 Conley RT: Thermal Stability of Polymers. New York, M. Dekker, 1970.

73 Zinke A: The Chemistry of Phenolic Resins and the Processes Leading to Their Formation. *Journal of Applied Chemistry* 1951; **1**: 257-266.

74 Shalin RE: Polymer Matrix Composite. London ; New York : Chapman & Hall, 1995.

75 Benjamin BM, Raaen VF, Maupin PH, Brown LL, Collins CJ: Thermal Cleavage of Chemical Bonds in Selected Coal-Related Structures. *Fuel* 1978; **57**: 269-272.

76 Allen DT, Gavalas GR: Reactions of Methylene and Ether Bridges. *Fuel* 1984; **63**: 586-592.

77 Ko TH, Kuo WS, Chang YH: Microstructural changes of phenolic resin during pyrolysis. *Journal of Applied Polymer Science* 2001; **81**: 1084-1089.

78 Ouchi K: Infra-red study of structural changes during the pyrolysis of a phenol-formaldehyde resin. *Carbon* 1966; **4**: 59-66.

79 Morterra C, Low MJD: I.R. studies of carbons--VII. The pyrolysis of a phenol-formaldehyde resin. *Carbon* 1985; **23**: 525-530.

80 Jha V, Banthia AK, Paul A: Thermal-Analysis of Phenolic Resin Based Pyropolymers. *Journal of Thermal Analysis* 1989; **35**: 1229-1235.

81 Martin RW: The chemistry of phenolic resins. New York, J. Wiley, 1956.

82 Malhotra HC, Gupta VK: Kinetics of Alkali-Catalyzed Meta-Cresol-Formaldehyde Reaction. *Journal of Applied Polymer Science* 1978; **22**: 343-351.

83 Choe CR, Lee KH: Effect of Processing Parameters on the Mechanical-Properties of Carbonized Phenolic Resin. *Carbon* 1992; **30**: 247-249.

84 Conley RT: Oxidative Degradation of Phenol-Formaldehyde Polycondensation Initial Degradation Reactions. *Journal of Applied Polymer Science* 1965; **9**: 1117-&.

85 Fromonteil C, Bardelle P, Cansell F: Hydrolysis and oxidation of an epoxy resin in sub- and supercritical water. *Industrial & Engineering Chemistry Research* 2000; **39**: 922-925.

86 Okajima I, Sugeta T, Sako T: Decomposition and debromination of flame-resistant polymers containing bromine atoms with subcritical water. *Kobunshi Ronbunshu* 2001; **58**: 692-696.

87 Okajima I, Yamada K, Sugeta T, Sako T: Decomposition of epoxy resin and recycling of CFRP with sub- and supercritical water. *Kagaku Kogaku Ronbunshu* 2002; **28**: 553-558.

88 Liu W-C, Yang C-C, Chen W-C, Dai B-T, Tsai M-S: The structural transformation and properties of spin-on poly(silsesquioxane) films by thermal curing. *Journal of Non-Crystalline Solids* 2002; **311**: 233-240.

89 Peacock AJ: Handbook of polyethylene;structures, properties, and applications. New York : Marcel Dekker, 2000.

90 Charlesby A: Radiation effects in materials. Oxford, London, New York, Paris : Pergamon Press, 1960.

91 Dole M: The radiation chemistry of macromolecules. New York, London : Academic Press, 1972.

92 Han SO, Lee DW, Han OH: Thermal degradation of crosslinked high density polyethylene. *Polymer Degradation and Stability* 1999; **63**: 237-243.

93 Premnath V, Bellare A, Merrill EW, Jasty M, Harris WH: Molecular rearrangements in ultra high molecular weight polyethylene after irradiation and long-term storage in air. *Polymer* 1999; **40**: 2215-2229.

94 Celina M, George GA: Characterization and Degradation Studies of Peroxide and Silane Cross-Linked Polyethylene. *Polymer Degradation and Stability* 1995; **48**: 297-312.

95 Clough RL: High-energy radiation and polymers: A review of commercial processes and emerging applications. *Nuclear Instruments and Methods in Physics Research Section B: Beam Interactions with Materials and Atoms* 2001; **185**: 8-33.

96 Briskman BA: Radiation effects in thermal properties of polymers. An analytical review. I. Polyethylene. *Nuclear Instruments & Methods in Physics Research Section B-Beam Interactions with Materials and Atoms* 2001; **185**: 116-122.

97 Sen AK, Mukherjee B, Bhattacharyya AS, De PP, Bhowmick AK: Degradation of silane- and peroxide-cross-linked polyethylene and ethylene propylene rubber. *Polymer Degradation and Stability* 1992; **36**: 281-289.

98 Swallow AJ: Radiation chemistry of organic compounds. London, Pergamon Press, 1960.

99 Wilson EJ: Radiation chemistry of monomers, polymers, and plastics. New York, Marcel Dekker, Inc., 1974.

100 Mitchell J: Applied polymer analysis and charaterization. New York, Macmillan, 1987.

101 Smedberg A, Hjertberg T, Gustafsson B: Crosslinking reactions in an unsaturated low density polyethylene. *Polymer* 1997; **38**: 4127-4138.

102 Callister WD: Material science and engineering: an introduction. New York :John Wiley & Sons, Inc., 1999.

103 Agari Y, Ueda A, Nagai S: Thermal-Conductivity of a Polyethylene Filled with Disoriented Short-Cut Carbon-Fibers. *Journal of Applied Polymer Science* 1991; **43**: 1117-1124.

104 Mather PJ, Thomas KM: Carbon black high density polyethylene conducting composite materials .2. The relationship between the positive temperature coefficient and the volume resistivity. *Journal of Materials Science* 1997; **32**: 1711-1715.

105 King JA, Weber EH, Quan CL, Tucker KW, Vogt BD: Conductive high temperature nylon. *Journal of Composite Materials* 2000; **34**: 2038-2060.

106 Krupa I, Chodak I: Physical properties of thermoplastic/graphite composites. *European Polymer Journal* 2001; **37**: 2159-2168.

107 Hernandez-Sanchez F, Herrera-Franco PJ: Electrical and thermal properties of recycled polypropylene- carbon black composites. *Polymer Bulletin* 2001; **45**: 509-516.

108 Weber EH, Clingerman ML, King JA: Thermally conductive nylon 6,6 and polycarbonate based resins. II. Modeling. *Journal of Applied Polymer Science* 2003; **88**: 123-130.

109 Weber EH, Clingerman ML, King JA: Thermally conductive nylon 6,6 and polycarbonate based resins. I. Synergistic effects of carbon fillers. *Journal of Applied Polymer Science* 2003; **88**: 112-122.

110 Calleja FJB, Bayer RK, Ezquerra TA: Electrical-Conductivity of Polyethylene Carbon-Fiber Composites Mixed with Carbon-Black. *Journal of Materials Science* 1988; **23**: 1411-1415.

111 Nagata K, Iwabuki H, Nigo H: Effect of particle size of graphites on electrical conductivity of graphite/polymer composite. *Composite Interfaces* 1999; **6**: 483-495.

112 Yang GC, Teng RR, Xiao P: Electrical properties of crosslinked polyethylene/carbon black switching composites as a function of morphology and structure of the carbon black. *Polymer Composites* 1997; **18**: 477-483.

113 Tsotra P, Friedrich K: Thermal, mechanical, and electrical properties of epoxy resin/polyaniline-dodecylbenzenesulfonic acid blends. *Synthetic Metals* 2004; **143**: 237-242.

114 Parrott JE, Stuckes AD: Thermal conductivity of solids. London : Pion, 1975.

115 Berman R: Thermal Conduction in Solids. Clarendon, Oxford, 1976.

116 Rusu M, Sofian N, Rusu D, Neagu E, Neagu R: Properties of iron powder filled high density polyethylene. *Journal of Polymer Engineering* 2001; **21**: 469-487.

117 Morgan VT: The Thermal-Conductivity of Cross-Linked Polyethylene Insulation in Aerial Bundled Cables. *Ieee Transactions on Electrical Insulation* 1991; **26**: 1153-1158.

118 Nakamura H, Matsuura M, Kawasaki K, Hiki Y, Kogure Y: Low-temperature thermal conduction in particle-dispersed polyethylene. *Journal of Applied Physics* 1996; **79**: 3994-4001.

119 Tavman IH: Effective thermal conductivity of isotropic polymer composites. *International Communications in Heat and Mass Transfer* 1998; **25**: 723-732.

120 Sofian NM, Rusu M, Neagu R, Neagu E: Metal powder-filled polyethylene composites. V. Thermal properties. *Journal of Thermoplastic Composite Materials* 2001; **14**: 20-33.

BIOGRAPHICAL SKETCH

Jinho Kim was born in Seoul, South Korea, on July 23, 1970. He entered Inha University to study polymer science and engineering and graduated with a bachelor's degree in 1996. He also served in the military during this bachelor's study. He joined the master's program in the same university and completed his study on polymer rheology and processing. After graduation in 1998, he began working as a member of the Polymer Processing Laboratory in the Korea Institute of Science and Technology (KIST) for two years.

In Fall 1999, he entered the Ph. D program in the Department of Materials Science and Engineering at the University of Florida.

I certify that I have read this study and that in my opinion it conforms to acceptable standards of scholarly presentation and is fully adequate, in scope and quality, as a dissertation for the degree of Doctor of Philosophy.

Ronald H. Baney

Ronald H. Baney, Chairman
Research Scientist of Materials Science and Engineering

I certify that I have read this study and that in my opinion it conforms to acceptable standards of scholarly presentation and is fully adequate, in scope and quality, as a dissertation for the degree of Doctor of Philosophy.

Darryl P. Butt
Associate Professor of Materials Science and Engineering

I certify that I have read this study and that in my opinion it conforms to acceptable standards of scholarly presentation and is fully adequate, in scope and quality, as a dissertation for the degree of Doctor of Philosophy.

Wolfgang Sigmund
Associate Professor of Materials Science and Engineering

I certify that I have read this study and that in my opinion it conforms to acceptable standards of scholarly presentation and is fully adequate, in scope and quality, as a dissertation for the degree of Doctor of Philosophy.

Laurie Gower

Laurie A. Gower
Associate Professor of Materials Science and Engineering

I certify that I have read this study and that in my opinion it conforms to acceptable standards of scholarly presentation and is fully adequate, in scope and quality, as a dissertation for the degree of Doctor of Philosophy.

James S. Tulenko
Professor of Nuclear and Radiological Engineering

This dissertation was submitted to the Graduate Faculty of Engineering and to the Graduate School and was accepted as partial fulfillment of the requirements for the degree of Doctor of Philosophy.

December 2004

Pramod P. Khargonekar
Dean, College of Engineering

Kenneth Gerhardt
Interim Dean, Graduate School